This dissertation has been
microfilmed exactly as received

69-2396

THORNE, John Kandelin, 1940-

ROLE OF CHEMICAL EQUILIBRIA IN THE SILICOTHERMIC REDUCTION OF MOLYBDENUM TRIOXIDE IN THE PRESENCE OF IRON.

The University of Michigan, Ph.D., 1968
Engineering, metallurgy

University Microfilms, Inc., Ann Arbor, Michigan

ROLE OF CHEMICAL EQUILIBRIA IN THE SILICOTHERMIC REDUCTION OF MOLYBDENUM TRIOXIDE IN THE PRESENCE OF IRON

by
John Kandelin Thorne

A dissertation submitted in partial fulfillment
of the requirements for the degree of
Doctor of Philosophy in
The University of Michigan
1968

Doctoral Committee:

Professor Lawrence H. Van Vlack, Chairman
Doctor James M. Dahl
Associate Professor Robert D. Pehlke
Professor Clarence A. Siebert
Professor Maurice J. Sinnott
Professor Edgar F. Westrum

ACKNOWLEDGMENTS

The author expresses his appreciation to the many people who have aided in this investigation and particularly to the following:

- Professor Lawrence H. Van Vlack, Chairman of the Doctoral Committee, for advice, suggestions, and encouragement throughout the course of this investigation;
- Professor Robert D. Pehlke, member of the Doctoral Committee, for his assistance and for serving as Acting Chairman of the Doctoral Committee during the chairman's sabbatical leave of absence;
- Professors Clarence A. Siebert, Maurice J. Sinnott, and Edgar F. Westrum, members of the Doctoral Committee, for their advice and cooperation;
- Dr. James M. Dahl of the Climax Molybdenum Company and member of the Doctoral Committee for patient guidance, helpful discussions, inspiration throughout this project; and
- D. V. Doane and Dr. M. Semchyshen of the Climax Molybdenum Company for suggesting this investigation and smoothly coordinating the company's interests in this project with those of the University.

The staff of the Ann Arbor Research Laboratory of the Climax Molybdenum Company of Michigan is acknowledged for its interest and assistance in the experimental program. A special tribute is due H. H. Blackett, E. Jamros, F. Lewellyn, F. Mass, R. M. Monroe, J. C. Raymoure, and W. W. Stine for their instruction and advice on the construction and use of equipment. Thanks are also expressed to R. H. Maurer, F. R. Fucek, B. Ivanycky, W. H. Price, and R. E. Rady for performing the chemical analyses, Mrs. Donna Kruzich for typing the manuscript, and to G. Choley for preparing the final drawings.

The author is also appreciative of the worthwhile discussions with his fellow graduate students as well as their helpful advice.

The financial support of the Climax Molybdenum Company and the National Aeronautics and Space Adminstration during the author's tenure as a graduate student at The University of Michigan is gratefully acknowledged.

TABLE OF CONTENTS

	Page
ACKNOWLEDGMENTS	ii
LIST OF TABLES	vi
LIST OF FIGURES	vii
ABSTRACT	1
INTRODUCTION	3
REVIEW OF THE LITERATURE	5
Metallothermic Production of Ferromolybdenum	6
Slag-Metal Relationships in the Metallothermic Production of Ferromolybdenum	9
Phase Equilibria	11
Fe-O	12
Mo-O	12
Fe-Mo	13
Fe-Mo-O	13
Fe-Si-O	15
EXPERIMENTAL PROCEDURE	16
Phase Rule Analysis	16
Equilibration Studies	18
Materials	18
Equilibration Studies at Molybdenum Saturation	18
Equilibration Studies at Silica Saturation	25
Analytical Procedure	27
EXPERIMENTAL RESULTS	30
Results of Equilibrations in the Fe-Mo System	30
Results of Equilibrations in the Fe-Mo-O System	32
Results of Equilibrations in the Fe-Mo-Si-O System	36
Results of Equilibrations with a Synthetic Commercial Slag	41
DISCUSSION OF EXPERIMENTAL RESULTS	43
Analysis of Experimental Technique	43
Thermochemical Relationships	47
Pertinence of Results to Commercial Practice	56
CONCLUSIONS	59
REFERENCES	61
APPENDIX A: USES OF FERROMOLYBDENUM	104

Page

APPENDIX B: DISCUSSION OF EXPERIMENTS UTILIZING A ROTATING CRUCIBLE APPARATUS 105

REFERENCES: APPENDIX B 108

LIST OF TABLES

		Page
Table I	Commercial Ferromolybdenum Specification.	5
Table II	Typical Ferromolybdenum Slag Compositions	10
Table III	Phase Rule Analysis of the Fe-Mo-Si-O and Fe-Mo-O Systems at Constant Temperature and Pressure for the Equilibria Studied in this Investigation	17
Table IV	Analysis of Materials Used in Sample Preparation. .	19
Table V	Schedule of Significant Experimental Runs	21
Table VI	Summary of Equilibrations in the Iron-Molybdenum System	31
Table VII	Summary of Equilibrations in the Fe-Mo-O System . .	33
Table VIII	Summary of Equilibrations in the Fe-Mo-Si-O System.	37
Table IX	Summary of Equilibrations Using a Synthetic Commercial Slag (Run 85).	42
Table X	Best Estimate of Liquidus Composition in the Fe-Mo System Using Data from Fe-Mo, Fe-Mo-O, and Fe-Mo-Si-O Equilibrations	48
Table XI	Gibbs Free Energy Data for the Fe-Mo-O System at 1873, 1973, and 2073 K	50
Table XII	Summary of Experimental Data from the Fe-Mo-O System Used to Calculate the Experimental Equilibrium Content ($K'_{eq.}$).	52
Table XIII	Summary of Experimental Data from the Fe-Mo-Si-O System Used to Calculate the Experimental Equilibrium Constant ($K'_{eq.}$)	55
Table B-I	Results of Rotating Crucible Experiments.	107

LIST OF FIGURES

		Page
Figure 1	Loading the Reaction Pot with the Thermite Mixture. .	67
Figure 2	Hoisting the Ferromolybdenum Button and Slag Cap from the Sand Pit to the Water-Quench Tank.	68
Figure 3	Separating the Ferromolybdenum Button from the Slag Cap.	69
Figure 4	Breaking the Ferromolybdenum Button to Feedstock Sizes for the Jaw Crushers.	70
Figure 5	Equilibrium Phase Diagram for the Iron-Oxygen Binary System	71
Figure 6	Equilibrium Phase Diagram for the Molybdenum-Oxygen Binary System	72
Figure 7	Equilibrium Phase Diagram for the Fe-Mo System. . . .	73
Figure 8	Pseudo-Binary Phase Diagram for the Fe_2O_3-MoO_3 System.	74
Figure 9	Pseudo-Binary Phase Diagram for the System FeO-MoO_3.	75
Figure 10	Pseudo-Binary Phase Diagram for the System $Fe_2(MoO_4)_3$-$FeMoO_4$	76
Figure 11	Schematic Isothermal Section through the Fe-Mo-O Ternary System in the Temperature Range 800 to 1100 C.	77
Figure 12	Equilibrium Phase Diagram for the Pseudo-Binary System FeO-SiO_2	78
Figure 13	Schematic Diagram of Inert-Atmosphere Induction-Heated Furnace Used for Molybdenum Crucible Experiments	79
Figure 14	Vertical Section of Molybdenum Crucible after Completion of Run 58.	80
Figure 15	Microstructure of Oxide Phase in Sample 68-2.	81
Figure 16	Microstructure of Oxide Phase in Sample 55-3.	82
Figure 17	Microstructure of Quenched Metal Phase in Sample 59-3	83
Figure 18	Interface between Metal Phase and Interior Wall of Molybdenum Crucible after Completion of Run 59 and Furnace Cooling	84

Page

Figure 19 Microstructure of Metal Phase in Sample 82-2. 85

Figure 20 Schematic Illustration of Experimental Runs to Determine the Partial 1600 C Isothermal Section of the Fe-Mo-O Phase Diagram. 86

Figure 21 Microstructure of Molybdenum-Rich Metal Phase, Molybdenum Dioxide Phase (Twinned), and Matrix of Iron-Molybdenum Oxide in Sample 45. 87

Figure 22 Interface between Contents of Crucible and Interior Wall of Molybdenum Crucible after Completion of Run 52. 88

Figure 23 Interface between Contents of Crucible and Interior Wall of Molybdenum Crucible after Equilibration of Run 50 at 1600 C 89

Figure 24 Schematic Illustration of Runs 55 and 83 in the Fe-Mo-O System. 90

Figure 25 Microstructure of Oxide Phase in Sample 83-1. 91

Figure 26 1600 C Isothermal Section through the Fe-Mo-O Phase Diagram Based on the Experimental Results of This Investigation 92

Figure 27 Iron-Molybdenum Equilibrium Phase Diagram Showing the Best Estimate of Liquidus Composition Using Data from Me-Mo, Fe-Mo-O, and Fe-Mo-Si-O Equilibrations. 93

Figure 28 Effect of Temperature and Silicon Concentration of Molybdenum-Saturated Fe-Mo-Si-O Slags in Equilibrium with Liquid Fe-Mo Metal on Molybdenum Concentration of These Slags. 94

Figure 29 Effect of Temperature and Silica Concentration of Molybdenum-Saturated Fe-Mo-Si-O Slags in Equilibrium with Liquid Fe-Mo Metal on the Molybdenum Concentration of These Slags. 95

Figure 30 Effect of Temperature and Silicon Concentration of Molybdenum-Saturated Fe-Mo-Si-O Slags in Equilibrium with Liquid Fe-Mo Metal on Iron Concentration of These Slags 96

Figure 31 Microstructure of Oxide Phase in Sample 84-1. 97

Figure 32 Microstructure of Oxide Phase in Sample 57-1. 98

Figure 33 Microstructure of Oxide Phase in Sample 58-1. 99

Page

Figure 34 Effect of Temperature and Molybdenum Concentration of Liquid Fe-Mo Metal in Equilibrium with Silica-Saturated Fe-Mo-Si-O Slags on Molybdenum Concentration of These Slags 100

Figure 35 Partitioning of Molybdenum between an Fe-Mo-Si-O Slag and Fe-Mo Metal (Molybdenum Saturation) as a Function of Silica Content of the Slag 101

Figure 36 Equilibrium Constants versus Reciprocal of Absolute Temperature. 102

Figure 37 Effect of SiO_2 Additions to Molybdenum-Saturated Liquid Fe-Mo-Si-O Slag in Equilibrium with Liquid Fe-Mo Metal on the Activity Coefficient Ratio $\gamma_{MoO_2}/\gamma^2_{FeO}$ $K_{eq.}/K'_{eq.}$ at 1873, 1973, and 2073 K. . . 103

Figure B-1 Schematic Diagram of Inert Atmosphere Induction Heated Rotating Crucible Apparatus 109

A B S T R A C T

ROLE OF CHEMICAL EQUILIBRIA IN THE SILICOTHERMIC REDUCTION OF MOLYBDENUM TRIOXIDE IN THE PRESENCE OF IRON

by

John Kandelin Thorne

Chairman: Lawrence H. Van Vlack

The purpose of this study was to determine experimentally the partition coefficient of molybdenum between the molybdenum weight fraction in the liquid slag and the weight fraction in the liquid metal for the Fe-Mo-Si-O system in the temperature range 1600 to 1800 C. The importance of this research arises from its applicability to the commercial production of ferromolybdenum by the silicothermic reduction of iron and molybdenum oxides.

The system was studied at molybdenum or silica saturation by equilibrating Fe-Mo-Si-O charges in molybdenum or silica crucibles. Samples of the equilibrated phases were obtained for analysis by (1) suction of liquid slag or liquid metal into Vycor tubes and water quenching, or (2) rapid cooling of the crucible and its contents. The samples were analyzed by x-ray powder diffraction, by metallographic examination, and by conventional wet chemical techniques. A series of samples in the iron-molybdenum-oxygen ternary system was prepared to determine a partial 1600 C isothermal section and to determine the molybdenum partition coefficient at 1600, 1700, and 1800 C. The effect of silica additions to the slag on the molybdenum partition coefficient was determined at 1600, 1700, and 1800 C for silica concentrations up to saturation.

For the molybdenum-saturated liquid metal and liquid slag in the Fe-Mo-O system, the results indicate that the molybdenum content of the slag increases from 18 weight percent at 1600 C to 24 weight percent at 1800 C, and that the partition coefficient increases from 0.34 at 1600 C

to 0.39 at 1800 C. At silica saturation, the molybdenum concentration of the slag is lowered to 0.2 weight percent at 1600 C and 0.3 weight percent at 1800 C; the corresponding values of the partition coefficient are 0.004 and 0.005 at 1600 and 1800 C, respectively. An ideal solution model describes the equilibrium relationship between iron and molybdenum in the slag and metal phases:

$$2(FeO) + \underline{Mo} = 2\ \underline{Fe} + (MoO_2)$$

The experimental equilibrium constants based on mole fractions of the components (0.186 and 0.184 at 1600 and 1800 C, respectively) agree well with the values calculated from published data. The model suggests that an interaction between FeO and SiO_2 in the slag causes a negative deviation in the activity of FeO and results in a lower molybdenum concentration in the slag than would be expected in an ideal solution.

Two general conclusions can be drawn from this investigation:

1. The partition coefficient of molybdenum between molybdenum-saturated liquid slag and liquid metal in the Fe-Mo-Si-O system is highly dependent on the silica content of the slag phase.
2. Within the temperature range studied, the partition coefficient of molybdenum is dependent on temperature, the dependency being less at higher silica concentrations in the slag.

INTRODUCTION

Research and development efforts on an existing metallurgical process frequently have as a goal an understanding of an idealized system from which information may be extrapolated to the actual system. Such is the case in this investigation, in which slag-metal equilibria in the Fe-Mo-Si-O system were examined with the goal of providing some insight into metallurgical phenomena encountered in the production of ferromolybdenum by the thermite process.

One of the key measurements of the efficiency of production of ferromolybdenum by the thermite process is the percentage of molybdenum charged that is recovered in the metal product, typically about 95%. It is often economical to attempt to recover the 5% of the charged molybdenum not appearing in the metallic product. About one-half of the "lost" molybdenum is recovered in a baghouse or by precipitators as dust evolved during the reaction and is recycled to the charge mixture. The other portion of the "lost" molybdenum appears in the slag as an oxide and as metallic iron-molybdenum prills that had not settled to the melt before the slag froze. The metal prills are often recovered by crushing and air elutriation of the slag and are recycled. However, molybdenum as oxide in the slag is not usually recovered. This investigation is concerned with providing some understanding of slag-metal relationships in ferromolybdenum production so that techniques may be developed for decreasing the molybdenum-content of the slag phase. A lower molybdenum concentration in the slag phase would increase the efficiency of the process as well as conserve a valuable natural resource.

To establish the nature and scope of the present investigation, the Fe-Mo-Si-O system was selected as being an appropriate first approximation to the more complex production situation. The system was studied at

equilibrium because it is the thermodynamic end point that is approached by the actual system and because it is the base point for any future kinetic studies. Because of experimental limitations, data were taken only at molybdenum or silica saturation. Despite these experimental limitations the approach was realistic because ferromolybdenum slags are silica-saturated and ferromolybdenum is nearly molybdenum-saturated within the temperature range studied.

REVIEW OF THE LITERATURE

The literature related to this research is presented in three sections. First, the metallothermic production of ferromolybdenum is briefly described and the open literature pertaining to this process is discussed. Second, literature is presented on slag-metal relationships in metallothermic processes. Finally, a discussion is given of the literature that pertains to phase equilibria in selected binary and ternary combinations of the elements iron, molybdenum, silicon, and oxygen.

The uses of ferromolybdenum are briefly discussed in Appendix A. A commercial specification[1] for this product is given in Table I.

Table I

Commercial Ferromolybdenum Specification

Composition	
Molybdenum[a]	60-64%
Carbon	0.10% max
Sulfur	0.15% max
Phosphorus	0.05% max
Copper	0.20% max
Silicon[b]	1.00% max
Balance	Principally Iron
Size	
Lump	+3/4 inch
Nut	3/4 to 1/5 inch
Ladle	4 mesh and under
Small Ladle	20 mesh and under
Powder	-40 mesh (100%); -80 mesh (60% min; 80% max); -325 mesh (10% min; 30% max)

[a] Powder contains 57 to 64% molybdenum.
[b] Powder contains 1.50% max silicon.

Metallothermic Production of Ferromolybdenum

The production of ferromolybdenum by the metallothermic reduction of molybdic oxide has been described by Durrer and Volkert[2] and Elyutin et al.[3] in their books on ferroalloy manufacture. A general description of the process is presented based on these books and on information provided by the Climax Molybdenum Company.[4-6] Other descriptions of the process have also been published.[7-10] Actual practices of individual plants would be expected to vary somewhat in details from those described below.

In the metallothermic production of ferromolybdenum,[2-6] molybdenum trioxide, iron oxide, silicon and aluminum are reacted as follows:

$$MoO_3 + 2Al \longrightarrow Mo + Al_2O_3 \quad (1)$$

$$Fe_2O_3 + 2Al \longrightarrow 2Fe + Al_2O_3 \quad (2)$$

$$3Fe_3O_4 + 8Al \longrightarrow 9Fe + 4Al_2O_3 \quad (3)$$

$$2MoO_3 + 3Si \longrightarrow 2Mo + 3SiO_2 \quad (4)$$

$$2Fe_2O_3 + 3Si \longrightarrow 4Fe + 3SiO_2 \quad (5)$$

$$Fe_3O_4 + 2Si \longrightarrow 3Fe + 2SiO_2 \quad (6)$$

The reaction is highly exothermic and burns violently to completion, leaving a liquid oxide slag floating over a pool of molten iron-molybdenum metal. Additions of lime, limestone, and fluorspar are generally included in the charge mixture to aid in slag-metal separation by the formation of a more fluid slag. After solidification, the slag cap and metal button are separated. The metal button is then fractured to sizes desired by ferromolybdenum consumers.

The relative quantities of reactants in the charge are governed by the stoichiometries of the reactions above and by the desired net heat release. The latter is controlled by the ratio of aluminum to silicon in the charge because the oxidation of aluminum is more exothermic than

that of silicon. The heat supplied by the reactions must be sufficient for the charge to burn smoothly to completion in a reasonable time and for the products to be left sufficiently molten for a good slag-metal separation before their solidification. The use of silicon alone as a reducing agent is not usually satisfactory from a heat-release standpoint. Therefore, the more expensive aluminum is added in the minimum amount necessary to achieve sufficiently high temperatures. Aluminum and silicon are included in the charge as ferrosilicon plus aluminum granules or as ferroaluminumsilicon.

Molybdic oxide is included in the charge as powder obtained, for example, from the roasting of molybdenum sulfide ore concentrates. The iron oxide is added as iron ore or mill scale. Some iron may also be charged, such as in the form of small pieces of unalloyed steel scrap. The fluxing ingredients (lime, limestone, and fluorspar) are added to the charge as powders or small chunks. Manganese ore may also be added as a flux.

After the ingredients are weighed and blended, they are charged to a bottomless reaction pot situated on a nest dug in a pit of silica sand. The reaction pot is a steel shell lined with refractory brick over which an exhaust hood is placed for collection of dust and gases evolved during burning. Figure 1 shows a reaction pot being charged.[11]

The charge is ignited by using an incandescent iron rod, a ladle of molten slag from a previous run, or an exothermic fuse material. The charge, weighing perhaps 6000 pounds, may burn to completion in only several minutes or take as long as an hour, depending on the specific formulary and particle size of materials used. After the reaction has ceased and the products are partially cooled, the reaction pot is lifted from the sand pit. The slag and metal are allowed to cool further and

solidify in the sand pit. A crane then removes the metal button and slag cap to a water-quench tank (Figure 2).[12] After quenching, the metal and slag are separated (Figure 3).[13] The metal is then fractured for crushing (Figure 4),[14] and crushed, screened, and packaged for sale.

Modifications of the process as described above include: (1) tapping the slag after the reaction subsides, (2) igniting a small amount of charge in the reaction pot followed by gradual feeding of the balance of the charge, (3) igniting from the bottom of the charge rather than the top, and (4) using a detachable insulated roof on the reaction pot.

The effect of variations in formulary and particle size of the charge components has been studied experimentally by Dubrovin et al.[15] These investigators show that a finer particle size causes a faster reaction and permits a decrease in the aluminum-to-silicon ratio in the charge. Too fast a reaction rate decreases the molybdenum recovery because of sublimation of some molybdic oxide before it is reduced and because of slag splashouts. However, too slow a rate increases the molybdenum lost in the slag. Rispel and Klokotina[16] reported studies on material and heat balances and on sources and distribution of impurities in ferromolybdenum production.

Dubrovin and Pliner[17] published temperature and heat-release calculations for thermite processes. The temperature is a function of the rate of the reaction, a matter examined experimentally in a later paper by Dubrovin and Kuznetsov.[18] The reaction rate was studied for various thermite charges by measuring the time of burning between thermocouples that were placed along the length of cylindrical containers. The effect on the reaction rate of the density of the charge, particle size, and gas pressure (air, inert gases, vacuum) was determined experimentally. The reaction rate was found to increase with increasing charge density

and increasing gas pressure up to about 2 atmospheres. A decline of the reaction rate at higher pressures was explained on the basis of the effective thermal conductivity of the charge. The authors found that the reaction rate could be regulated by controlling the gas pressure as well as other variables, such as charge density and composition. Pliner[19] proposed equations to characterize the dependence of the temperature of thermite melts on their heat content. These equations were applied to the thermite reduction of a number of oxides, including MoO_3.

Slag-Metal Relationships in the Metallothermic Production of Ferromolybdenum

The control of ferromolybdenum slag composition and fluidity is of considerable importance to minimize molybdenum losses in the slag as oxide and entrapped metallic prills. By minimizing these losses the subsequent effort necessary to recover the molybdenum in the slag may also be reduced. Table II lists a typical slag composition as reported by Elyutin et al.[20] and by the Climax Molybdenum Company.[5] Molybdenum contained in the slag as oxide has been reported as being about 0.2% MoO_3.[21]

Several research studies for decreasing the molybdenum content of ferromolybdenum slags have been published. Zhilo and Sobolev[22] investigated the viscosity of ferromolybdenum slags as a function of slag composition in the temperature range 1500 to 1800 C. Viscosities ranged between 125 and 15 poises with increasing temperature and FeO content favoring a more fluid slag. The role of slag viscosity on the coagulation rate of metal drops in thermite melts was discussed by Pliner et al.[23] With increasing viscosity, the rate of collision of drops decreases, and movement of the coagulated drops into the metal button is slower, causing an increased loss of metal as prills in the slag. Recommendations were made on the particle size of the reactants for the formation of optimal

Table II

Typical Ferromolybdenum Slag Compositions

Component	Concentration (Weight Percent)	
	Climax Molybdenum Company[a]	Elyutin et al.[b]
SiO_2	65.1	62.56
Al_2O_3	17.4	9.59
FeO	13.5	23.13
CaO	2.8	2.96
CaF_2	--	1.75
P_2O_5	--	0.01

[a] "Ferromolybdenum Development Manual of Information," Internal Publication Climax Molybdenum Company, New York, 1965.

[b] V. P. Elyutin, Yu. A. Pavlov, B. E Levin, and E. M. Alekseev, Production of Ferroalloys, second edition, translated by B. Shapira, National Science Foundation, Washington, D.C., 1961 (OTS 61-11429), p. 277.

size metal drops. For example, if aluminum powder is used for reduction, the recommended size range is 0.003 to 0.005 mm.

The possibility of enhancing the rate of movement of metal prills from the slag into the metal button by applying an electric current to the system was reported by several authors. Utilizing an "electrocapillary effect," Khlynov and Esin[24] showed that droplets of ferromolybdenum could be more completely removed from the slag if the droplets were electrically charged. Later experiments by Nikitin et al.[25] showed this method to be equally effective for ferrotungsten slags.

The relatively low concentration of molybdenum oxide in ferromolybdenum slags has been rationalized on a thermodynamic basis by Pliner and Ignatenko[26] and by Elyutin et al.[20] By assuming ideal solution behavior of the slag components, the latter authors calculated the equilibrium

molybdenum oxide content of the slag to be about 10^{-9} weight percent at 2000 K. In practice such a low value is never attained, which the authors suggest is because of the kinetic conditions of the process.

Molybdenum-containing oxide phases in ferromolybdenum slags were examined by Rusakov et al.[27] by metallographic and x-ray analysis. The authors conclude that molybdenum in the molten slag is present as MoO_2 and lower oxides of molybdenum. With decreasing temperature these oxides crystallize as complex oxides of the types $2MO \cdot MoO_2$ (MO = FeO or MgO) or decompose into metal and MoO_2.

Although the effect of ferromolybdenum slag composition on molybdenum oxide solubility has not been examined, some information may be obtained from a paper by Dittrich.[28] This investigator studied methods of making an iron-molybdenum alloy by removing molybdenum from copper smelting wastes containing 2 to 10% molybdenum. It was found that additions of SiO_2 to the slag decreased the MoO_3 content of the slag until at 40% SiO_2 no molybdenum could be found in the slag phase. The movement of molybdenum from slag to metal was explained according to the two-step reaction:

$$2FeMoO_4 + SiO_2 \longrightarrow 2FeO \cdot SiO_2 + 2MoO_3 \qquad (7)$$

$$6Fe + 3SiO_2 + 2MoO_3 \longrightarrow 3(2FeO \cdot SiO_2) + 2Mo \qquad (8)$$

By adding SiO_2 to the copper smelting wastes it was possible to concentrate molybdenum in the metal phase.

Phase Equilibria

A literature review of phase equilibria related to the present research is presented below. The Fe-O, Mo-O, and Fe-Mo binary systems and the Fe-Mo-O and Fe-Si-O ternary systems are considered. The Fe-Mo-Si-O quaternary system has been studied by only Dittrich.[28]

Fe-O Binary System

The Fe-O binary system has been studied by numerous investigators, excellently referenced by Hansen[29] and Elliott.[30] The most outstanding study is that of Darken and Gurry,[31,32] who equilibrated the condensed phases at oxygen potentials controlled by known mixtures of CO and CO_2 gases. In earlier work, Chipman and Marshall[33] used the H_2/H_2O equilibrium in a similar manner. More recent investigations by Dastur and Chipman[34] and Gokcen[35] have helped to confirm the essential validity of the earlier data. The phase diagram as determined by Darken and Gurry is reproduced in Figure 5.

The solubility of oxygen in alpha iron is reported by Seybolt[36] to be about 0.002 weight percent at 850 C. In gamma iron the solubility is about 0.003 weight percent in the temperature range 1325 to 1423 C, according to Kitchener et al.[37] The solubility in delta iron, as determined by Tankins and Gokcen,[38] follows the relationship log (%O) = 5.51 - 12,630/T, (T in degrees Kelvin), being 0.015 weight percent at 1450 C.

Mo-O Binary System

The Mo-O equilibrium phase diagram has recently been delineated by Phillips and Chang[39] by equilibration of molybdenum and MoO_3 powders in sealed platinum capsules in the temperature range 600 to 1700 C. Figure 6 shows the phase diagram according to these investigators. Four stable compounds exist at lower temperatures: MoO_2, Mo_4O_{11}, Mo_9O_{26}, and MoO_3. At 818 C, Mo_4O_{11} melts incongruently to MoO_2 + liquid; whereas Mo_9O_{26} has a transition temperature at 765 C and melts incongruently at 780 C to a mixture of Mo_4O_{11} + liquid. The trioxide of molybdenum, MoO_3, melts congruently at 782 C. Its vapor pressure is one atmosphere at about 1155 C,[40] the vapor phase species being predominantly MoO_3 trimers.[41]

At high temperatures $MoO_2(s)$ disproportionates,[41,42] the gaseous phase being primarily MoO_3:

$$3MoO_2(s) = 2MoO_3(g) + Mo(s)$$

The temperature at which the equilibrium pressure over $MoO_2(s)$ is one atmosphere is estimated to be 1777 C.[43]

Molybdenum oxides other than those shown by Phillips and Chang are known to exist. It is possible that these oxides are intermediate reaction products and not thermodynamically stable phases. Information on these oxides has been summarized by Elliott.[44]

The solubility of oxygen in solid molybdenum has been determined by Few and Manning[45] to be 0.006 weight percent at 1600 C. The solubility is reported to decrease linearly to about 0.004 weight percent at 1100 C.

Fe-Mo Binary System

Hansen[46] and Elliott[47] have summarized early work on Fe-Mo equilibrium phase relationships. The diagram shown by Hansen has been considerably modified by two recent investigations. Sinha, Buckley, and Hume-Rothery[48] have re-determined the diagram for 0 to 45 atomic percent molybdenum. They have identified two additional equilibrium phases: an R phase, containing about 37.4 atomic percent molybdenum, forms peritectically at 1488 C and decomposes eutectoidally at 1245 C, and a Laves phase λ, or Fe_2Mo, forms peritectoidally at 950 C. The solidus and liquidus relations on the iron-rich side of the system have been re-determined by Gibson, Lee, and Hume-Rothery[49] by thermal analysis at temperatures up to about 1570 C. Figure 7 shows the Fe-Mo phase diagram as determined by these two studies.

Fe-Mo-O Ternary System

The most definitive work on phase equilibria in the Fe-Mo-O ternary system is that of Jäger, Rahmel, and Becker.[50] By x-ray and thermal

analyses, these investigators found the following equilibrium compounds: $Fe_2(MoO_4)_3$, $FeMoO_4$, Fe_2MoO_4, and $Fe_4Mo_6O_{16}$. Pseudo-binary phase diagrams for Fe_2O_3-MoO_3, $FeMoO_4$-MoO_3, and $FeMoO_4$-$Fe_2(MoO_4)_3$ are reproduced in Figures 8, 9, and 10, respectively. Figure 11 shows a schematic isothermal section through the ternary phase diagram proposed by the authors to illustrate the probable nature of this diagram in the temperature range 800 to 1100 C. The compounds $Fe_2(MoO_4)_3$ and $FeMoO_4$ are reported to melt congruently at 956 and 1068 C, respectively. The melting points of Fe_2MoO_4 and $Fe_4Mo_6O_{16}$ are above 1150 C, the maximum temperature of Jäger's investigation. Jäger's paper confirms the earlier findings of Tamman and Westerhold,[51] who studied the FeO-MoO_3 and Fe_2O_3-MoO_3 systems, and reported the existence of the compound $FeMoO_4$.

In addition to the Fe-Mo-O compounds reported by Jäger et al., other compounds are known to exist. Schönberg[52,53] prepared and characterized the compounds FeMoO, Fe_3Mo_3O, and $FeMoO_x$, where x varies between 0.4 and 1. McCarroll et al.[54,55] described the preparation and structure of $Fe_2Mo_3O_8$. Work by Meijering and Rathenau[56-58] on the rapid attack of MoO_3 on metal and alloys by formation of low melting oxides has indicated the eutectics described by Jäger et al.[50] Structural information of $Fe_2(MoO_4)_3$ by Jäger et al. has been supplemented by that of Nassau et al.[59] Kozmanov and Ugolnikova,[60] and Kozmanov[61,62] have also characterized the compounds $FeMoO_4$, Fe_2MoO_4, and $Fe_2(MoO_4)_3$.

Phase equilibria in the Fe-Mo-O system have not been clarified at temperatures higher than about 1150 C. The activity of oxygen in liquid Fe-Mo metal, however, has been studied by Tankins et al.[63] and Floridis and Chipman.[64] The stable liquid and solid oxides in equilibrium with liquid and solid metallic phases have not been examined.

Fe-Si-O Ternary System

Phase equilibria in the Fe-Si-O ternary system have been summarized by Levin et al.[65] Of primary interest to the present investigation is the $FeO-SiO_2$ pseudo-binary phase diagram. This system may be considered truly binary only when the small amount of trivalent iron in the melt is neglected. Figure 12 shows this diagram according to the work of Bowen and Schairer,[66] who studied the system by equilibration of the phases in iron crucibles in an inert atmosphere and quenching to obtain samples for analysis. More recent studies on the ternary system have been made by Darken[67] and by Michal and Schuhmann,[68] who studied the phase equilibria as a function of temperature and gas composition above the melt. Liquidus surfaces for the $FeO-Fe_2O_3-SiO_2$ system have been determined by Schuhmann et al.[69] and by Maun.[70]

EXPERIMENTAL PROCEDURE

In this investigation, phase rule considerations were applied to the Fe-Mo-Si-O system to assist in the design of experiments, and then equilibration studies were conducted on this system. The equilibration studies were performed in three parts: (1) equilibration at molybdenum saturation by holding the melt in molybdenum crucibles, (2) equilibration at silica saturation by holding the melt in silica crucibles, and (3) equilibration in a rotating crucible apparatus. The procedure is discussed in the order in which it was followed, except for the discussion of the rotating crucible experiments, which is reserved for Appendix B because they did not yield significant data.

Phase Rule Analysis

This investigation of high-temperature equilibria in the Fe-Mo-Si-O system is facilitated by application of the phase rule to hypothesize the phase equilibria in the system. Since the study was conducted at essentially constant gas pressure of one atmosphere, the Gibbs phase rule, as discussed by Case,[71] reduces to

$$V = C - P + 1 \tag{10}$$

where V = the variance or degrees of freedom,

C = the number of components, and

P = the number of phases in equilibrium.

In a four-component system, phase equilibria may be described by an isothermal tetrahedron in which the sides are the four triangular isothermal sections from the four respective ternary phase diagrams. The phase rule for four components at constant temperature and pressure is

$$V = 4 - P \tag{11}$$

The phase rule for a three-component system at constant temperature and pressure is similar except that the maximum possible variance is reduced

by one:

$$V = 3 - P \tag{12}$$

Table III shows the phase rule variance for the four-component Fe-Mo-Si-O system and the three-component Fe-Mo-O system for the equilibria studied in this investigation. In these studies the system was saturated with the material used for the crucible. The univariant systems listed in Table III therefore become invariant at equilibrium because of this saturation requirement.

Table III

Phase Rule Analysis of the Fe-Mo-Si-O and Fe-Mo-O Systems at Constant Temperature and Pressure for the Equilibria Studied in this Investigation

Phases in Equilibrium[a]	Variance	Phase Diagram Representation
Fe-Mo-Si-O System		
Solid metal, liquid metal, solid oxide I, liquid oxide II	Invariant	Tie-tetrahedron
Solid metal, liquid metal, liquid oxide I, liquid oxide II	Invariant	Tie-tetrahedron
Solid oxide I, liquid metal, liquid oxide II	Univariant	Tie-triangles
Solid metal, liquid metal, liquid oxide II	Univariant	Tie-triangles
Fe-Mo-O System		
Solid metal, liquid metal, liquid oxide II	Invariant	Tie-triangle
Solid metal, liquid oxide II, solid oxide III	Invariant	Tie-triangle
Solid metal, liquid oxide II	Univariant	Tie-lines

[a] Solid metal: primarily molybdenum; liquid metal: primarily iron-molybdenum; oxide I: primarily silica; liquid oxide II: iron oxide-rich slag; solid oxide III: primarily molybdenum dioxide.

Equilibration Studies

The experiments performed in this investigation were of two types: equilibration at molybdenum saturation and equilibration at silica saturation. Following a discussion of materials used for these experiments, the details of each type of experiment are presented. The procedure for analysis of specimens is the same for both experiments and is presented in the final portion of the section.

Materials

The materials used for sample preparation in this investigation were Climelt arc-cast molybdenum bar and tubing, molybdenum powder, molybdenum dioxide powder, molybdenum trioxide powder, Ferro-vac E iron bar, reagent grade iron powder, reagent grade ferric oxide powder, silicon dioxide powder, and fused silica crucibles and tubing. Table IV lists typical compositions of these materials as supplied by the manufacturers. All materials were used in the as-received condition with the exception of the Ferro-vac E iron bar, which was cleaned by pickling in a 1:1 aqueous HCl solution, rinsed in water, rinsed in alcohol, and air-dried.

Equilibration Studies at Molybdenum Saturation

Equilibria in the Fe-Mo, Fe-Mo-O, and Fe-Mo-Si-O systems at molybdenum saturation were studied by equilibrating the desired elements in molybdenum crucibles in an argon atmosphere. Specimens were obtained for analysis by quenching the equilibrated phases. The molybdenum crucibles were machined from bar stock to form 2-1/4-inch-diameter crucibles about 2 inches tall having a cavity 1-1/8 inches in diameter and 1-1/2 inches deep. The crucibles were cleaned in concentrated HF, rinsed in water, swabbed with alcohol, and air-dried.

The equilibration experiments were performed in an inert atmosphere, 30-kw, 3-kc induction furnace. This furnace was constructed by winding

Table IV

Analysis of Materials Used in Sample Preparation

Material	Chemical Composition (Weight Percent)				
	Mo	Fe	Si	C	O
Climelt arc-cast molybdenum bar and tubing[a]	>99.9	<0.001	<0.001	0.003	0.0006
Molybdenum powder	>99.9	<0.001	<0.001	--	--
Molybdenum dioxide powder	>74.9	--	--	--	>25.0
Molybdenum trioxide powder	66.62	<0.003	<0.014	--	33.33
Ferro-vac E iron bar	--	>99.9	--	0.005	--
Iron powder, reagent grade[b]	--	>98.0	--	--	--
Ferric oxide powder, reagent grade[c]	--	69 45	--	--	29.85
Silicon dioxide powder[d]	--	0.007	>46.28	--	>52.72
Fused silica crucibles and tubing[e]	--	<0.1 ppm	>46.74	--	>53.25

[a] Laboratory analysis of 2-1/4-inch-diameter bar used for crucibles substantiated this analysis.
[b] Also contains <0.001% sulfur.
[c] Also contains 0.10% $SO_4^=$.
[d] Also contains 0.006% calcium and a trace amount of sodium.
[e] Also contains <0.1 ppm calcium.

a 22-turn, 7-inch-i.d. by 1-foot-long induction coil from 3/8-inch copper tubing. The coil was centered in a 1-foot-i.d. by 2-foot-tall transite cylinder, and the annular space between the coil and the transite cylinder was filled with alumina bubble. For the present experiments, a 4-inch-diameter by 4-inch-high cylindrical molybdenum chamber was constructed to fit inside a zirconia crucible, as shown schematically in Figure 13. The space between the walls of the zirconia crucible and those of the molybdenum

chamber was filled with zirconia powder. A circular, 1/4-inch-thick molybdenum plate having a 1-inch-diameter center hole served as the top of the chamber. Charging and sampling were accomplished through a 1-inch-i.d. zirconia tube, which served as a sight hole and entry into the hot zone from the top of the furnace. Tank argon was flooded into the furnace through a molybdenum tube at the rate of about 10 ft^3/hr. In addition to acting as a susceptor, the molybdenum chamber provided a more uniform temperature in the hot zone by serving as a baffle for the argon gas. In all experiments conducted in this furnace, oxidation of the molybdenum components was not observed. This would imply an oxygen partial pressure of less than approximately 0.04 atmosphere at 1900 C based on thermodynamic information from Glassner.[72]

Temperature was measured with a tungsten, tungsten-26% rhenium thermocouple attached to the side of the molybdenum crucible with molybdenum wire. During some runs the thermocouple became contaminated because of splashing during sampling or charging. If contamination was suspected, a new thermocouple was suspended down the sight hole into the hot zone along side the crucible, and the run was continued. The measured temperature is considered to be within 20 deg C of the scheduled temperature. A typical run was made by charging a molybdenum crucible with weighed amounts of Mo, MoO_2, Fe, Fe_2O_3, and SiO_2 powders that had been blended in a high-speed impact shaker. After meltdown of this initial charge, pellets of the powdered mixture were added to the crucible until it was almost full. The crucible contributed significant amounts of molybdenum to the melt, as evidenced by the extent of dissolution of the interior wall of the crucible. Figure 14 is a photograph of a vertical section of the molybdenum crucible after completion of Run 58. This photograph shows the extent of dissolution of the crucible from its original interior diameter

and shows the slag and metal phases, liquid at temperature, which remained after sampling was completed. After the melt was held for the scheduled time and temperature samples were withdrawn, and another time-temperature hold was begun. Runs 55 through 59 and 82 through 85 were made in this manner. A summary of these runs is given in Table V. Sampling was accomplished by drawing the liquid slag or liquid metal into 6-mm Vycor tubing using the partial vacuum created by expanding a compressed rubber bulb attached to the end of the tubing. After the tube was quickly

Table V

Schedule of Significant Experimental Runs

Run	Charge (Weight Percent)						Crucible Material	Sample	Time (hr)	Temperature (C)
	Mo	MoO_2	MoO_3	Fe	Fe_2O_3	SiO_2				
Iron-Molybdenum Binary System: Molybdenum Saturation										
59	30.00	--	--	70.00	--	--	Molybdenum	1 2 3 4 5	1 1 1 0.5 0.5	1550 1600 1700 1800 1900
82	67.74	--	--	32.26	--	--	Molybdenum	1 2 3	1 3.5 1	1700 1700 1600
Molybdenum-Oxygen Binary System: Molybdenum Saturation										
42	57.14	--	42.86	--	--	--	Molybdenum	--	3	1600
Fe-Mo-O Ternary System: Molybdenum Saturation										
44	54.31	--	40.75	1.28	3.66	--	Molybdenum	--	12	1600
45	51.16	--	38.38	2.71	7.75	--	Molybdenum	--	7	1600
48	43.56	--	32.68	6.16	17.61	--	Molybdenum	--	5	1600
50	--	--	40.04	15.54	44.42	--	Molybdenum	--	4.5	1600
51	--	--	56.89	22.07	21.04	--	Molybdenum	--	4.5	1600
52	--	--	60.04	10.35	29.60	--	Molybdenum	--	4.5	1600
55	20.88	--	--	38.53	40.59	--	Molybdenum	1 2 3 4 6	1 2 3 1 0.25	1600 1600 1600 1700 1800
83	--	53.39	--	46.61	--	--	Molybdenum	1 2	2.5 2.5	1600 1700

Table V (Continued)

Schedule of Significant Experimental Runs

Run	Charge (Weight Percent)						Crucible Material	Sample	Time (hr)	Temperature (C)
	Mo	MoO_2	MoO_3	Fe	Fe_2O_3	SiO_2				
Fe-Mo-Si-O Quaternary System: Molybdenum Saturation										
56	20.00	--	--	42.29	35.22	2.49	Molybdenum	1 2 5	1 1 0.25	1600 1700 1800
57	20.00	--	--	41.01	31.52	7.48	Molybdenum	1 2 4	1 1 0.25	1600 1700 1800
58	20.00	--	--	38.40	24.08	17.52	Molybdenum	1 2 3 4	1 1 0.5 0.25	1600 1700 1800 1900
84	1.65	45.14	--	50.00	--	3.21	Molybdenum	1 2	2.5 2.5	1600 1700
Fe-Mo-Si-O Quaternary System: Silica Saturation										
68	12.69	--	--	73.71	5.13	8.47	Silica	1 2 3	1 1 1	1550 1600 1650
69	29.79	--	--	57.06	4.96	8.19	Silica	1 2 3	1 1 1	1550 1600 1650
71	23.34	--	--	47.22	11.11	18.34	Silica	--	2	1550
72	23.34	--	--	47.22	11.11	18.34	Silica	--	2	1600
Fe-Mo-Si-O Quaternary System: Molybdenum and Silica Saturation[a]										
74	33.33	--	--	37.20	11.13	18.33	Molybdenum	--	2	1600
75	33.33	--	--	37.20	11.13	18.33	Molybdenum	--	2	1800
76	33.33	--	--	37.20	11.13	18.33	Molybdenum	--	2	1900
78	33.33	--	--	37.20	11.13	18.33	Molybdenum	--	2	1750
80	33.33	--	--	37.20	11.13	18.33	Molybdenum	--	2	1650
81	33.33	--	--	37.20	11.13	18.33	Molybdenum	--	7	1550
Multicomponent: Molybdenum Saturation										
85[b]	30.00	--	--	21.75	5.00	33.00	Molybdenum	1 2	2.5 2.5	1600 1700

[a] Systems were silica-saturated by including additional silica as pieces of Vitreosil fused silica.

[b] Charge also contained 1.50% CaO and 8.75% Al_2O_3.

filled with several inches of liquid, it was withdrawn from the furnace and quenched in water. The solid sample was then pulled from the glass tube or the tube was fractured and the sample separated from the glass. No reaction was ever observed between the Vycor tube and the liquid sample. However, it was necessary to sample quickly because the temperature of the sample was above the softening temperature of the glass. This sampling method proved to be reliable and convenient after some experience was gained in its performance.

Runs 74, 75, 76, 80, and 81, also summarized in Table V, were made in smaller molybdenum crucibles, 1-1/2-inch-o.d. by 1-1/2-inch-long, having a 1-1/4-inch-i.d. by 1-1/4-inch-deep cavity. These crucibles were charged with the desired powders and with several pieces of Vitreosil silica to saturate the system with silica as well as molybdenum. They were individually suspended into the hot zone of the inert atmosphere induction furnace using a molybdenum wire harness and suspension wire. A tungsten, tungsten-26% rhenium thermocouple was wired to the side of the crucible. The hot zone of the furnace was identical to that previously described except that a larger 2-inch-diameter entry hole was constructed to permit the removal of the crucible from the hot zone. After equilibration for the scheduled time and temperature, the crucible was carefully removed from the top of the furnace, and immediately quenched in water. This sampling procedure was followed because the Vycor tube technique was not satisfactory for sampling the three-phase contents of these crucibles.

Several additional experimental runs were made by encapsulating Fe-Mo-Si-O charges in molybdenum containers, heating each capsule in a high-temperature vacuum furnace, and quenching the capsule and its contents in tin powder. The capsules were prepared by charging weighed amounts of Mo, MoO_3, Fe, Fe_2O_3, and SiO_2 powders into molybdenum cylinders closed

at one end. The powders were previously blended in a high-speed impact shaker. Each charge was then encapsulated in its container by electron beam welding a molybdenum cap onto the open end of the cylinder in a vacuum of less than 5 microns. By focusing the electron beam to a small diameter spot and by holding each container in a steel heat sink, it was possible to encapsulate with no observed heat effects on the charge. The molybdenum containers were of two types: (1) 3-inch-long by 3/8-inch-diameter thin-wall molybdenum tubing, and (2) 3-inch-long by 3/4-inch-o.d. by 3/8-inch-i.d. capsules drilled from molybdenum bar stock. Containers of the first type were used for charges that contained an excess of molybdenum in the powdered mixture. The second type of container was used for molybdenum-lean charges in which molybdenum saturation was approached by partial dissolution of the interior wall of the capsule.

Each sealed capsule was heated for the scheduled time and temperature in a high-temperature vacuum furnace. The cylindrical hot zone of this furnace was 5-1/2 inches tall and 2-3/4 inches in diameter and heated by tantalum resistance elements. A molybdenum wire harness was fashioned around the end of each capsule so that the capsule could be suspended into the hot zone. The molybdenum suspension wire was held from above the hot zone by a chuck having jaws that could be manipulated outside the vacuum chamber.

The temperature of the capsule during a run was measured using a tungsten, tungsten-26% rhenium thermocouple suspended into the hot zone adjacent to the capsule. The temperature was controlled manually by adjusting the current through the tantalum heating elements and was estimated to be within 20 deg C of the scheduled temperature throughout a run.

A run was made by heating the suspended capsule for the scheduled time and temperature, after which the capsule was quenched by opening a

door at the bottom of the hot zone and opening the jaws of the chuck. This permitted the capsule to fall from the hot zone into a copper heat sink filled with tin powder. The tin was melted and the sample quenched, for example, from 1800 C to about 400 C in about 45 seconds. The capsule was then sectioned and the contents analyzed. Runs 42, 44, 45, 48, 50, 51, and 52 were made in this manner and are included in the schedule of significant experimental runs shown in Table V.

In addition to the experiments designed to yield data on the Fe-Mo-Si-O equilibria, one experiment was run which included CaO (prepared by calcining reagent grade $CaCO_3$) and reagent grade Al_2O_3 in the charge to better approximate the slag-metal compositions encountered in ferromolybdenum production by the thermite method. The procedure for this run (85) was the same as described on page 21 using molybdenum crucibles, and included in Table V.

Equilibration Studies at Silica Saturation

In addition to the equilibrations at both molybdenum and silica saturation using molybdenum crucibles as described on page 23, several equilibrations at silica saturation and lower molybdenum concentrations were made using silica crucibles in the inert atmosphere induction furnace. Each fused silica crucible, 3 inches in diameter and 4-7/8 inches deep, was placed into the induction furnace in a bed of silica sand. Following the procedure of Kojima and Sano[73] who studied silica saturated slag - metal equilibria in the Fe-Cr-Si-O system, a graphite sleeve was fitted around the outside of the top two-thirds of the crucible. This sleeve served as a susceptor to heat the slag phase while the metal phase in the bottom part of the crucible was heated by self-induction. A run was made by charging a silica crucible with molybdenum powder and several pieces of Ferro-vac E iron to approximate the liquid metal composition. The

silica-saturated slag phase was approximated by charging mixed powders to SiO_2, Fe_2O_3, and Fe. After the charge was melted and the scheduled temperature was reached, the viscous slag phase was periodically agitated with an iron bar to encourage more rapid equilibration with the liquid metal. The liquid metal and slag were sampled after the hold time had elapsed and then a new time-temperature sequence was begun. Table V includes a schedule of the two significant runs made in this manner, Runs 68 and 69.

In this series of experiments, sampling of the liquid metal phase was performed by suction into Vycor tubing and water quenching. However, the silica-saturated slags could not be sampled in the same way because of their high viscosity. Instead, slag samples were obtained by scooping out a portion of this phase with a cold iron spoon and water quenching. The temperature of the melt was measured by a platinum, platinum-13% rhodium thermocouple in which the hot junction touched the outside of the bottom of the crucible at its center. The measured temperature during a run was estimated to be within 20 deg C of the scheduled temperature.

In Runs 68 and 69, difficulty was encountered in obtaining slag samples free of metallic inclusions. An alternative sampling technique was tried which did not require agitation of the phases during sampling. For this purpose, Runs 71 and 72 were made using 4-inch-long by 3/4-inch-i.d. fused silica bulbs open at the top. Each bulb was placed inside a tubular molybdenum holder and suspended in the inert atmosphere induction furnace in a manner similar to that used for molybdenum crucibles (page 23). Temperature was measured by wiring a tungsten, tungsten-26% rhenium thermocouple to the outside of the holder. A run was made by charging the desired powders into a silica bulb and equilibrating the system for the scheduled time and temperature. The bulb, holder, and thermocouple assembly were

then withdrawn from the top of the furnace and water-quenched. This technique did not completely remedy the problem of metallic inclusions in these highly viscous slags.

Analytical Procedure

Chemical analyses of the slag and metal samples were performed by the Ann Arbor Research Laboratory of the Climax Molybdenum Company of Michigan. The procedures followed in these analyses are outlined below. A more detailed description of the procedure for molybdenum determinations in these materials is available elsewhere.[74-76]

Metal samples were analyzed for molybdenum, silicon, and oxygen. After dissolution of each sample in acid and preparation of suitable aliquots, the molybdenum was determined by gravimetric precipitation with the reagent alpha benzoin oxime. Silicon was determined gravimetrically as SiO_2. The determination of oxygen was performed conductrimetrically using a barium hydroxide solution. Oxygen in the metal was reacted with carbon black to form CO, which is catalyzed to CO_2 and passed through the conductrimetric solution.

Slag samples were analyzed for molybdenum, total iron, and silica. The slags were fused with sodium carbonate and the silica determined gravimetrically. Slags containing greater than about 1% molybdenum were analyzed for molybdenum by the alpha benzoin oxime method. For molybdenum concentrations below about 1%, a colorimetric determination was followed in which the molybdenum is extracted in an organic solution and the color of the solution compared with standards using a spectrophotometer. Iron was determined by titration with a potassium dichromate standard solution.

Most chemical analyses were made by taking two aliquots of the master solution of the sample and running duplicate determinations. In some analyses, four determinations were made by preparing two master solutions

and making duplicate determinations on each solution. The average value of these determinations was taken as the best estimate of the true value. As a general rule, if the reported determination was greater than about 1 weight percent, the true value was considered to be within ±1% of the reported value. If the reported concentration was less than about 1 weight percent, an error of ±10% of the reported value was ascribed to it. An individual determination was generally repeated if it fell outside the estimated range of error applied to the average value of the determinations.

Metal and slag samples were also examined by conventional x-ray and metallographic techniques to identify the phases in the quenched samples. A second purpose of these examinations was to determine if it was reasonable to assume that the samples obtained for chemical analysis were actually single-phased at the equilibration temperature. For example, large spherical particles of metal in a slag sample, such as those shown in Figure 15, were assumed to have been present as inclusions in the liquid slag phase at the equilibration temperature. However, a small dendritic metallic particle in a slag sample, such as that shown in Figure 16, was assumed to have precipitated from solution in the liquid slag upon quenching. A chemical analysis of the oxide plus the metallic dendrites was assumed to be representative of the slag phase at the equilibration temperature.

Conventional x-ray powder diffraction techniques were followed using a General Electric XRD-5 diffractometer. Specimens were ground to -300 mesh and exposed to nickel-filtered copper radiation or, if iron fluoresence was intolerable, vanadium-filtered chromium radiation.

Mounted specimens were prepared for metallographic examination using standard polishing procedures with a final polish on a Syntron polishing machine using the proprietary Cer-Cre compound containing cerium oxide.

Slag specimens were examined unetched. A potassium ferricyanide + sodium hydroxide etch was used on iron-molybdenum and molybdenum metal samples.

An Applied Research Laboratories electron beam microanalyzer was used to examine a specimen obtained from Run 45. Because of operating difficulties with this newly installed instrument only qualitative results were obtained. However, these results were of considerable assistance in identifying the phases in this specimen and in similar specimens.

EXPERIMENTAL RESULTS

The experimental results of this investigation are presented as additional information pertaining to the Fe-Mo, Fe-Mo-O, and Fe-Mo-Si-O equilibrium phase diagrams. The thermochemical relationships developed from these results are presented in the discussion section of this report.

Results of Equilibrations in the Fe-Mo System

Runs 59 and 82 were made to determine the liquidus composition in the Fe-Mo system between 1550 and 1900 C. A second purpose of these experiments was to examine the feasibility of alternative methods of approaching the equilibrium liquidus composition and to design experiments in the Fe-Mo-O and Fe-Mo-Si-O systems accordingly. In Run 59, the liquidus composition was established by saturating a molybdenum-lean charge with molybdenum by partially dissolving the molybdenum crucible. In particular, the molybdenum content of the charge was less than the liquidus composition at 1550 C, the lowest temperature studied. When the molten charge was held at 1550 C the liquid became saturated with molybdenum by partial dissolution of the crucible. After the liquid metal was sampled, the temperature was increased, the liquid became further enriched with molybdenum, and another sample was taken. By using a molybdenum-lean charge and an increasing temperature series, it was possible to obtain samples of the liquid metal phase having the liquidus composition and no molybdenum-rich solid particles. Figure 17 shows a photomicrograph of one such metal sample, quenched from 1700 C. The angular, dendritic shape of the several etched phases in this microstructure suggest that they were formed on quenching. Figure 18 shows the interface between the interior wall of the molybdenum crucible and its contents after completion of this run. Table VI summarizes the chemical analyses of specimens from this run.

Table VI

Summary of Equilibrations in the Iron-Molybdenum System

Run	Sample	Time (hr)	Temperature (C)	Phases Present[a]	Analysis of Liquid Metal Phase[b] (Weight Percent)	
					Molybdenum	Iron[c]
59	1	1	1550	I	52.2 (38.9)[d]	47.8 (61.1)
	2	1	1600	I	55.9 (42.5)	44.1 (57.5)
	3	1	1700	I	62.1 (48.8)	37.9 (51.2)
	4	0.5	1800	I	63.0 (49.8)	37.0 (50.2)
	5	0.5	1900	I	68.3 (55.6)	31.7 (44.4)
82[e]	1	1	1700	II	--	--
	2	3.5	1700	II	--	--
	3	1	1600	II	--	--

[a] I = liquid Fe-Mo metal; solid Fe-Mo metal on wall of molybdenum crucible.
II = liquid Fe-Mo metal; solid Fe-Mo metal on wall of molybdenum crucible and dispersed as particles in liquid metal phase.

[b] Semiquantitative spectrographic analysis of three liquid metal samples (Samples 1, 2, and 3 of Run 59) showed the approximate impurity levels to be the same in each sample, i.e., 10 to 100 ppm Mn, ~10 ppm Mg, ~10 ppm V, ~100 ppm Cr, 100 to 1000 ppm Ni, ~100 ppm Ti, ~100 ppm Zr, <300 ppm W, 10 to 100 ppm Sn, and ~100 ppm Si.

[c] Obtained by difference.

[d] Figures in parentheses are values in atomic percent.

[e] Chemical analyses not obtained because of inadequate phase segregation.

An alternative approach, taken in Run 82, was to cool a molybdenum-rich charge to the equilibration temperature and to sample the liquid metal after holding at that temperature. It was assumed that the excess molybdenum had been deposited on the interior wall of the molybdenum crucible. This approach was considered to be unsuccessful because the molybdenum-rich solid particles remained in suspension in the liquid metal phase and

prevented obtaining a single phase sample of liquid metal for chemical analysis. Figure 19 is a photomicrograph of a sample quenched from 1700 C containing large, spherical molybdenum-rich particles. The details of this run are also summarized in Table VI.

The results of molybdenum-saturated equilibrations in the Fe-Mo system indicate that the most satisfactory experimental approach to equilibrium is from the molybdenum-lean, low-temperature side. This approach produces a liquid metal phase free of molybdenum-rich solid particles, a necessary requirement for interpretation of results from wet chemical analyses. This approach to equilibrium was followed in the majority of the molybdenum-saturated equilibrations in the Fe-Mo-O and Fe-Mo-Si-O systems. However, additional experiments were performed to approach equilibrium from other directions in these systems. The results and discussion on the ternary and quaternary systems are presented below.

Results of Equilibrations in the Fe-Mo-O System

The primary purpose of the equilibrations which were made in the Fe-Mo-O system was to develop a partial 1600 C isothermal section through the ternary phase diagram. Of particular interest in this isothermal section was the location of the liquid oxide corner, i.e., the composition of the oxide phase of the oxide(ℓ) + metal(ℓ) + metal(s) three-phase region. This corner is identified as point A in Figure 20. The position of this isothermally invariant point over the temperature range 1600 to 1800 C was also determined. A summary of the equilibrations made in this system is given in Table VII.

For the 1600 C isotherm, samples were prepared to lie in the oxide(ℓ) + metal(ℓ) + metal(s), the oxide(ℓ) + MoO_2(s), and the metal(s) + oxide(ℓ) regions, as shown in Figure 20. The approximate width of the two-phase metal(s) + oxide (ℓ) region was determined by preparing samples in the two adjoining three-phase regions to establish the corners of these regions.

Table VII

Summary of Equilibrations in the Fe-Mo-O System

Run	Sample	Time (hr)	Temperature (C)	Phases Present[a]	Analysis of Liquid Metal Phase[b] (Weight Percent)			Analysis of Liquid Oxide Phase (Weight Percent)		
					Mo	Fe[c]	Si	Mo	Fe	O[c]
42[d]	--	3	1600	I	--	--	NA[e]	--	--	--
44	--	12	1600	II	--	--	NA	NA	NA	NA
45	--	7	1600	II	--	--	NA	NA	NA	NA
48	--	5	1600	II	--	--	NA	NA	NA	NA
50	--	4.5	1600	III	--	--	NA	34.0 (13.3)[f]	40.7 (27.4)	25.3 (59.3)
51	--	4.5	1600	II	--	--	NA	NA	NA	NA
52	--	4.5	1600	II	--	--	NA	NA	NA	NA
55[g]	1	1	1600	IV	52.1 (38.8)	47.9 (61.2)	0.02 --	16.5 (6.0)	56.5 (35.2)	27.0 (58.8)
	2	2	1600	IV	55.0 (41.6)	45.0 (58.4)	0.03 --	16.8 (6.1)	56.3 (35.2)	26.9 (58.7)
	3	3	1600	IV	55.2 (41.8)	44.8 (58.2)	0.04 --	17.1 (6.2)	55.7 (34.7)	27.2 (59.1)
	4	1	1700	IV	56.8 (43.3)	43.2 (56.7)	0.02 --	19.9 (7.2)	52.2 (32.4)	27.9 (60.4)
	6	0.25	1800	IV	61.9 (48.6)	38.1 (51.4)	0.10 --	24.4 (8.9)	47.7 (29.9)	27.9 (61.1)
83	1	2.5	1600	IV	NA	NA	NA	19.7 (7.6)	56.4 (37.3)	23.9 (55.1)
	2	2.5	1700	IV	NA	NA	NA	19.8 (7.5)	55.2 (35.8)	25.0 (56.7)

[a] I = Solid MoO_2, solid molybdenum as crucible and dispersed as particles.
II = Solid MoO_2, liquid oxide, solid Fe-Mo on wall of molybdenum crucible and dispersed as particles.
III = Liquid oxide, solid Fe-Mo metal on wall of molybdenum crucible.
IV = Liquid oxide, liquid metal, solid Fe-Mo metal on wall of molybdenum crucible.

[b] Oxygen concentration of the liquid metal phase was not determined, but was assumed to be small.

[c] Determined by difference.

[d] This run is in the molybdenum-oxygen binary system.

[e] NA = Not analyzed.

[f] Figures in parentheses are values in atomic percent.

[g] In this run, the silica pickup in the slags is a measure of contamination by Vycor sampling tubes.

For the three-phase region, oxide(ℓ) + MoO_2(s) + metal(s), Runs 42, 44, 45, and 48 represent a series of increasing iron additions starting from the Mo-O binary. The phases were not sufficiently segregated in

these samples to be separated for wet chemical analysis; metallographic and x-ray examination were used to determine if it was reasonable to conclude that the samples were, in fact, in the three-phase region at temperature as pictured. The microstructure of one such sample (Run 45) is shown in Figure 21. The phases are identified as a molybdenum-rich metal phase and an MoO_2 phase, both solid at 1600 C, and an iron-molybdenum oxide matrix phase, which was liquid at 1600 C. Examination of this sample with an electron beam microanalyzer confirmed the identity of the phases. The charge compositions for Runs 50, 51, and 52 placed these samples in the single-phase liquid oxide region. However, by reaction with the interior of the molybdenum capsules these charges became saturated with molybdenum. An examination of samples from Runs 51 and 52 placed the contents of these capsules in the three-phase oxide(ℓ) + MoO_2(s) + metal(s) region. A representative microstructure of these samples is shown in Figure 22 as the sample from Run 52.

One run (50) was made in the two-phase metal(s) + oxide(ℓ) region. No MoO_2 solid phase was observed in a quenched sample, nor was there a metal phase that could be considered liquid at temperature. A photomicrograph of this sample (Run 50) is shown in Figure 23. The walls of the molybdenum capsule in contact with the oxide phase represent the composition of the solid metal phase in equilibrium with the oxide at 1600 C. The oxide phase was separated from the capsule and submitted to chemical analysis, the results of which are given in Table VII. These results aided in the placement of the phase boundary between the single phase oxide(ℓ) and the two phase oxide(ℓ) + metal(s) regions.

The three-phase metal(s) + metal(ℓ) + oxide(ℓ) region of the isothermal section was examined in Runs 55 and 83. The results are shown schematically in Figure 24. The charge in Run 55 placed the contents of the molybdenum

crucible in the two-phase metal(ℓ) + oxide(ℓ) region. By partial dissolution of the crucible, each phase became saturated with molybdenum at the equilibration temperature. Liquid metal and liquid oxide samples were taken at 1600, 1700, and 1800 C. The results of chemical analyses of these samples are included in Table VII and illustrated in Figure 24, which shows that the three-phase triangle shifts toward the molybdenum corner of the diagram with increasing temperature. Run 83 was made using a different approach to the equilibrium position of Run 55. In Run 55, no molybdenum was charged as oxide, whereas all the oxide charged in Run 83 was MoO_2. Therefore, in Run 55 the equilibrium molybdenum content of the liquid oxide was approached from the iron-rich, molybdenum-lean side and in Run 83 the approach was from the iron-lean, molybdenum-rich side. The results of chemical analyses on the oxide phase of samples from Run 83 are included in Table VII and Figure 24. These results show the liquid oxide phase to be slightly higher in molybdenum and iron in Run 83 than in Run 55. An average of the 1600 and 1700 C values obtained from each run was taken as the best estimate of the true value. In addition to the reasonably good agreement in chemical analysis of the oxide phase resulting from these two approaches to equilibrium, the microstructures and x-ray diffraction patterns of the quenched specimens are also in agreement. The microstructures of the oxide phase of Samples 55-3 and 83-1, both quenched from 1600 C, are shown in Figures 16 and 25, respectively. These microstructures are representative of the other oxide samples obtained in these two runs. The phases in these microstructures were identified by x-ray diffraction as FeO and Fe_2MoO_4 (or, $2FeO{\cdot}MoO_2$). The presence of FeO and Fe_2MoO_4 in these samples suggests that at the equilibration temperature the liquid oxide phase contained iron and molybdenum primarily as the lower valence species Fe^{+2} and Mo^{+4}.

The x-ray diffraction pattern of Fe_2MoO_4 obtained in the samples above is in agreement with studies on this compound made by Rahmel et al.,[77] Jäger et al.,[50] and Kozmanov et al.[60] The pattern is very similar to that of Fe_3O_4. The lattice of Fe_2MoO_4 is of the spinel type (a = 8.45 A), and is slightly expanded over that of Fe_3O_4 (a = 8.396 A). The 2θ diffraction angles of Fe_2MoO_4 are about 1 degree smaller than those of Fe_3O_4. Fe_2MoO_4 was also found in the quenched oxide specimens, liquid at temperature, which were obtained in the previously described studies on the three-phase metal(s) + MoO_2(s) + oxide(ℓ) and the two-phase metal(s) + oxide(ℓ) regions.

Figure 26 presents a 1600 C isothermal section through the Fe-Mo-O diagram using the data of this investigation. The liquid oxide corner of the metal(s) + metal(ℓ) + oxide(ℓ) three-phase region is placed at 6.9 atomic percent molybdenum, 36.0 atomic percent iron, and balance oxygen. The position of this corner changes to 7.4 atomic percent molybdenum, 34.1 atomic percent iron, and balance oxygen at 1700 C and 8.9 atomic percent molybdenum, 29.9 atomic percent iron, and balance oxygen at 1800 C. The liquid oxide corner of the metal(s) + MoO_2(s) + oxide(ℓ) three-phase region is placed at 15.0 atomic percent molybdenum, 26.0 atomic percent iron, and balance oxygen at 1600 C. Within the errors of this investigation the compositions of the metallic phases are those of the binary Fe-Mo system shown in Figure 27.

Results of Equilibrations in the Fe-Mo-Si-O System

The purpose of equilibrations in the Fe-Mo-Si-O system was to determine the effect of silica on the molybdenum content of liquid slag in equilibrium with liquid metal. The system was studied as a function of temperature under three conditions:

1. The system was molybdenum-saturated and the silica content of the liquid slag was varied.

2. The system was silica-saturated and the molybdenum content of the liquid metal was varied.

3. The system was silica-saturated and molybdenum-saturated.

Table VIII summarizes the equilibrations made in this quaternary system.

Table VIII

Summary of Equilibrations in the Fe-Mo-Si-O System

Run	Sample	Time (hr)	Temperature (C)	Phases Present[a]	Analysis of Liquid Metal Phase[b] (Weight Percent)				Analysis of Liquid Oxide Phase (Weight Percent)			
					Mo	Fe[c]	Si	O	Mo	Fe	Si	O[c]
Molybdenum Saturation												
56	1	1	1600	I	50.5 (37.0)[e]	49.2 (61.9)	NA[d] (NA)	0.26 (1.1)	11.3 (4.1)	60.6 (37.5)	2.5 (3.1)	25.6 (55.3)
	2	1	1700	I	57.1 (43.7)	42.9 (56.3)	NA (NA)	NA (NA)	14.4 (5.2)	56.7 (35.1)	3.0 (3.7)	25.9 (56.0)
	5	0.25	1800	I	63.1 (49.9)	36.9 (50.1)	NA (NA)	NA (NA)	18.0 (6.7)	54.3 (34.5)	2.7 (3.4)	25.0 (55.4)
57	1	1	1600	I	51.7 (38.1)	48.1 (60.9)	NA (NA)	0.22 (1.0)	6.0 (2.0)	58.8 (33.6)	6.7 (7.6)	28.5 (56.8)
	2	1	1700	I	56.4 (43.0)	43.6 (57.0)	NA (NA)	NA (NA)	6.9 (2.3)	57.6 (33.5)	6.7 (7.8)	27.8 (56.4)
	4	0.25	1800	I	62.8 (49.6)	37.2 (50.4)	NA (NA)	NA (NA)	8.4 (2.8)	53.6 (30.0)	8.3 (9.2)	29.7 (58.0)
58	1	1	1600	I	54.6 (41.0)	45.2 (58.2)	NA (NA)	0.17 (0.8)	1.3 (0.39)	50.0 (25.2)	15.1 (15.2)	33.6 (59.2)
	2	1	1700	I	62.2 (48.9)	37.8 (51.1)	NA (NA)	NA (NA)	2.1 (0.62)	48.7 (24.5)	15.5 (15.5)	33.7 (59.3)
	3	0.5	1800	I	62.8 (49.6)	37.2 (50.4)	NA (NA)	NA (NA)	2.4 (0.69)	46.7 (23.2)	16.3 (16.1)	34.6 (60.0)
	4	0.25	1900	I	67.4 (54.6)	32.6 (45.4)	NA (NA)	NA (NA)	1.9 (0.53)	41.5 (19.7)	19.7 (18.6)	36.9 (61.2)
84	1	2.5	1600	I	NA NA	NA NA	NA (NA)	NA (NA)	12.6 (4.5)	59.0 (36.6)	2.9 (3.6)	25.5 (55.2)
	2	2.5	1700	I	61.2 (47.8)	38.8 (52.2)	NA (NA)	NA (NA)	15.4 (5.6)	55.6 (34.6)	3.5 (4.4)	25.5 (55.4)

[a] I = Liquid oxide, liquid metal, solid Fe-Mo metal on wall of molybdenum crucible.
II = Liquid oxide, liquid metal, solid silica as crucible.
III = Liquid oxide, liquid metal, solid silica, solid Fe-Mo metal on wall of molybdenum crucible.
IV = Liquid oxide, liquid metal, liquid silica, solid Fe-Mo metal on wall of molybdenum crucible.

[b] Oxygen and silicon concentrations of the liquid metal phase were not usually determined but were assumed to be small.

[c] Determined by difference.

[d] NA = Not analyzed.

[e] Figures in parentheses are values in atomic percent.

Table VIII (Continued)

Summary of Equilibrations in the Fe-Mo-Si-O System

Run	Sample	Time (hr)	Temperature (C)	Phases Present[a]	Analysis of Liquid Metal Phase[b] (Weight Percent)				Analysis of Liquid Oxide Phase (Weight Percent)			
					Mo	Fe[c]	Si	O	Mo	Fe	Si	O[c]
Silica Saturation												
68	1	1	1550	II	14.4 (8.9)	85.6 (91.1)	NA (NA)	NA (NA)	0.110 (0.027)	33.5 (14.8)	25.5 (22.3)	40.9 (62.9)
	2	1	1600	II	13.8 (8.5)	86.2 (91.4)	NA (NA)	NA (NA)	0.043 (0.011)	31.0 (13.4)	26.8 (23.0)	42.2 (63.6)
	3	1	1650	II	13.6 (8.4)	86.4 (91.6)	NA (NA)	NA (NA)	0.029 (0.007)	34.0 (15.0)	25.1 (22.0)	40.9 (63.0)
69	1	1	1550	II	33.7 (22.8)	66.3 (77.2)	NA (NA)	NA (NA)	0.069 (0.018)	34.2 (15.1)	25.1 (22.1)	40.6 (62.8)
	2	1	1600	II	33.5 (22.7)	66.5 (77.3)	NA (NA)	NA (NA)	0.062 (0.016)	34.5 (15.4)	25.4 (22.5)	40.0 (62.2)
	3	1	1650	II	33.4 (22.6)	66.6 (77.4)	NA (NA)	NA (NA)	0.047 (0.012)	30.9 (13.4)	27.1 (23.3)	42.0 (63.3)
71	--	2	1550	II	36.6 (25.2)	63.4 (74.8)	NA (NA)	NA (NA)	0.15 (0.04)	36.6 (16.5)	24.0 (21.6)	39.2 (61.9)
72	--	2	1600	II	37.8 (26.1)	62.2 (73.9)	NA (NA)	NA (NA)	0.15 (0.04)	35.5 (15.8)	23.9 (21.2)	40.4 (63.0)
Molybdenum and Silica Saturation												
74	--	2	1600	III	54.2 (40.8)	45.7 (59.1)	0.044 (0.11)	NA (NA)	0.56 (0.15)	35.5 (16.0)	24.5 (21.9)	39.4 (62.0)
75[f]	--	2	1800	IV	64.4 (51.3)	35.5 (48.6)	0.042 (0.11)	NA (NA)	0.28 (0.07)	30.0 (13.0)	28.0 (24.1)	41.7 (62.9)
76[g]	--	2	1900	IV	72.0 (59.9)	28.0 (40.0)	0.026 (0.07)	NA (NA)	0.35 (0.09)	28.1 (12.0)	29.3 (24.9)	42.2 (63.0)
78[h]	--	2	1750	IV	61.2 (47.9)	38.7 (52.1)	0.007 (0.02)	NA (NA)	0.24 (0.06)	28.5 (12.1)	27.6 (23.3)	43.7 (64.6)
80	--	2	1650	III	56.8 (43.4)	43.1 (56.5)	0.065 (0.17)	NA (NA)	0.29 (0.08)	34.5 (15.4)	25.4 (22.5)	39.8 (62.0)
81[i]	--	7	1550	III	NA	NA	NA	NA	NA	NA	NA	NA

[f] The liquid silica phase contained 0.44 weight percent molybdenum and 0.23 weight percent iron.

[g] The liquid silica phase contained 0.41 weight percent molybdenum and 0.15 weight percent iron.

[h] The liquid silica phase contained 0.14 weight percent molybdenum and 0.22 weight percent iron.

[i] No chemical analysis was obtained because of inadequate phase segregation.

Runs 56, 57, 58, and 84 represent the molybdenum-saturated experiments below silica saturation. These samples contained various silica concentrations in the slag phase. The experimental runs were made in a manner similar to Run 55 (page 20). Molybdenum-lean, iron-rich charges were melted in molybdenum crucibles and the phases saturated with molybdenum by partial dissolution of the crucible. Whereas the charge in Runs 56, 57, and 58 contained no molybdenum as oxide, that of Run 84 contained no iron as oxide so that the equilibrium molybdenum concentration of the slag phase could be approached from the molybdenum-lean and molybdenum-rich sides. The agreement between the two approaches to the equilibrium molybdenum content of the slag phase is considered satisfactory. The results of these experiments are shown in Figures 28 and 29 where the molybdenum content in the liquid slag phase is plotted as a function of the silicon content in the slag at several equilibration temperatures. Figure 30 shows the variation of iron concentration in these slags with the silicon concentration in the slag. The effect of silica additions on the molybdenum content of the slag may be visualized as movement of the oxide(ℓ) corner of the three-phase metal(s) + metal(ℓ) + oxide(ℓ) region in the Fe-Mo-O system toward the Fe-Si-O side of the isothermal tetrahedron in the Fe-Mo-Si-O quaternary system. Figures 28 and 29 indicate that the concentration of the liquid oxide phase is lowered by relatively low silica additions. This behavior implies that the line representing the composition of this phase in the isothermal tetrahedron may be drawn from the Fe-Mo-O face to almost touch the Fe-Si-O face at low silicon concentrations.

Representative microstructures of the quenched oxide phase, liquid at temperature, are shown in Figures 31, 32, and 33. As confirmed by x-ray diffraction analyses, the addition of silica to this phase caused

an increasing amount of fayalite, $2FeO \cdot SiO_2$, to be found upon solidification. The oxide phase of Sample 84-1, having 6.2 weight percent SiO_2, was composed of FeO, Fe_2MoO_4, and Fe_2SiO_4. At higher silica concentrations such as that of Sample 58-1 (32.3 weight percent SiO_2) fayalite predominated the microstructure and no other phase was detected by x-ray diffraction.

Table VIII presents the results of experimental runs made at 1550, 1600, and 1650 C in silica crucibles for silica saturation and several molybdenum concentrations. In Figure 34 the molybdenum concentration of the liquid slag phase is plotted as a function of the molybdenum concentration of the liquid metal phase with which it was equilibrated. These data do not correlate well, although the expected trend of a decreasing molybdenum concentration in the slag phase with decreasing molybdenum content of the metal phase is evident. The failure of these data to be better correlated is attributed to the entrapment of small metallic prills in the highly viscous, silica-saturated slag phase. Although efforts were made to obtain a satisfactory phase separation during equilibration and to mechanically remove the prills before submitting the slags to chemical analysis, it is believed that enough metal remained in these samples to mask the relatively low concentration of molybdenum as oxide. The expected trend of increasing molybdenum concentration in the slag with increasing temperature is not evident because of the metal prill retention of the more viscous slags at lower temperatures. A representative photomicrograph of these slags is shown in Figure 15 as Sample 68-2. The microstructure contained fayalite, cristobalite, and small spherical metallic inclusions.

Despite the problem of obtaining satisfactory samples for chemical analysis, this series of experiments is considered to be significant because

it offers some insight into the extent of stability of metallic prills in these viscous slags. The retention of metallic prills in the liquid slag is an important problem in the production of ferromolybdenum by the thermite process and the relationship of these experiments to the process is discussed later in this report.

The results of experiments at both silica and molybdenum saturation are also included in Table VIII. These results are shown graphically as the silica saturated end points of Figures 28, 29, and 30 and the molybdenum-saturated end points of Figure 34. The slag specimens at 1600 and 1650 C contained metallic inclusions similar to those in the silica-saturated specimens previously described. The inconsistency of these two points with the rest of the data is attributed to the presence of these inclusions. At 1750, 1800, and 1900 C the slag was considerably less viscous and much lower in metallic inclusions. These higher temperature data correlate well with the balance of the data obtained in this investigation at lower silica concentrations. The microstructures of slag specimens obtained in this series of experimental runs were similar to that of Sample 68-2 shown in Figure 15.

In the 1750, 1800, and 1900 C molybdenum-saturated, silica-saturated runs (75, 76, and 78), three liquid phases were present at temperature: liquid slag, liquid metal, and liquid silica. The liquid silica phase was analyzed for iron and molybdenum, the results being shown as a footnote to Table VIII. These few data indicate that the molybdenum and iron contents of this phase are low, as anticipated. However, the change of concentration of these elements with temperature is not clearly evident.

Results of Equilibrations with a Synthetic Commercial Slag

One experimental run was made to equilibrate liquid ferromolybdenum with a synthetic commercial slag in a molybdenum crucible. This run was

made to approximate more closely the slag-metal compositions occurring in ferromolybdenum production by including CaO and Al_2O_3 in the slag phase. The results of this run (85) are shown in Table IX. In contrast to the silica-saturated Fe-Mo-Si-O specimens obtained at temperatures below 1700 C, relatively few metallic inclusions were present in quenched specimens of the liquid slag phase in Run 85. This lower inclusion content was attributed to a somewhat lower slag viscosity caused by the calcium oxide additions. The molybdenum analysis of the slag phase in Samples 85-1 and 85-2 was believed to represent primarily molybdenum as oxide.

Table IX

Summary of Equilibrations Using a Synthetic Commercial Slag (Run 85)

Sample	Time (hr)	Temperature (C)	Phases Present[a]	Analysis of Liquid Metal Phase (Weight Percent)		Analysis of Liquid Oxide Phase[b] (Weight Percent)
				Mo	Fe[c]	Mo
1	2.5	1600	I	57.7 (44.3)[d]	42.3 (55.7)	0.17
2	2.5	1700	I	61.1 (47.7)	38.9 (52.3)	0.22

[a] I = liquid oxide; liquid metal; solid Fe-Mo metal on wall of molybdenum crucible.

[b] Slag composition estimated by charge composition as approximately 66 weight percent SiO_2, 17.5 weight percent Al_2O_3, 13.5 weight percent FeO, and 3.0 weight percent CaO.

[c] Obtained by difference.

[d] Figures in parentheses are values in atomic percent.

DISCUSSION OF EXPERIMENTAL RESULTS

The discussion of the experimental results of this investigation is presented as (1) an evaluation of the experimental technique and accuracy of the results, (2) thermochemical relationships derivable from the results and the literature, and (3) the pertinence of the results to the commercial production of ferromolybdenum.

Analysis of Experimental Technique

The experimental approach used in this investigation was selected, primarily, by experimental limitations rather than by choosing the best of several possible techniques. In particular, two limitations were determinant in the type of experiment that could be performed:

1. The crucible material should not contaminate the system under study.
2. Samples for wet chemical analysis should be single-phased at the equilibration temperature if an interpretation was to be made of the data.

No known crucible material is inert to molten iron oxide and iron-molybdenum oxides. To circumvent the crucible problem two techniques were used to prepare the melts:

1. Melts were made in crucibles of one of the materials under study (molybdenum or silica) and thus the phases were saturated with that material.
2. Melts were held in a rotating crucible described in Appendix B.

Although these experimental limitations restricted the scope of the investigation, it was fortunate that the experiments conducted were also of particular interest to ferromolybdenum production: Restricting the study to the molybdenum-saturated and silica-saturated samples did not destroy the usefulness of the study because ferromolybdenum is almost

molybdenum-saturated at the temperatures of interest and ferromolybdenum slags are silica-saturated.

Although the magnitude of error attributable to a given measurement in this study was difficult to determine accurately, the sources, approximate magnitudes, and relative importance of possible deviations from the unknown true values were considered. Of primary concern to this study were errors originating from the following causes:

1. the extent to which equilibrium was approached,
2. the accuracy of temperature measurement and control,
3. the extent of impurity contamination, and
4. the extent to which samples for chemical analysis were single-phased at the equilibration temperature.

With respect to the attainment of equilibrium, experimental checks were made to approach several isothermally invariant compositions from opposite directions. For example, experimental runs were made in the Fe-Mo-O and Fe-Mo-Si-O systems to approach the equilibrium molybdenum content of the liquid slag phase from the molybdenum-rich and molybdenum-lean sides. Thus, in the ternary system, a concentration of 19.7 weight percent molybdenum was determined after a charge in which the initial oxide content was 75.0 weight percent molybdenum (Sample 83-1) was equilibrated at 1600 C for 2-1/2 hours. The same invariant point was approached starting with no molybdenum as oxide in the charge and obtaining 17.1 weight percent molybdenum after equilibration at 1600 C for three hours (Sample 55-3). Although longer holding times at temperature would probably produce closer agreement, an average value of these two determinations was accepted as reasonably accurate. Duplicate determinations such as these were not made for every data point; however, it would be reasonable to assume that such determinations would yield results in which the extent of agreement was

similar. Based on kinetic arguments, the equilibrations at higher temperatures, such as those made at 1700 and 1800 C, would be expected to approach the true invariant compositions more rapidly. A second means of examining the extent to which equilibrium was attained is to compare experimental values with those published by other investigators. Although an invariant equilibrium composition is reproducible, the agreement, per se, of experimental and literature values does not ensure that equilibrium was actually attained in both investigations. Unfortunately, no literature values were available with which to contrast the results of the phase diagram studies in this investigation.

Errors in the measurement and control of temperature were considered in the design and evaluation of experiments in this study. Since the experiments were to be conducted by equilibration at constant elevated temperatures, a furnace was designed and constructed to provide as uniform a hot zone and as constant a temperature as was experimentally feasible. With this goal, the furnace was extensively insulated and molybdenum baffles and susceptors were used to reduce thermal gradients in the hot zone. The temperature of the hot zone was continuously monitored during a run to detect and correct for any fluctuations with time. New tungsten, tungsten-26% rhenium thermocouples, calibrated by the manufacturer, were installed for every run and were replaced during a run if deterioration was suspected. As a result of these efforts the temperature of the crucible and melt was considered to be within 20 deg C of the scheduled temperature throughout an isothermal hold. Because the system being equilibrated was thought to react rather sluggishly to small temperature fluctuations, the average temperature during a hold was used as the equilibration temperature rather than the temperature at the moment of sampling, which might have been slightly different. Even though better temperature control

might have been desirable, the accumulation of a volume of data over a comparatively large temperature range assisted in minimizing the effects of small, random temperature errors in individual measurements.

Errors attributable to impurity contamination were reduced by attempting to minimize the concentration of impurities in the system. Thus, efforts were made to use high-purity materials in these experiments and to prevent contamination of the melt during a run. Spectrographic analyses (Table VI) were made on one series of metal samples, liquid at temperature, to determine the approximate concentrations of trace elements and if any large impurity pickup was obtained during the run. These results showed no detectable change in trace element concentration with equilibration temperature or time at temperature. These considerations suggest that errors resulting from the presence of impurity elements were maintained relatively small.

The accuracy of the chemical analyses, as discussed on page 28, was considered to be excellent and the resulting errors relatively negligible. However, a major problem in this study was obtaining specimens for chemical analysis that were single-phased at the equilibration temperature. Thus, an error in the interpretation of the chemical analysis of a slag sample would result if the slag contained metallic inclusions at the equilibration temperature and these inclusions were included in the sample to be analyzed. The problem of metallic inclusions in slag samples became more critical in slags having a high-silica concentration for two reasons:

1. The viscosity of these slags was much higher and reduced the rate of gravitational separation of the liquid slag and liquid metal phases.
2. The molybdenum content of these slags was relatively low and the inclusion of a few molybdenum-rich metal particles

could cause a proportionally large error in the analysis for molybdenum in slag.

To reduce errors of this type sampling of the liquids was carefully performed to minimize agitation and mixing of the phases. All the quenched samples were examined metallographically before chemical analysis to determine if it was reasonable to assume that they were single-phased at temperature. This type of error was considered to be acceptably small in all the reported analyses except those on slag specimens obtained at both silica saturation and temperatures of 1550 to 1650 C. For the latter specimens, the results were generally scattered and inconsistent and preference was given to extrapolation of data obtained at lower silica contents and higher temperatures.

As a consequence of the errors discussed above, the experimental techniques of this investigation were not considered sufficiently accurate to determine the minor effects of small amounts of dissolved oxygen and silicon on the liquidus composition of the Fe-Mo binary system. Thus, chemical analyses of the molybdenum-saturated metal phase, liquid at temperature, which was obtained from equilibrations in the Fe-Mo-O and Fe-Mo-Si-O systems were considered to be statistically identical to those obtained in the binary system. Data from all three systems were used to obtain a statistically better estimate of the true liquidus values at the temperatures studied. The experimental liquidus values obtained in this manner are tabulated in Table X and shown graphically in the binary phase diagram in Figure 27, which also shows the hypothetical curve of Hansen.[29]

Thermochemical Relationships

One purpose of the present investigation was to determine the equilibrium partitioning of molybdenum between liquid slag and liquid metal as a function of temperature and slag-metal composition. The partitioning

Table X

Best Estimate of Liquidus Composition in the Fe-Mo System Using Data from Fe-Mo, Fe-Mo-O, and Fe-Mo-Si-O Equilibrations

Temperature (C)	Number of Data Points	Molybdenum (Atomic Percent)	Standard Deviation
1550	1	38.9	--[a]
1600	7	40.8	2.3
1650	1	43.4	--[a]
1700	7	46.2	2.5
1750	1	47.9	--[a]
1800	6	49.8	0.8
1900	3	56.7	2.3

[a] Insufficient data points for statistical analysis.

of molybdenum is conveniently described by means of the partition coefficient, or distribution coefficient. This coefficient is defined as the weight ratio of the molybdenum in the slag phase to the molybdenum in the metal phase. The empirical relationship between the partition coefficient and the equilibration temperature at several silica concentrations in the slag phase is illustrated in Figure 35 for molybdenum saturation. Figure 35 was prepared using the best correlations of the experimental data as shown in Table X and Figure 29. The partition coefficient of molybdenum decreased with increasing silica content of the slag phase and with decreasing temperature, the dependency of temperature becoming less at higher silica concentrations.

The physical nature of liquid slags is not completely known, and various molecular and ionic theories have been advanced to describe slag behavior. A review of these theories is presented by Ward.[78] A molecular model has been successfully used to describe slag-metal interactions in a number of classic investigations, such as those of Chipman et al.,[79] Taylor et al.,[80] and Winkler et al.[81] Although a slag model based on various molecular species is an oversimplification and slags are ionic,

one must agree with Winkler and Chipman[82]:

> Probably the most easily visualized, most widely and easily used hypothesis for the constitution of liquid slag, particularly where thermodynamic calculations are employed, assumes that the oxide components of the slags form more or less stable chemical compounds somewhat similar to the combinations that appear in the same slags in the solid state. Even though no definite compounds may form in the liquid state, the assumption at least affords a logical pattern for the attraction between the slag components that must exist in order to account for the slag-metal reactions in any metallurgical refining process.....This does not mean that the authors believe that such chemical species necessarily exist; The immediate usefulness of the assumption is not dependent on its ultimate truth.

A molecular model may be used to represent the equilibria studied in this investigation. FeO, MoO_2, and SiO_2 were selected as the slag species, based on the presence of FeO, Fe_2MoO_4 (or $2FeO \cdot MoO_2$), Fe_2SiO_4, and SiO_2 in the various quenched samples of this study. The equilibrium reaction under consideration can be represented as follows:

$$2FeO\ (\text{in slag}) + Mo\ (\text{in metal}) = MoO_2\ (\text{in slag}) + 2Fe\ (\text{in metal}) \quad (13)$$

where the equilibrium constant can be written as

$$K_{eq.} = (a_{Fe}^2\ a_{MoO_2})/(a_{FeO}^2\ a_{Mo}) \quad (14)$$

where a_{MoO_2}, a_{FeO} = activities of components in the liquid slag phase,

and a_{Fe} and a_{Mo} = activities of components in the liquid metal phase.

The standard free energy change and equilibrium constant as a function of temperature for Equation (13) may be estimated from the published data summarized in Table XI. The standard states were taken as the pure substances at the temperature of interest. With reference to Table XI, the free energies of formation of MoO_2(s) and FeO(ℓ) were obtained from Elliott et al.[83] The free energy as a function of temperature for the fusion of molybdenum was calculated from the enthalpy of fusion and melting point as tabulated by Kubaschewski et al.[84] The free energy of fusion of MoO_2 as a function of temperature is not known. It was estimated using

Table XI

Gibbs Free Energy Data for the Fe-Mo-O System at 1873, 1973, and 2073 K

Reaction	Function (cal)	Temperature (K)			Reference
		1873	1973	2073	
$Mo(s) + O_2(g) = MoO_2(s)$	$\Delta F°$	-66,800	-63,380	-59,970	Elliott et al.[a]
$Fe(\ell) + \frac{1}{2}O_2(g) = FeO(\ell)$	$\Delta F°$	-34,760	-33,580	-32,400	Elliott et al.[a]
$Mo(s) = Mo(\ell)$	$\Delta F°$	+2,330	+2,100	+1,870	$\Delta H°$ and $T_{m.p.}$ from Kubaschewski et al.[b]
$MoO_2(s) = MoO_2(\ell)$	$\Delta F°$	+4,680	+3,930	+3,190	Data unavailable. Estimated from data for WO_2 of Wicks and Block[c,d] using procedure of Chipman et al.[e]
2FeO (in slag) + Mo = MoO_2 (in slag) + 2Fe	$\Delta F°$ $K_{eq.}$	+5,070 0.256	+5,610 0.239	+6,150 0.225	Calculated Calculated

[a] J. F. Elliott, M. Gleiser, and V. Ramakrishna, Thermochemistry for Steelmaking, vol. II, Addison-Wesley, Reading, Massachusetts, 1963, pp. 619-620.

[b] O. Kubaschewski, E. LL. Evans, and C. B. Alcock, Metallurgical Thermochemistry, fourth edition, Pergamon Press, New York, 1967, p. 376.

[c] C. E. Wicks and F. E. Block, "Thermodynamic Properties of 65 Elements--Their Oxides, Halides, Carbides, and Nitrides," U.S. Bureau of Mines Bulletin 605 (1963), 125.

[d] Reference c, p. 79.

[e] J. Chipman, J. B. Gero, and T. B. Winkler, "The Manganese Equilibrium," AIME Trans. 188 (1950), 344.

the procedure of Chipman et al.,[85] who assumed that the heats of formation of similar substances were proportional to their melting points. By using data for the similar compound WO_2 to estimate the heat of fusion of MoO_2, the heat of fusion and melting point of WO_2 were obtained from Wicks and Block[86] as 11,500 cal/mole and 1543 K, respectively. The melting temperature of MoO_2 is unknown, but was estimated as 2500 K after Wicks and Block.[40] The heat of fusion of MoO_2 was then estimated as 18,600 cal/mole. The values for ΔF° and $K_{eq.}$ for Equation (13) were calculated from these data within the temperature range studied:

$$\Delta F^\circ = -4970 + 5.36\ T \tag{15}$$

$$\log K_{eq.} = (1086/T) - 1.17 \tag{16}$$

An estimate of the equilibrium constant can be obtained from the results of this investigation and compared with that calculated from literature data. Experimental values of the activities of the components can not be calculated from the results of this study. However, if it is assumed that the liquid metal and liquid slag phases behave as ideal solutions to a first approximation, the mole fractions of the components may be used as an estimate of their activities. The assumption of the ideality of the liquid iron-molybdenum metal phase is considered reasonable and has been made by other authors such as Chipman.[87] Any deviation from Raoult's law in this system would be expected to be in the negative direction because of chemical attraction between these elements as evidenced by the intermetallic compounds existing at lower temperatures. The experimental equilibrium constant is defined as

$$K'_{eq.} = (X^2_{Fe}\ X_{MoO_2})/(X^2_{FeO}\ X_{Mo}) \tag{17}$$

where X_{FeO} and X_{MoO_2} = the mole fractions of the components in the liquid slag phase,

and X_{Fe} and X_{Mo} = the atomic fractions of the respective elements in the liquid metal phase.

The relationship between $K_{eq.}$ and $K'_{eq.}$ is given by

$$K_{eq.} = K'_{eq.} \left[(\gamma^2_{Fe} \ \gamma_{MoO_2}) / (\gamma^2_{FeO} \ \gamma_{Mo}) \right] \qquad (18)$$

where γ_{Fe}, γ_{Mo}, γ_{FeO}, and γ_{MoO_2} represent the activity coefficients of the respective species in solution.

The experimental equilibrium constant, $K'_{eq.}$, was calculated from the data obtained from the Fe-Mo-O system, where the liquid slag and liquid metal were equilibrated at molybdenum saturation in molybdenum crucibles. Table XII summarizes the data used to calculate $K'_{eq.}$. In this calculation, data from Table X pertaining to the metal phase and data on the slag phase (page 36) were employed to represent the best correlation of the experimental results. Using the method of least squares the best straight line representing $\log K'_{eq.}$ as a function of the reciprocal of the absolute temperature was derived as

$$\log K'_{eq.} = (67.81/T) - 0.7675 \qquad (19)$$

According to this equation, the value of $K'_{eq.}$ at 1873, 1973, and 2073 K is 0.1856, 0.1849, and 0.1842, respectively. The agreement between $K'_{eq.}$ and $K_{eq.}$ is shown graphically in Figure 36. The extent of agreement may be measured in terms of $RT(\ln K'_{eq.} - \ln K_{eq.})$. At the median temperature of this study, 1700 C, this factor is RT(ln 0.185 - ln 0.239), or about 1.3 kcal. This value is considered to be well within the combined error

Table XII

Summary of Experimental Data from the Fe-Mo-O System Used to Calculate the Experimental Equilibrium Content ($K'_{eq.}$)

Temperature (K)	X_{Fe}	X_{Mo}	X_{FeO}	X_{MoO_2}	$K'_{eq.} = \frac{X^2_{Fe} \ X_{MoO_2}}{X^2_{FeO} \ X_{Mo}}$
1873	0.592	0.408	0.839	0.161	0.1965
1973	0.538	0.462	0.822	0.178	0.1650
2073	0.502	0.498	0.771	0.229	0.1949

attributable to the literature calculations and the experimental data, and it offers some justification for the ideal solution assumption. The agreement between $K'_{eq.}$ and $K_{eq.}$ becomes better at higher temperatures. This trend is consistent with the general thermodynamic observation that solutions become more ideal as temperature is increased. By comparing the van't Hoff relation [log K = ($-\Delta H/4.575$ T) + constant] and Equation (19), a value of -310 calorie was obtained for ΔH. A negative value of ΔH indicates that an increase in temperature cuases the equilibrium to be shifted toward the left, in accordance with the principle of Le Chatelier. However, as shown in Figure 36, the equilibrium constant is nearly a constant over the 300 C temperature range of this study, and within the errors of this study, the sign of ΔH is not determined with certainty.

The molybdenum-saturated Fe-Mo-O experiments of this study may be considered to be typical of a more general slag-metal study: the equilibration of liquid slag and liquid metal over a range of molybdenum concentrations using an inert crucible material. At constant temperature the equilibrium constant, as based on activities, is a true constant over the entire range of molybdenum concentration from zero to saturation. If the slag and metal solutions obey Raoult's law over this range of concentration, then the equilibrium constant determined experimentally at molybdenum saturation would apply to the more general slag-metal study. However, the applicability of the experimental equilibrium constant to systems more dilute in molybdenum is indeterminable from the results of the present investigation.

The thermodynamic effect of silica additions to the Fe-Mo-O slag-metal system on the experimental equilibrium constant may be examined from the results of this study. If it is assumed that the liquid metal phase is approximately an ideal solution ($\gamma_{Mo} = \gamma_{Fe} = 1$) then the relation

between $K_{eq.}$ and $K'_{eq.}$ of Equation (18) becomes

$$K_{eq.} = K'_{eq.} \ (\gamma_{MoO_2}/\gamma^2_{FeO}) \qquad (20)$$

A value of $K'_{eq.}$ may be calculated from the molybdenum-saturated experiments in which silica was added. The value of the activity coefficient ratio $\gamma_{MoO_2}/\gamma^2_{FeO}$ is then obtained by dividing $K_{eq.}$, as determined from the literature data, by $K'_{eq.}$. Table XIII summarizes these calculations, for which the best correlations of the experimental data were used (Figures 28 and 30 and Table X). By using the values for $K'_{eq.}$ obtained by least squares, the values of $K_{eq.}/K'_{eq.}$ for the Fe-Mo-O ternary were determined to be 1.38, 1.29, and 1.22 at 1873, 1973, and 2073 K, respectively. In Figure 37, the ratio $\gamma_{MoO_2}/\gamma^2_{FeO}$ is plotted as a function of the mole fraction of silica in the slag at the three temperatures studied. If the slag solution containing silica behaves ideally, then $K'_{eq.}$, as defined in Equation (17), remains constant at constant temperature over the range of silica additions and is equal to $K_{eq.}$. If so, then silica acts only as a diluent, the activity coefficients of the components are unity, and the curves shown in Figure 37 would be overlapping horizontal straight lines with y-intercept of $\gamma_{MoO_2}/\gamma^2_{FeO} = 1$. From Figure 37, in which the ratio $\gamma_{MoO_2}/\gamma^2_{FeO}$ increases with increasing silica additions it is evident that this behavior does not occur. The change of this ratio with silica additions is consistent with the hypotheses that (1) the MoO_2-SiO_2 attraction is very weak compared to the preference for like neighbors, causing a positive deviation from ideality and γ_{MoO_2} to be greater than unity, and (2) the FeO-SiO_2 attraction is strong, causing a negative deviation from ideality and γ_{FeO} to be less than unity. Since γ_{FeO} is less than unity and enters the ratio $\gamma_{MoO_2}/\gamma^2_{FeO}$ as a squared term, the ratio becomes much larger than unity. A negative deviation of FeO from ideality in the FeO-SiO_2 system is consistent with the work of

Table XIII

Summary of Experimental Data from the Fe-Mo-Si-O System Used to Calculate the Experimental Equilibrium Constant ($K'_{eq.}$)

Temperature (K)	X_{Fe}	X_{Mo}	X_{FeO}	X_{MoO_2}	X_{SiO_2}	$K'_{eq.} = \frac{X^2_{Fe}\ X_{MoO_2}}{X^2_{FeO}\ X_{Mo}}$	$\frac{K_{eq.}}{K'_{eq.}} \approx \frac{\gamma_{MoO_2}}{\gamma^2_{FeO}}$
1873	0.592	0.408	0.838	0.117	0.045	0.1431	1.79
1973	0.538	0.462	0.805	0.149	0.046	0.1440	1.66
2073	0.502	0.498	0.780	0.174	0.046	0.1447	1.55
1873	0.592	0.408	0.826	0.085	0.089	0.1070	2.39
1973	0.538	0.462	0.795	0.114	0.091	0.1130	2.12
2073	0.502	0.498	0.770	0.140	0.090	0.1195	1.88
1873	0.592	0.408	0.804	0.061	0.135	0.0810	2.95
1973	0.538	0.462	0.781	0.082	0.137	0.0842	2.84
2073	0.502	0.498	0.756	0.109	0.136	0.0965	2.33
1873	0.592	0.408	0.737	0.030	0.233	0.0474	5.40
1973	0.538	0.462	0.720	0.043	0.237	0.0519	4.60
2073	0.502	0.498	0.701	0.062	0.237	0.0638	3.53
1873	0.592	0.408	0.626	0.011	0.364	0.0241	10.6
1973	0.538	0.462	0.610	0.015	0.375	0.0253	9.46
2073	0.502	0.498	0.598	0.023	0.379	0.0326	6.91
1873	0.592	0.408	0.492	0.003	0.505	0.0107	24.0
1973	0.538	0.462	0.477	0.004	0.519	0.0110	21.7
2073	0.502	0.498	0.469	0.007	0.524	0.0161	14.0

Turkdogan and Pearson,[88] and might be expected on the basis of compound formation (Fe_2SiO_4) at lower temperatures. At a given value of X_{SiO_2} the ratio $\gamma_{MoO_2}/\gamma^2_{FeO}$ has values closer to unity at higher temperatures (Figure 37). This is consistent with the expectation that the system become more ideal at higher temperatures.

This thermochemical analysis suggests that a model may be successfully used to describe the system studied, although for engineering purposes an empirical description of the molybdenum partition coefficient may be adequate. In the model proposed, the relationship between molybdenum-

saturated Fe-Mo liquid metal and $FeO-MoO_2$ liquid slag is determined by an equilibrium constant based with reasonable accuracy on the mole fractions of the various components. The addition of SiO_2 to the system causes a marked deviation from ideality which is attributed, primarily, to a strong interaction between FeO and SiO_2.

Pertinence of Results to Commercial Practice

The results of the present investigation offer some further understanding of slag-metal relationships in commercial ferromolybdenum production by the thermite method. These implications are considered in the order of (1) the importance of slag constitution, (2) the effect of temperature as a process variable, and (3) the feasibility and suggested directions of further research in this area.

Slag constitution plays a major role in determining the equilibrium concentration of molybdenum as oxide in the slag. This role is shown in Figure 35 where the molybdenum partition coefficient is plotted as a function of temperature at several silica concentrations. The high silica content of commercial slags is dictated by the requirement of high silicon in the thermite charge for the reaction to be sufficiently exothermic. It is apparently fortuitous that commercial slag compositions are such that the molybdenum oxide concentration is low relative to slags more dilute in silica. Within the range of compositions studied, the experimental slags having the lowest molybdenum oxide content are those nearest in composition to the commercial slags. Therefore, for molybdenum oxide solubility, this research has not made evident a slag composition better than the empirically developed composition now in use. However, while showing the desirable effect of silica in lowering the molybdenum solubility as oxide, this study also shows that silica-rich Fe-Mo-Si-O slags are sufficiently viscous to essentially prevent complete gravimetric

separation of the metal and slag phases at temperatures below about 1700 C. For example, Fe-Mo-Si-O silica-saturated slags contained spherical metallic inclusions in suspension even after 7 hours at 1550 C. When CaO and Al_2O_3 were added to approximate commercial slag compositions more closely, the metallic inclusions decreased in concentration but were not completely eliminated. This decrease was presumably the result of a decrease in slag viscosity caused by the additions. However, as the concentration of CaO is further increased, the slag viscosity would eventually be expected to increase because of the formation of dicalcium silicate. In the experimental slag containing CaO and Al_2O_3 there was no significant difference in the concentration of molybdenum as oxide compared with similar experimental slags not containing these additions. This study has therefore helped to confirm the desirability of high-silica slags for maintaining a low concentration of molybdenum as oxide; nonetheless additional investigation should be pursued to reduce metallic inclusions by determining a less viscous slag composition.

The effect of temperature on the solubility of molybdenum as oxide was also examined in Fe-Mo-Si-O slags. The solubility invariably increases with increasing temperature, and in silica-rich slags the temperature dependency is less than in slags low in silica. In addition, the concentration of metallic inclusions entrapped in the liquid slag decreases with increasing temperature, probably because of decreasing slag viscosity with increasing temperature. These results suggest that the concentration of metal prills in the slag phase may be lowered in the commercial process by slow cooling of the products while they are still liquid. This procedure change would permit additional time for the metal phase to separate gravimetrically while the slag phase is still relatively fluid. Slower cooling would also permit the equilibrium content of molybdenum as oxide

in the slag to be approached more closely at lower temperatures (for example, 1600 C), rather than "quenching in" the higher molybdenum content of the slag at higher temperatures (for example, 1900 C).

Finally, the results of this investigation suggest directions for further related research. This study examined the Fe-Mo-Si-O system and one experiment was made in which CaO and Al_2O_3 were added to the slag. A more detailed examination of the effects of CaO and Al_2O_3 on the equilibrium concentration of molybdenum as oxide in the slag is needed to describe more adequately the effects of compositional deviations in the commercial formulary. Another suggested area of investigation is that of ferromolybdenum slag viscosity, which has been shown in the present study to be important to slag-metal separation. From viscosity data for simple oxide systems published in the literature and, perhaps, from additional experiments, it may be possible to determine a more fluid slag composition that is also compatible with the exothermic requirements of the charge materials.

CONCLUSIONS

The liquidus composition of the Fe-Mo binary system is 40.8, 46.2, 49.8, and 56.7 atomic percent molybdenum at 1600, 1700, 1800, and 1900 C, respectively.

The concentration of molybdenum in molybdenum-saturated Fe-Mo-O liquid slags in equilibrium with Fe-Mo liquid metal increases from about 18 weight percent molybdenum at 1600 C to about 24 weight percent molybdenum at 1800 C.

Silica additions to these slags lower the molybdenum concentration of the slag to about 0.2 weight percent at 1600 C and 0.3 weight percent at 1800 C when the slag is silica-saturated.

The partition coefficient of molybdenum, defined as the molybdenum weight fraction in the slag divided by the molybdenum weight fraction in the metal, decreases with increasing silica in the slag and with decreasing temperature. For molybdenum-saturated slags containing no silica, the partition coefficient increases from 0.34 at 1600 C to 0.39 at 1800 C. For slags saturated with molybdenum and silica the values are 0.004 at 1600 C and 0.005 at 1800 C.

An ideal solution model describing the equilibrium relationship between iron and molybdenum in the slag and metal is

$$2(FeO) + \underline{Mo} = 2\ \underline{Fe} + (MoO_2)$$

where $K'_{eq.} = (X^2_{Fe}\ X_{MoO_2})/(X_{Mo}\ X^2_{FeO})$. Within the temperature range studied, the agreement between this calculated equilibrium constant and an equilibrium constant calculated from published data is considered to be good. The model suggests that the presence of SiO_2 in the slag causes the activity of FeO to deviate negatively from Raoult's law and lowers the concentration of molybdenum in the slag more than would be expected by simple dilution.

The results of the study confirm the suitability of commercial ferromolybdenum slag compositions for minimizing the concentration of molybdenum as oxide. The viscosity of these slags probably plays a determinant role in the extent of slag-metal separation, and the possible development of lower viscosity slag compositions should be considered.

REFERENCES

1. "Molybdenum Product Specification-Ferromolybdenum," Climax Molybdenum Company, New York, 1963.

2. R. Durrer and G. Volkert, Metallurgy of Ferroalloys, Springer-Verlag, Berlin, 1953, pp. 281-285.

3. V. P. Elyutin, Yu. A. Pavlov, B. E. Levin, and E. M. Alekseev, Production of Ferroalloys, second edition, translated by B. Shapira, National Science Foundation, Washington, D. C., 1961 (OTS 61-11429), pp. 265-287.

4 L. W. Coffer, "Production of Ferromolybdenum by the Thermite Reduction of Molybdenum Concentrates," Climax Molybdenum Company, Internal Publication, 1943.

5. "Ferromolybdenum Development Manual of Information," Climax Molybdenum Company, Internal Publication, 1965.

6. "Ferromolybdenum Development Manual of Information," Supplement, Climax Molybdenum Company, Internal Publication, 1966.

7. H. Haag, "The Production of Ferromolybdenum and Metallic Molybdenum," Z. Erzbergbau Metallhuttenwesen 15 (1962), 229-234.

8. A. Triandaf and F. Olaru, "Production of Ferromolybdenum from Indigenous Molybdenum Concentrates," Met. Constr. Masini 1 (1963), 1-9.

9. Z. Kulinski and B. Paczula, "Making of Ferromolybdenum by Alumino-Silicothermic Method," Prace Inst. Hutnic 10 (1958), 143-145.

10. Z. Kulinski, "Improvement in the Production of Some Iron Alloys," Prace Inst. Hutnic 17 (1965), 137-139.

11. J. Evans, "Tailor Moly to Suit Industry," AMAX J. 2 (1964), 4.

12. Ibid., cover.

13. J. Evans, Unpublished, Courtesy AMAX Journal.

14. Reference 11, p. 5.

15. A. S. Dubrovin, N. A. Agarkova, S. S. Shestakov, K. S. Lastovitskaya, and L. I. Klokotina, "Optimum Conditions for Making Ferromolybdenum," Stal 26 (1966), 46-49.

16. K. N. Rispel and L. I. Klokotina, "Material and Heat Balances of Alumino-Silicothermic Smelting of Ferromolybdenum," Izv. Akad. Nauk SSSR, Metally 3 (1966), 34-41.

17. A. S. Dubrovin and Yu. L. Pliner, "Temperature of Aluminothermal Processes," Izv. Sibirsk Otd. Akad. Nauk SSSR 12 (1962), 9-15.

18. A. S. Dubrovin and V. L. Kuznetsov, "The Part Played by Pressure and Heat Transfer in Metallothermic Processes," Izv. Akad. Nauk SSSR, Metally, 4 (1965), 82-88.

19. Yu. L. Pliner, "Temperature Dependence of the Heat Content of a Thermite Melt," Sb. Tr. Klyuchevsk. Zavoda Ferrosplavov 2 (1965), 5-15.

20. Reference 3, p. 277.

21. Reference 3, p. 286.

22. N. L. Zhilo and G. I. Sobolev, "Viscosity of Ferromolybdenum Slags," Izv. Akad. Nauk SSSR, Metally 5 (1966), 31-33.

23. Yu. L. Pliner, G. A. Babushkin, E. A. Rubinshtein, B. M. Lepinskikh, and G. F. Ignatenko, "Coagulation of Metal Drops in a Thermite Melt," Sb. Tr Klyuchevsk. Zavoda Ferrosplavov 2 (1965), 57-66.

24. V. V. Khlynov and O. A. Esin, "Reduction of Metal Losses in a Ferrous Slag by an Electrocapillary Process," Izv. VUZ Chern. Met. 7 (1959), 3-11.

25. Yu. P. Nikitin, O. A. Esin, and A. I. Sotnikov, "On the Extraction of Ferrotungsten from Waste Slag with the Aid of an Electric Current," Izv. VUZ Chern. Met. 2 (1963), 12-15.

26. Yu. L. Pliner and G. F. Ignatenko, "Effect of Temperature on the Equilibrium State of Thermite Reduction of Metal Oxides," Sb. Tr. Klyuchevsk. Zavoda Ferrosplavov 2 (1965), 22-26.

27. L. N Rusakov, I. A. Novokhatskii, L. M. Lenev, A. S. Dubrovin, and A. A. Savinskaya, "Molybdenum-Containing Oxide Phases in Slags from Ferromolybdenum Smelting," Eksperiment v Tekhn. Mineralog. i Petrogr., po Materialam Soveshch., 7th, Lvov 1964, (1966), pp. 246-250.

28. W. Dittrich, "Equilibrium Investigations of the System Fe-Mo-O," Freiberger Forschungsh. 51B (1959), 33-48.

29. M. Hansen, Constitution of Binary Alloys, McGraw-Hill Book Company, Inc., New York, 1958, pp. 684-691.

30. R. P. Elliott, Constitution of Binary Alloys, First Supplement, McGraw-Hill Book Company, Inc., New York, 1965, pp. 423-424.

31. L. S. Darken and R. W. Gurry, "The System Iron-Oxygen. I. The Wustite Field and Related Equilibria," J. Am. Chemical Soc. 67 (1945), 1398-1412.

32. L. S. Darken and R. W. Gurry, "The System Iron-Oxygen. II. Equilibrium and Thermodynamics of Liquid Oxide and Other Phases," J. Am. Chemical Soc. 68 (1946), 798-816.

33. J. Chipman and S. Marshall, "The Equilibrium $FeO + H_2 = Fe + H_2O$ at Temperatures up to the Melting Point of Iron," J. Am. Chemical Soc. 62 (1940), 299-305.

34. M. N. Dastur and J. Chipman, "Equilibrium in the Reaction of Hydrogen with Oxygen in Liquid Iron," AIME Trans. 185 (1949), 441-445.

35. N. A. Gokcen, "Equilibria in Reactions of Hydorgen, and Carbon Monoxide with Dissolved Oxygen in Liquid Iron: Equilibrium in Reduction of Ferrous Oxide with Hydrogen, and Solubility of Oxygen in Liquid Iron," AIME Trans. 206 (1956), 1558-1567.

36. A. U Seybolt, "Solubility of Oxygen in Alpha Iron: A Revision," AIME Trans. 215 (1959), 298-300.

37. J. A. Kitchener, J. O'M. Bockris, M. Gleiser, and J. W. Evans, "The Solubility of Oxygen in Gamma Iron," Acta Met. 1 (1953), 93-101.

38. E. S. Tankins and N. A. Gokcen, "Solubility of Oxygen in Delta Iron," ASM Trans. 53 (1961), 843-852.

39. B. Phillips and L. L. Y. Chang, "Condensed-Phase Relations in the System Mo-O," AIME Trans. 233 (1965), 1433-1436.

40. C. E. Wicks and F. E. Block, "Thermodynamic Properties of 65 Elements--Their Oxides, Halides, Carbides, and Nitrides," U.S. Bureau of Mines Bul. 605 (1963), 79.

41. P. E Blackburn, M. Hoch, and H. L. Johnston, "The Vaporization of Molybdenum and Tungsten Oxides," J. Phys. Chem. 62 (1958), 769-773.

42. R. P. Burns, G. DeMaria, J. Drowart, and R. T. Grimley, "Mass Spectrometric Investigation of the Sublimation of Molybdenum Dioxide," J. Chem. Phys. 32 (1960), 1363-1366.

43. K. K. Kelly, "Thermodynamic Properties of Molybdenum Compounds," Climax Molybdenum Company Bulletin Cdb-2 (1954), p. 2.

44. Reference 30, pp. 623-624.

45. W. E. Few and G. K. Manning, "Solubility of Carbon and Oxygen in Molybdenum," AIME Trans. 194 (1952), 271-274.

46. Reference 29, pp. 668-670.

47. Reference 30, p. 420.

48. A. K. Sinha, R. A. Buckley, and W. Hume-Rothery, "Equilibrium Diagram of the Iron-Molybdenum System," J Iron and Steel Inst. 205 (1967), 191-195.

49. W. S. Gibson, J. R. Lee, and W. Hume-Rothery, "Liquidus-Solidus Relations in Iron-Rich Iron-Niobium and Iron-Molybdenum Alloys," J. Iron and Steel Inst. 198 (1961), 64-66.

50. W. Jäger, A. Rahmel, and K. Becker, "Ternary System Iron-Molybdenum-Oxygen," Arch. Eisenhüttenw. 30 (1959), 435-439.

51. G. Tamman and F. Westerhold, "Chemical Reactions in Powdered Mixtures of Two Kinds of Crystals. I. Reactions of WO_3 and MoO_3 on Basic Oxides and Carbonates," Z. anorg. allg. Chem. 149 (1925), 35-46.

52. N. Schönberg, "Existence of Ternary Transition Metal Oxides," Acta Chem. Scand. 8 (1954), 932-936.

53. N. Schönberg, "Existence of Metallic Ternary Oxides M'M''O with the Metal Atoms in Hexagonal Close Packing," Acta Chem. Scand. 8 (1954), 630-632.

54. W. H. McCarroll, R. Ward, and L. Katz, "Ternary Oxides of Tetravalent Molybdenum," J. Am. Chemical Soc. 78 (1956), 2909-2910.

55. W. H. McCarroll, R. Ward, and L. Katz, "Some Ternary Oxides of Tetravalent Molybdenum," J. Am. Chemical Soc. 79 (1957), 5410-5414.

56. J. K. Meijering and G. W. Rathenau, "Oxidation of Heat Resistant Alloys in the Presence of Foreign Oxides," Phillips Tech. Rev. 12 (1951), 213-220.

57. J. K. Meijering and G. W Rathenau, "Rapid Oxidation of Metals and Alloys in the Presence of Molybdenum Trioxide," Nature 165 (1950), 240-241.

58. G. W. Rathenau and J. K. Meijering, "Rapid Oxidation of Metals and Alloys in the Presence of Molybdenum Trioxide," Metallurgia 42 (1950), 167-172.

59. K. Nassua, H. J Levinstein, and G. M. Loiacono, "A Comprehensive Study of Trivalent Tungstates and Molybdates of the Type $L_2(MoO_4)_3$," J. Phys Chem. Solids 26 (1965), 1805-1816.

60. Yu. D. Kozmanov and T. A. Ugolnikova, "On Iron Molybdates," Zhur. Neorg. Khim. 3 (1958), 1267.

61. Yu. D. Kozmanov, "Solid Phase Reactions Between Ferrous Oxide and Molybdenum and Tungsten Oxides," Russian J. Inorganic Chem. 5 (1960), 996-997.

62. Yu. D. Kozmanov, "X-ray Investigation of the Reaction Between Solid Iron Oxides and Tungsten and Molybdenum Oxides," Zhur. Fiz. Khim. 31 (1957), 1861-1865.

63. E. S. Tankins, M. K. Thomas, J. F. Erthal, and F. S. Williams, "The Activity of Oxygen in Liquid Iron-Molybdenum and Iron-Tungsten Alloys," ASM Trans. 58 (1965), 245-252.

64. T. P. Floridis and J. Chipman, "Activity of Oxygen in Liquid Iron Alloys," AIME Trans. 212 (1958), 549-553.

65. E. M. Levin, C. R. Robbins, and H. F. McMurdie, Phase Diagrams for Ceramists, American Ceramic Society, Columbus, Ohio, 1964. pp. 59-61.

66. N. L. Bowen and J. F. Schairer, "The System FeO-SiO_2," Am. J. Science 24 (1932), 177-213.

67. L. S. Darken, "Melting Points of Iron Oxides on Silica; Phase Equilibria in the System Fe-Si-O as a Function of Gas Composition and Temperature," J. Am. Chemical Soc. 70 (1948), 2046-2053.

68. E. J. Michal and R. Schuhmann, "Thermodynamics of Iron-Silicate Slags: Slags Saturated with Silica," AIME Trans. 194 (1952), 723-728.

69. R. Schuhmann, R. G. Powell, and E. J. Michal, "Constitution of the FeO-Fe_2O_3-SiO_2 System at Steel-Making Temperatures," AIME Trans. 197 (1953), 1097-1104.

70. A. Maun, "Phase Equilibria in the System FeO-Fe_2O_3-SiO_2," AIME Trans. 203 (1955), 965-976.

71. L. O. Case, Elements of the Phase Rule, Edwards Letter Shop, Ann Arbor, Michigan, 1939.

72. A. Glassner, The Thermochemical Properties of the Oxides, Fluorides, and Chlorides to 2500 K, U.S.A.E.C., ANL-5750, 1957.

73. Y. Kojima and K. Sano, "On the Equilibrium Between Liquid Iron-Chromium Alloy and Silica-Saturated Acidic Slag," Tetsu-to-Hagane Overseas 5 (1965), 11-19.

74. "The Determination of Molybdenum in Iron and Steel," Climax Molybdenum Company, 1947, 14 pp.

75. "The Determination of Molybdenum in Iron and Steel (Umpire Benzoin Antioxime Method)," Procedure 503, Climax Molybdenum Company, Internal Publication.

76. "The Determination of Molybdenum in Iron and Steel (Umpire Thiocyanate-Photometric Method)," Procedure 506, Climax Molybdenum Company, Internal Publication.

77. A. Rahmel, W. Jäger, and K. Becker, "On the Oxidation of Iron-Molybdenum Alloys in Air at High Temperatures," Arch. Eisenhüttenw. 30 (1959), 351-360.

78. R. G. Ward, An Introduction to the Physical Chemistry of Steelmaking, Edward Arnold, London, 1962, Chapter 5.

79. J. Chipman, J. B. Gero, and T. B. Winkler, "The Manganese Equilibrium," AIME Trans. 188 (1950), 341-345.

80. C. R. Taylor and J. Chipman, "Equilibria in Liquid Iron and Simple Basic and Acid Slags in a Rotating Induction Furnace," AIME Trans. 154 (1943), 228-245.

81. T. B. Winkler and J. Chipman, "An Equilibrium Study of the Distribution of Phosphorus Between Liquid Iron and Basic Slags," AIME Trans. 167 (1946), 111-133.

82. Reference 81, p. 120.

83. J. F. Elliott, M. Gleiser, and V. Ramakrishna, Thermochemistry for Steelmaking, II, Addison-Wesley, Reading, Mass., 1963, pp. 619-620.

84. O. Kubaschewski, E. LL. Evans, and C. B. Alcock, Metallurgical Thermochemistry, Pergamon Press, New York, 1967, p. 376.

85. Reference 79, p. 344.

86. Reference 40, p. 125.

87. J. Chipman, "The Physical Chemistry of Liquid Steel," in Basic Open Hearth Steelmaking, W. O. Philbrook and M. B. Bever, editors, AIME New York, 1951, p. 637.

88. E. T. Turkdogan and J. Pearson, "Activities of Constituents in Iron and Steelmaking Slags, Part I: Iron Oxides," J. Iron and Steel Inst. 173 (1953), 217-223.



Figure 1 Loading the Reaction Pot with the Thermite Mixture



Figure 2 Hoisting the Ferromolybdenum Button and Slag Cap from the Sand Pit to the Water-Quench Tank

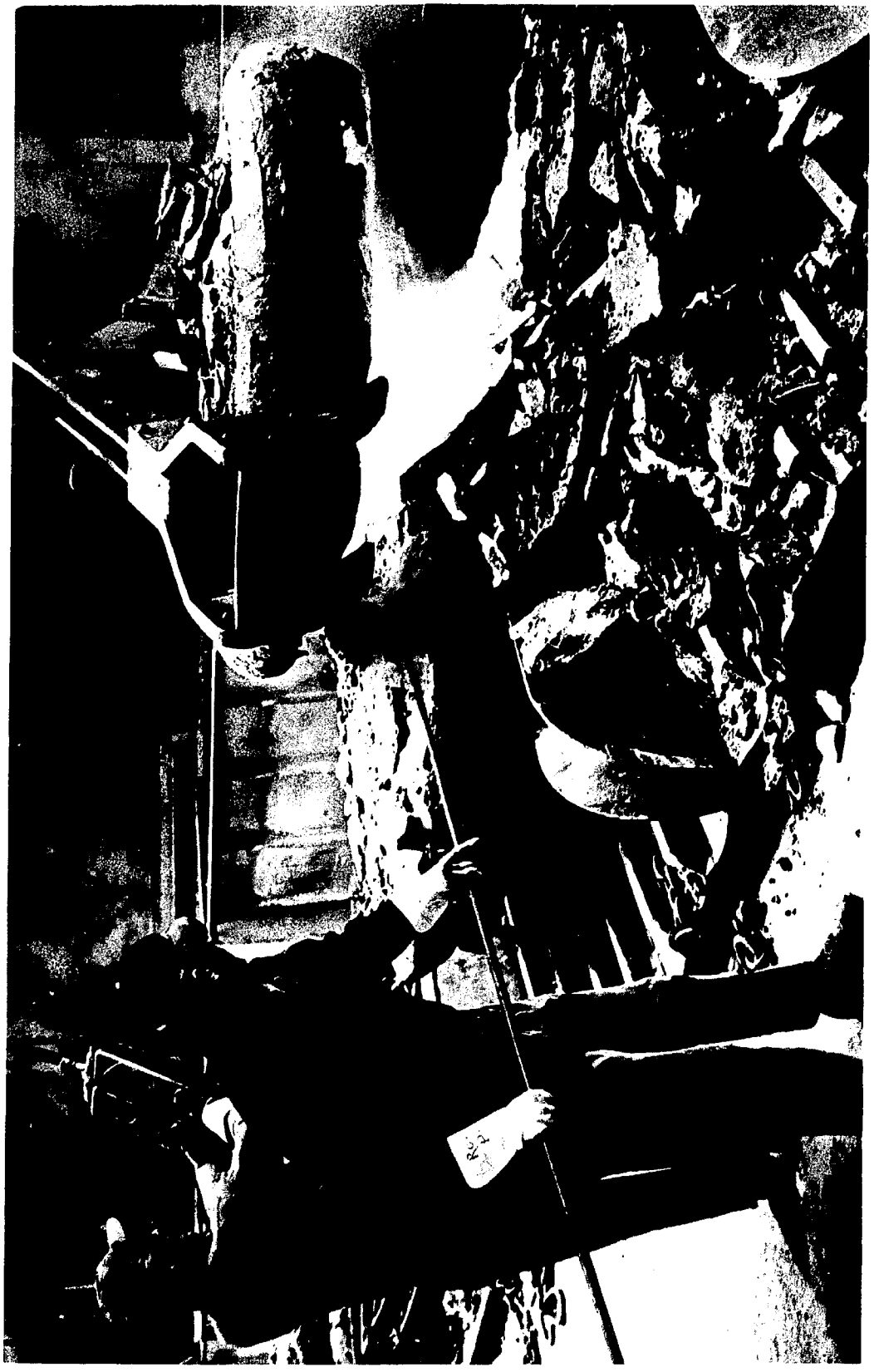


Figure 3 Separating the Ferromolybdenum Button from the Slag Cap



Figure 4 Breaking the Ferromolybdenum Button to Feedstock Sizes for the Jaw Crushers

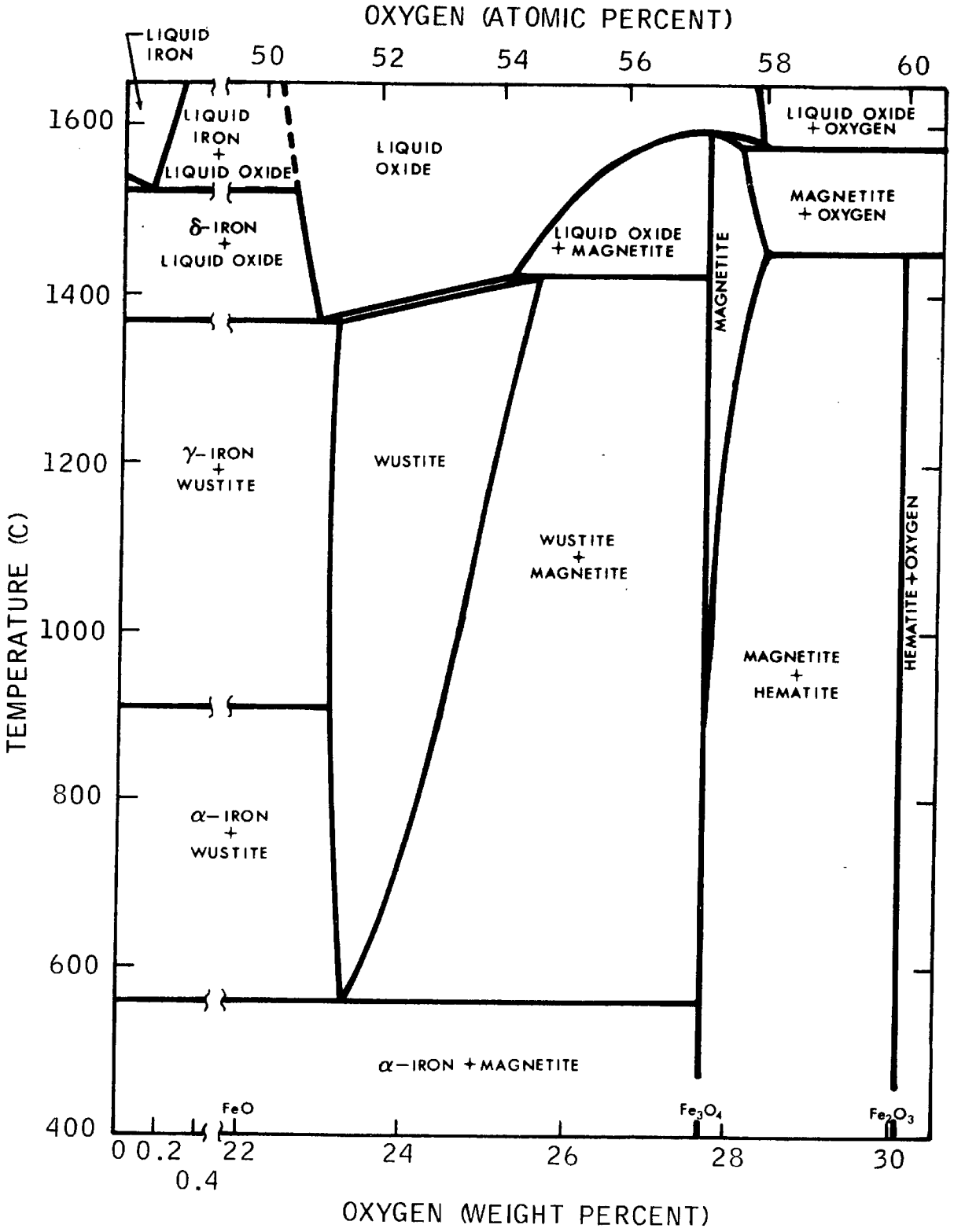


Figure 5 Equilibrium Phase Diagram for the Iron-Oxygen Binary System after L. S. Darken and R. W. Gurry, "The System Iron-Oxygen. II. Equilibrium and Thermodynamics of Liquid Oxide and Other Phases," J. Am. Chemical Soc 68 (1946), 798-816.

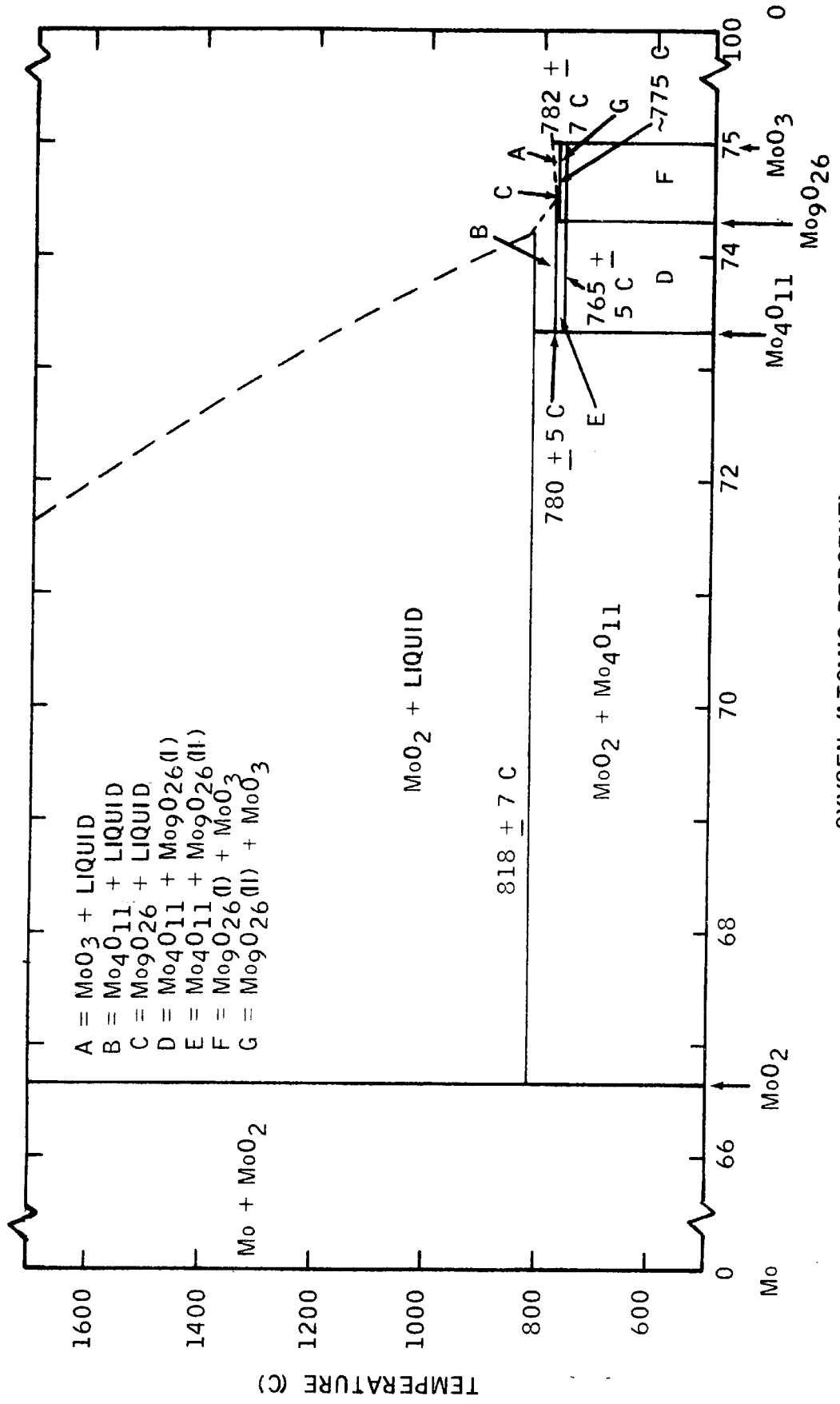


Figure 6 Equilibrium Phase Diagram for the Molybdenum-Oxygen Binary System after B. Phillips and L. L. Y. Chang, "Condensed-Phase Relations in the System Mo-O," AIME Trans. 233 (1965), 1433-1436.

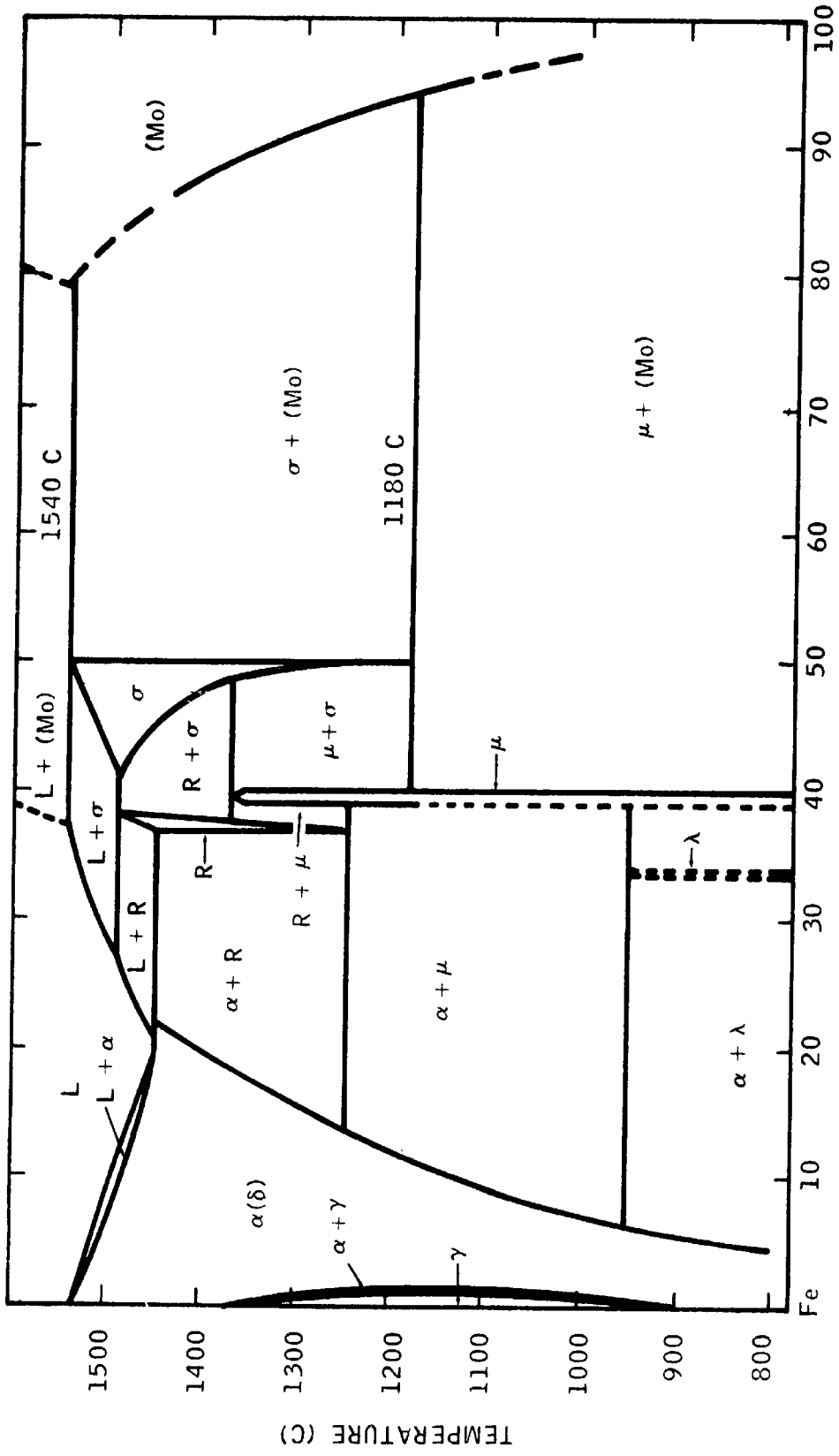


Figure 7 Equilibrium Phase Diagram for the Fe-Mo System after A. K. Sinha, R. A. Buckley, and W. Hume-Rothery, "Equilibrium Diagram of the Iron-Molybdenum System," J. Iron and Steel Inst. 205 (1967), 191-195.

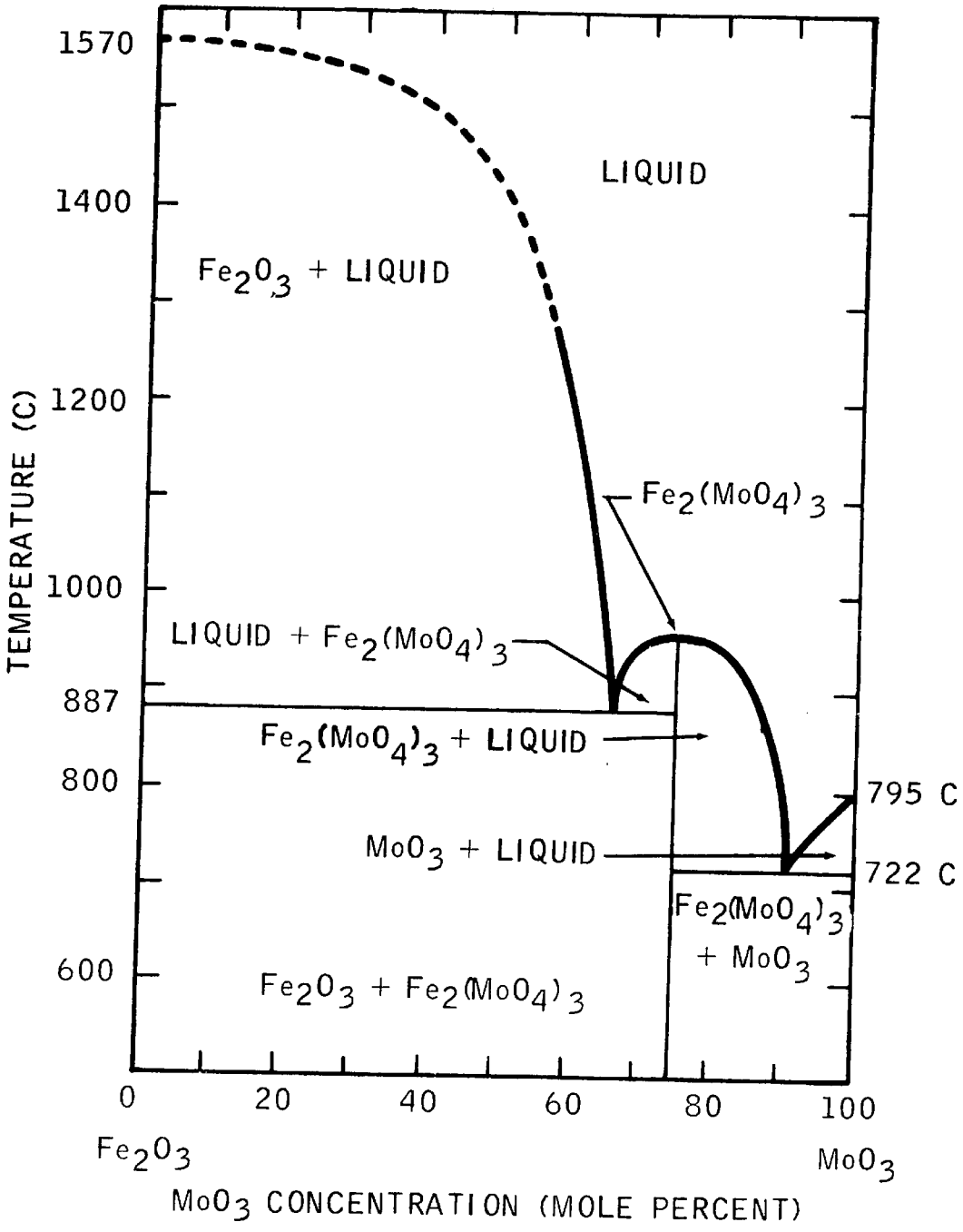


Figure 8 Pseudo-Binary Phase Diagram for the Fe_2O_3-MoO_3 System after W. Jager, A. Rahmel, and K. Becker, "Ternary System Iron-Molybdenum-Oxygen," Arch. Eisenhuttenw. 30 (1959), 435-439.

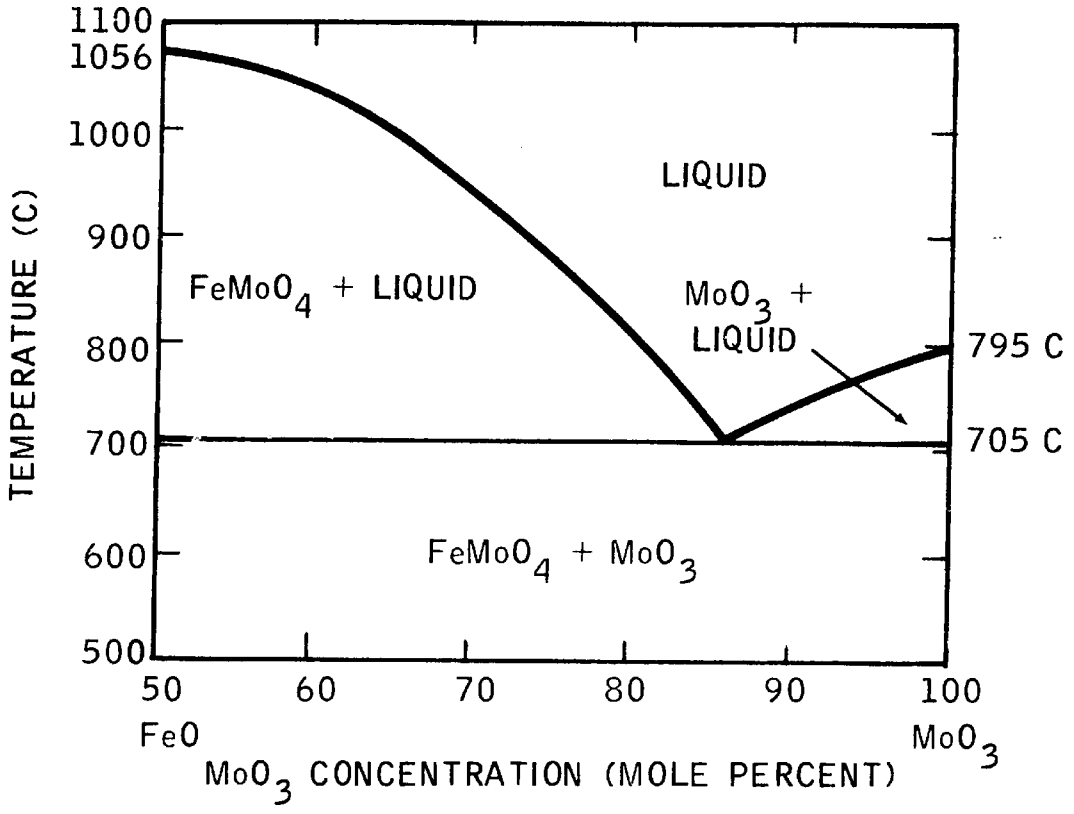


Figure 9 Pseudo-Binary Phase Diagram for the System FeO-MoO_3

after W. Jager, A. Rahmel, and K. Becker, "Ternary System Iron-Molybdenum-Oxygen," Arch. Eisenhuttenw. 30 (1959), 435-439.

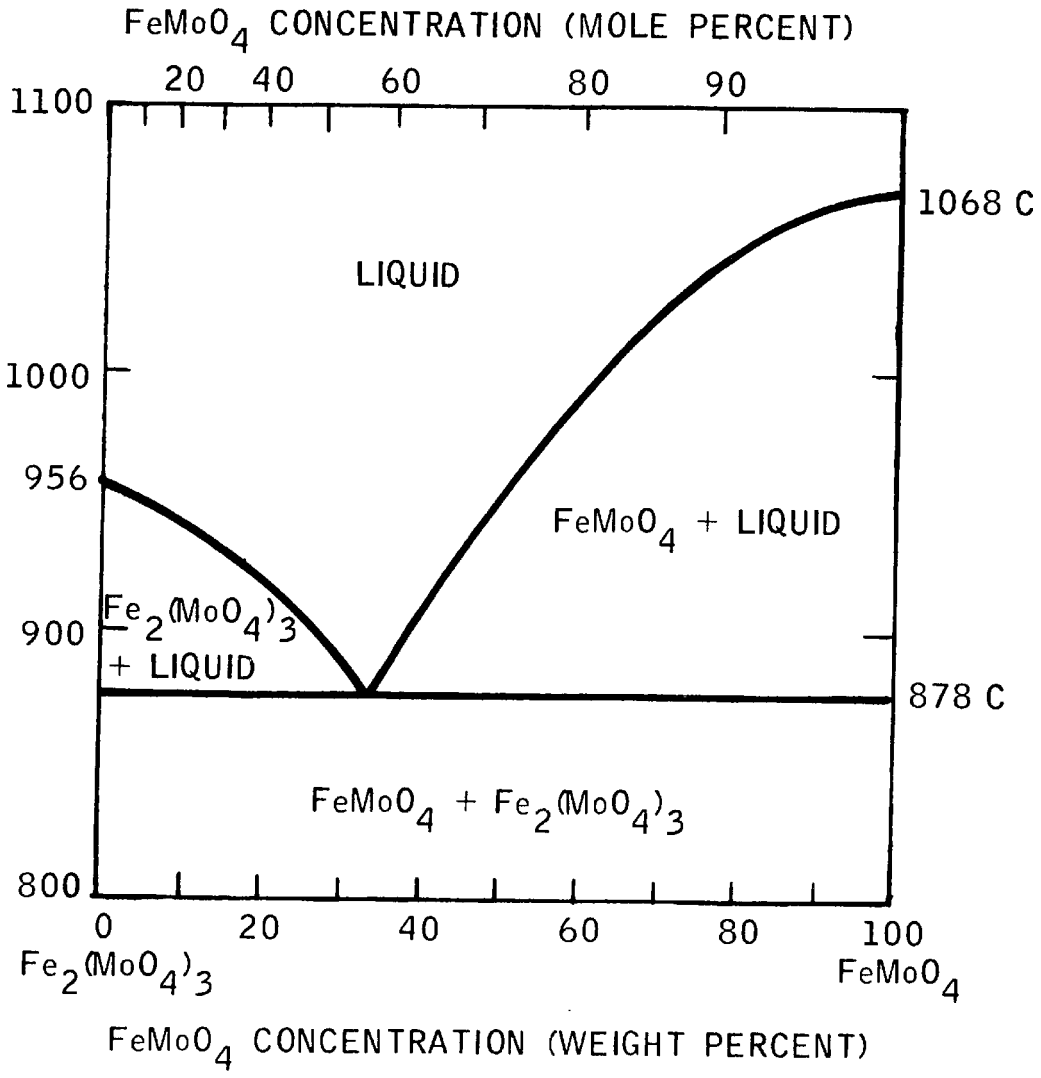


Figure 10 Pseudo-Binary Phase Diagram for the System $Fe_2(MoO_4)_3$-$FeMoO_4$ after W. Jager, A. Rahmel, and K. Becker, "Ternary System Iron-Molybdenum-Oxygen," Arch. Eisenhuttenw. 30 (1959), 435-439.

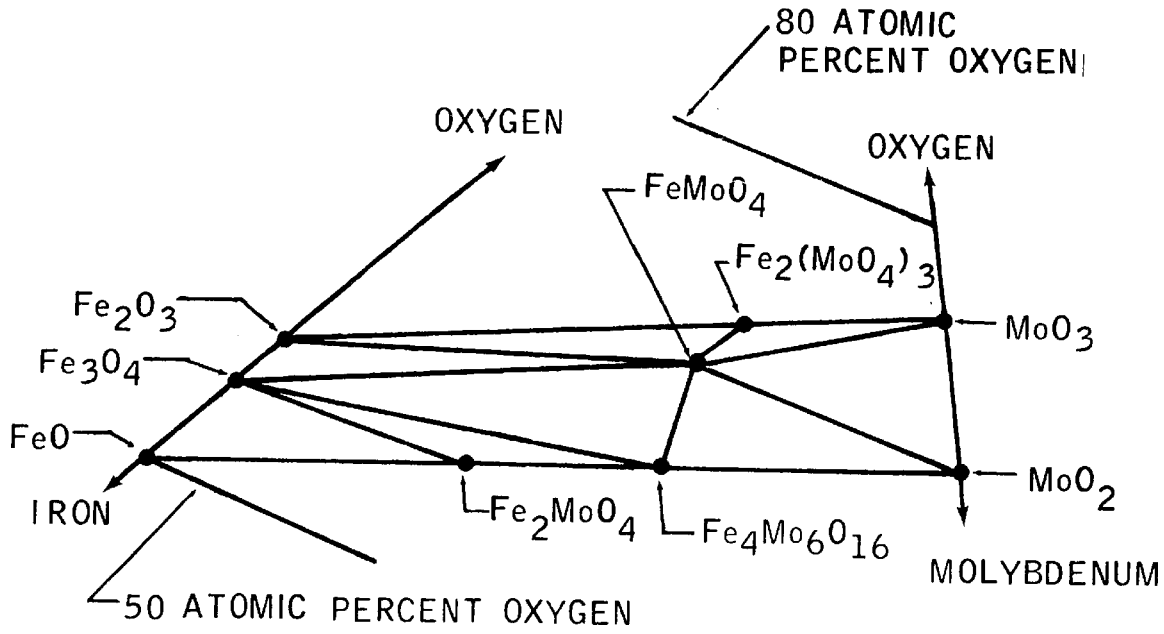


Figure 11 Schematic Isothermal Section through the Fe-Mo-O Ternary System in the Temperature Range 800 to 1100 C

As proposed by Jager et al., "Ternary System Iron-Molybdenum-Oxygen," Arch. Eisenhuttenw 30 (1959), 435-439.

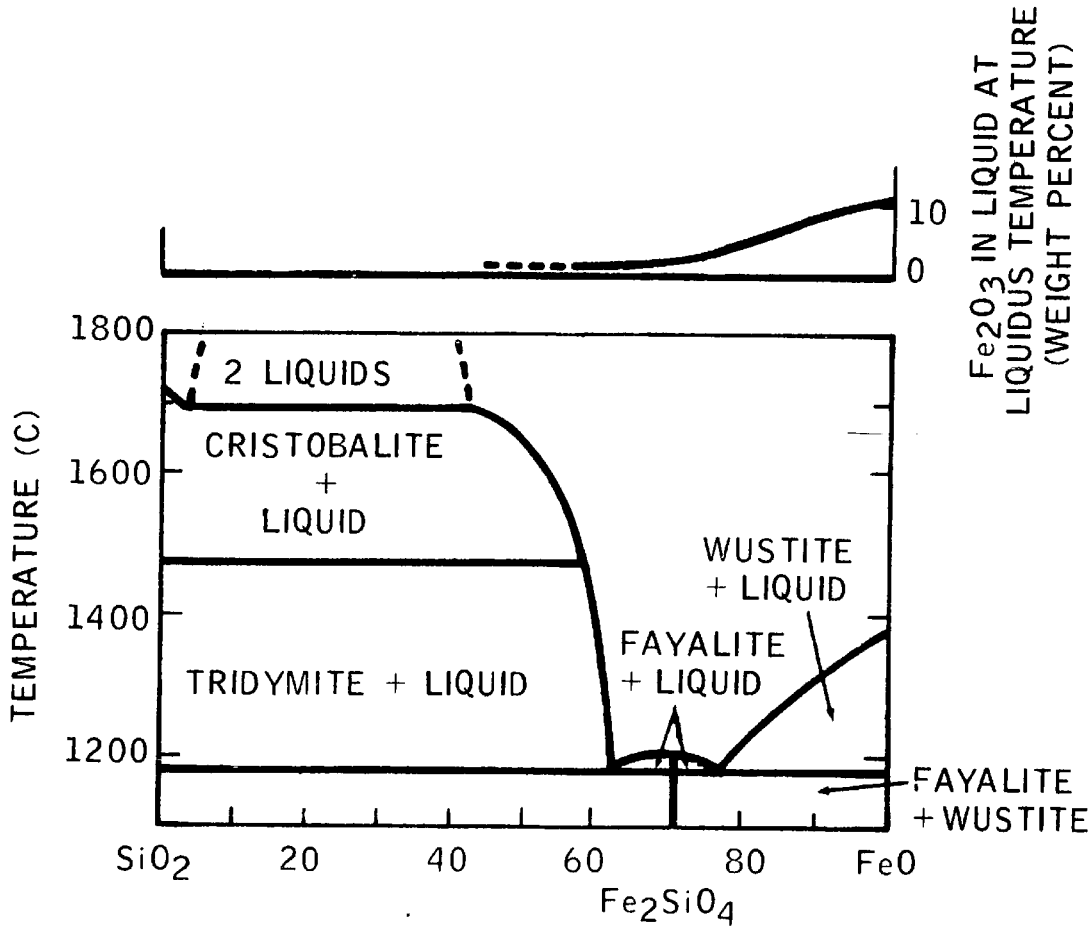


Figure 12 Equilibrium Phase Diagram for the Pseudo-Binary System FeO-SiO_2

after N. L. Bowen and J. F. Schairer, "The System FeO-SiO_2," Am. J. Science 24 (1932), 177-213.

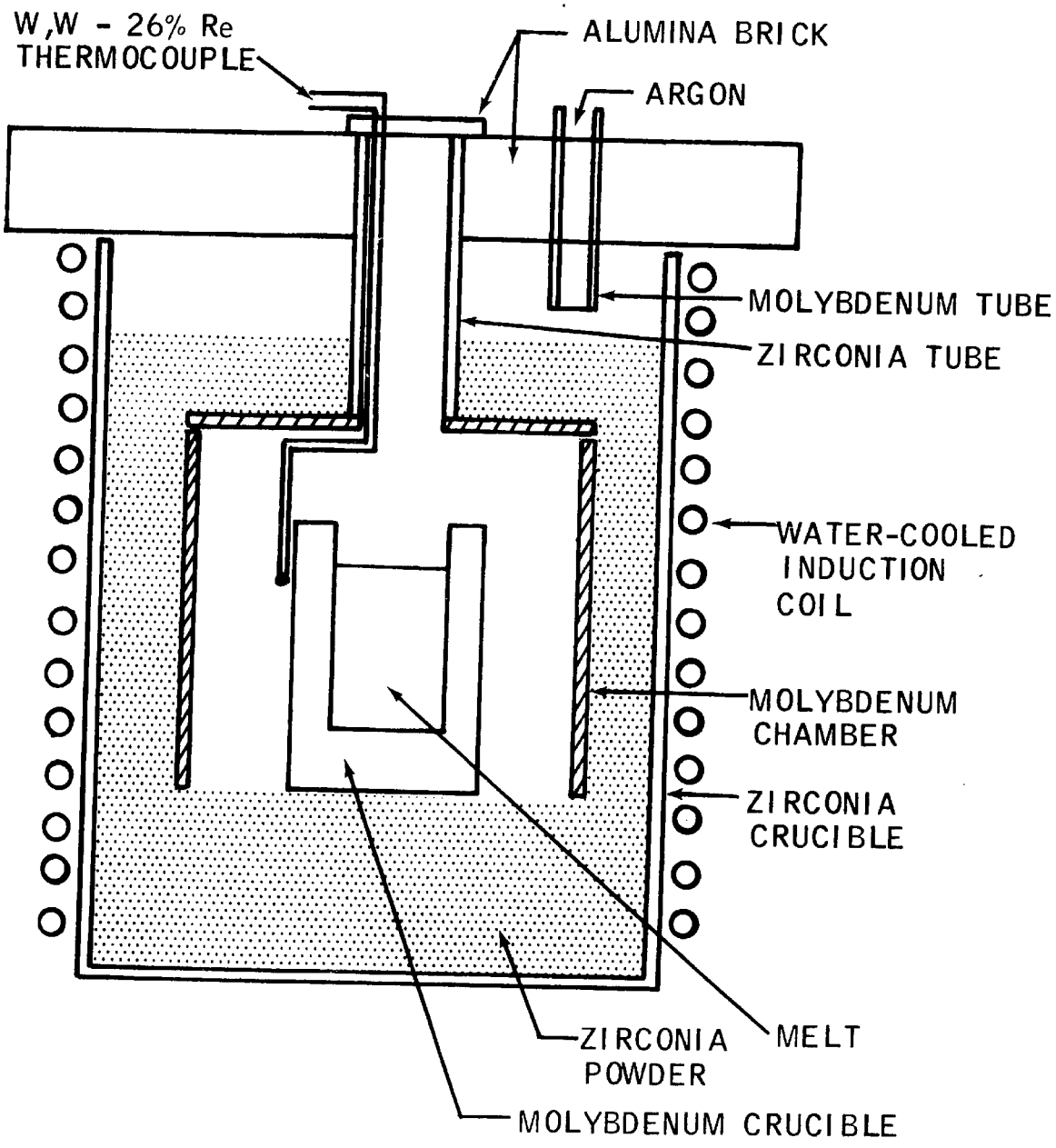


Figure 13 Schematic Diagram of Inert-Atmosphere Induction-Heated Furnace Used for Molybdenum Crucible Experiments

The apparatus shown above was packed in alumina bubble to the top of the induction coil.

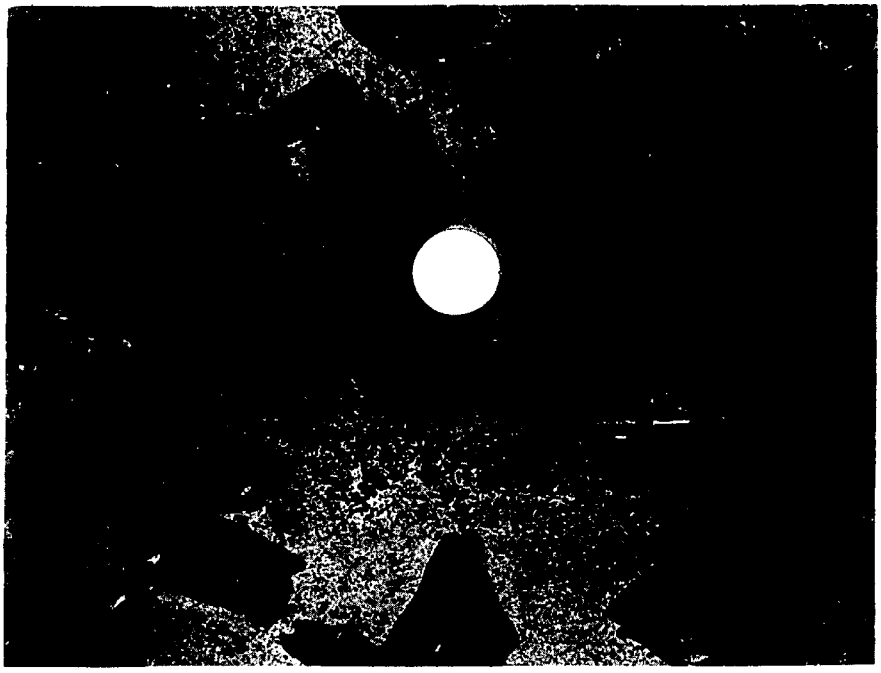


X1.75

Figure 14 Vertical Section of Molybdenum Crucible after Completion of Run 58

Photograph shows remaining slag and metal phases, which were liquid at temperature.

Note extent of dissolution of the crucible.



Unetched X500

Figure 15 Microstructure of Oxide Phase in Sample 68-2

Oxide phase was liquid at the 1600 C equilibration temperature.

Quenched sample contains cristobalite (dark phase), a fayalite matrix, and spherical metallic inclusions.



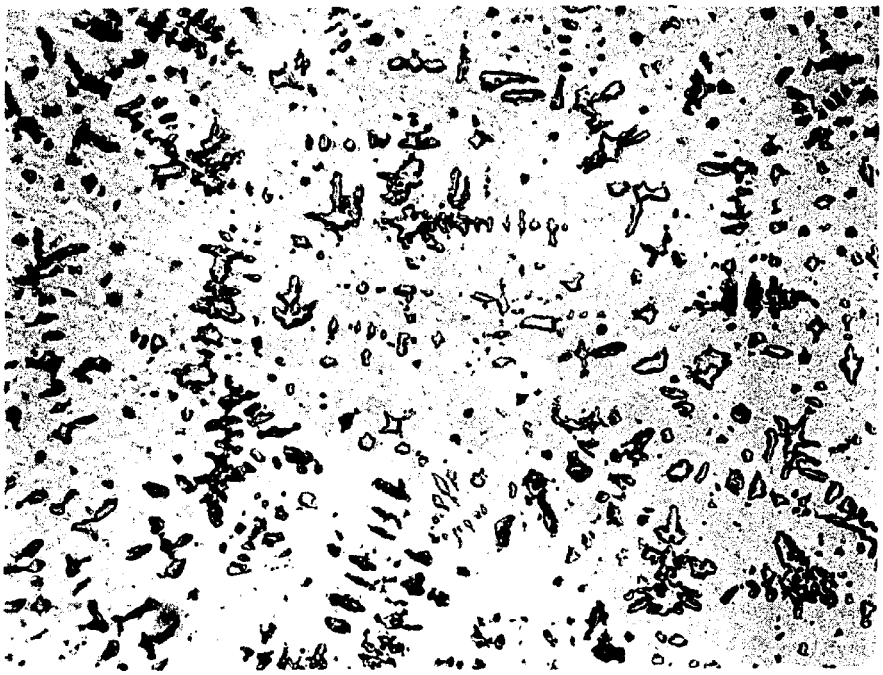
Unetched X500

Figure 16 Microstructure of Oxide Phase in Sample 55-3

Oxide phase was liquid at the 1600 C equilibration temperature.

Equilibrium oxide composition was approached from the molybdenum-lean side.

Light phase is believed to be Fe_2MoO_4; dark matrix is believed to be FeO.



$K_3Fe(CN)_6$ Etchant X500

Figure 17 Microstructure of Quenched Metal Phase in Sample 59-3

Quenched metal phase was liquid at the 1700 C equilibration temperature.

Metal Phase

Molybdenum Crucible

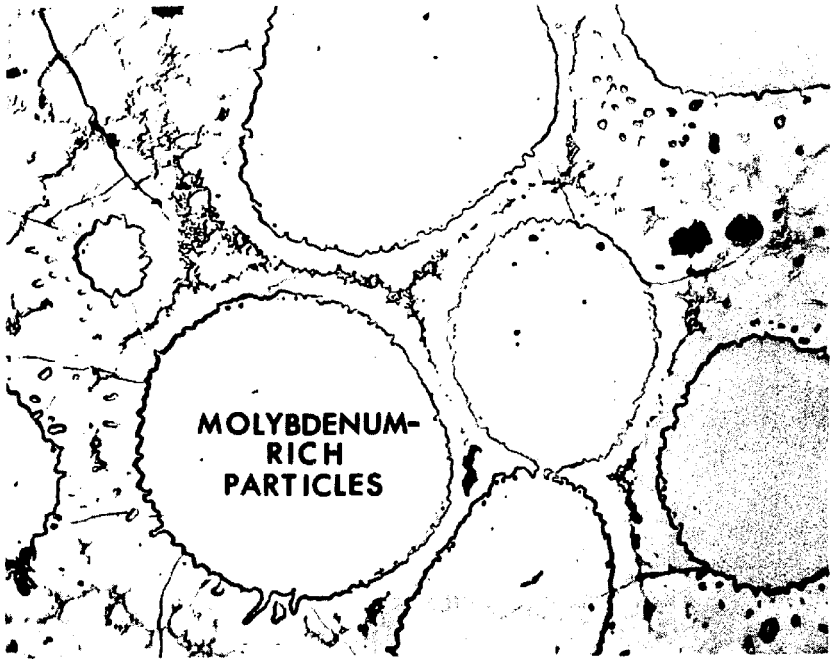


$K_3Fe(CN)_6$ Etchant

X500

Figure 18 Interface between Metal Phase and Interior Wall of Molybdenum Crucible after Completion of Run 59 and Furnace Cooling

Metal phase was liquid at the equilibration temperature (1550 C for Sample 59-1; 1600 C for Sample 59-2; 1700 C for Sample 59-3; 1800 C for Sample 59-4; and 1900 C for Sample 59-5).



$K_3Fe(CN)_6$ Etchant X500

Figure 19 Microstructure of Metal Phase in Sample 82-2

Metal phase was quenched from 1700 C ; it contained dispersed molybdenum-rich particles (solid at temperature) in a matrix that was liquid at temperature.

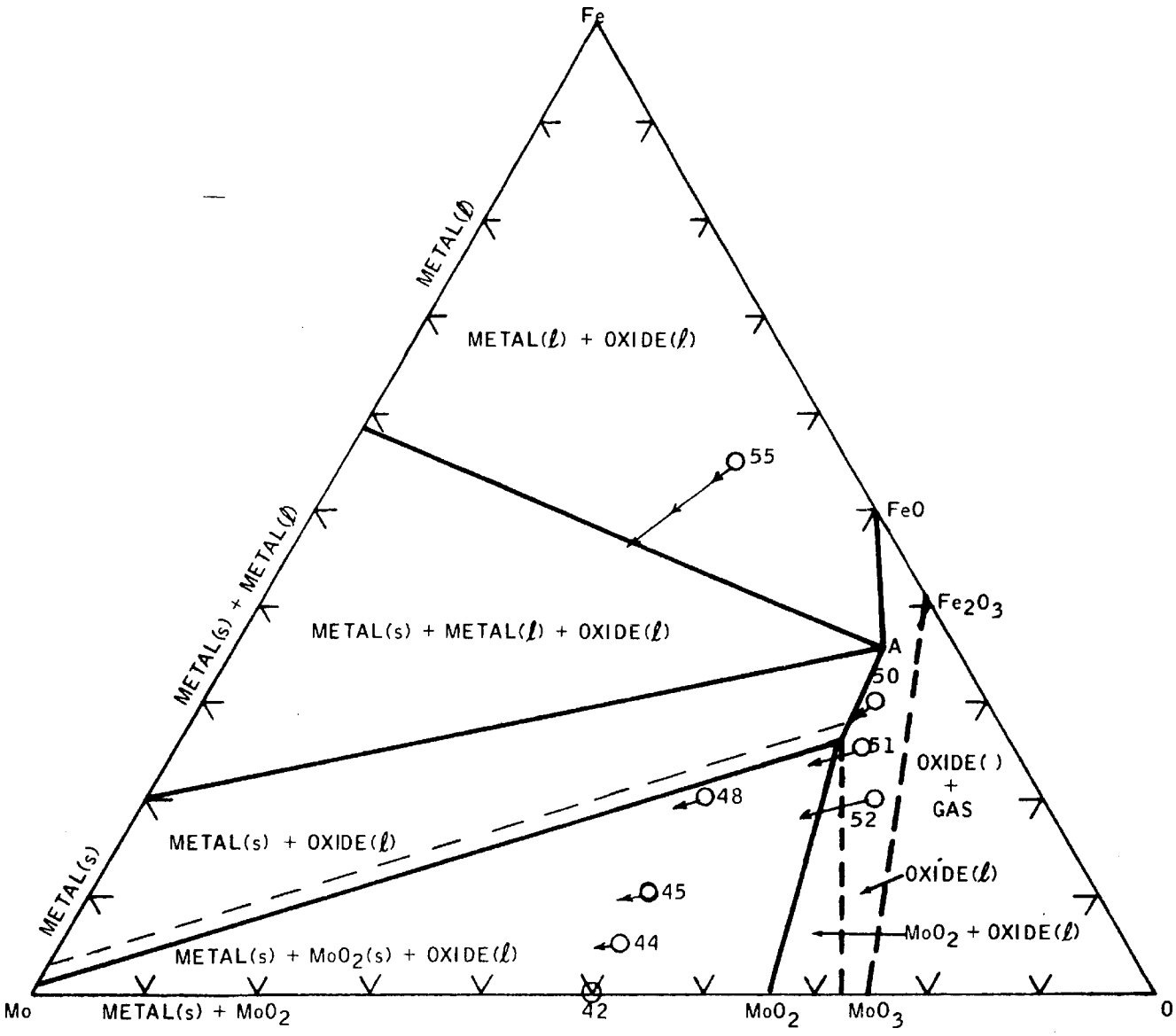


Figure 20 Schematic Illustration of Experimental Runs to Determine the Partial 1600 C Isothermal Section of the Fe-Mo-O Phase Diagram

Arrows represent compositional change in charge as molybdenum was added by reaction with crucible.



Unetched X500

Figure 21 Microstructure of Molybdenum-Rich Metal Phase, Molybdenum Dioxide Phase (Twinned), and Matrix of Iron-Molybdenum Oxide in Sample 45

Metal and molybdenum dioxide phases were solid at temperature; matrix was liquid at the 1600 C equilibrium temperature.



Figure 22 Interface between Contents of Crucible and Interior Wall of Molybdenum Crucible after Completion of Run 52

Dark, twinned phase is MoO_2, which was solid at the 1600 C equilibration temperature.

Matrix phase is an Fe-Mo oxide, which was liquid at temperature.



Figure 23 Interface between Contents of Crucible and Interior Wall of Molybdenum Crucible after Equilibration of Run 50 at 1600 C

Crucible contents were single-phased Fe-Mo liquid oxide at temperature.

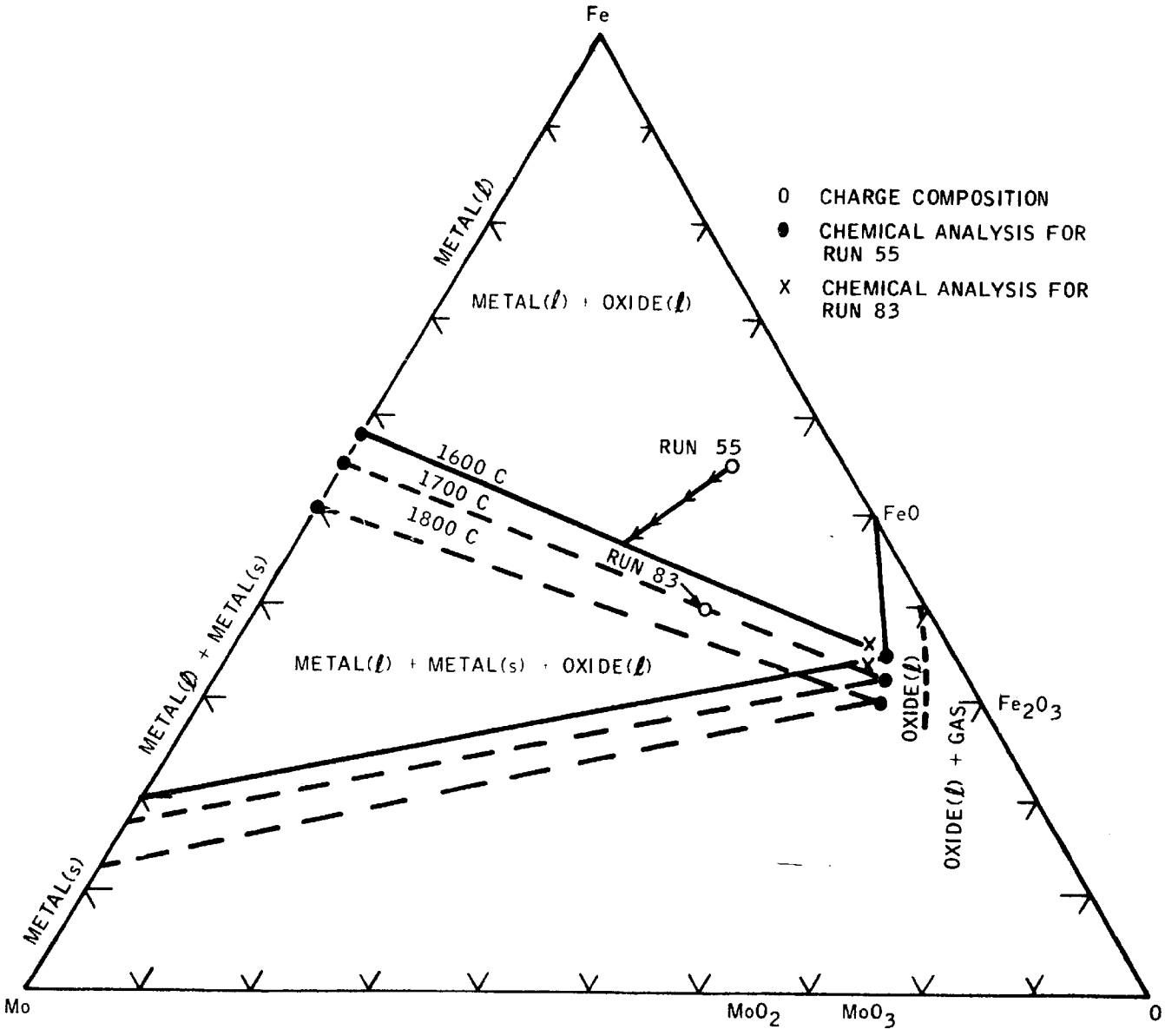
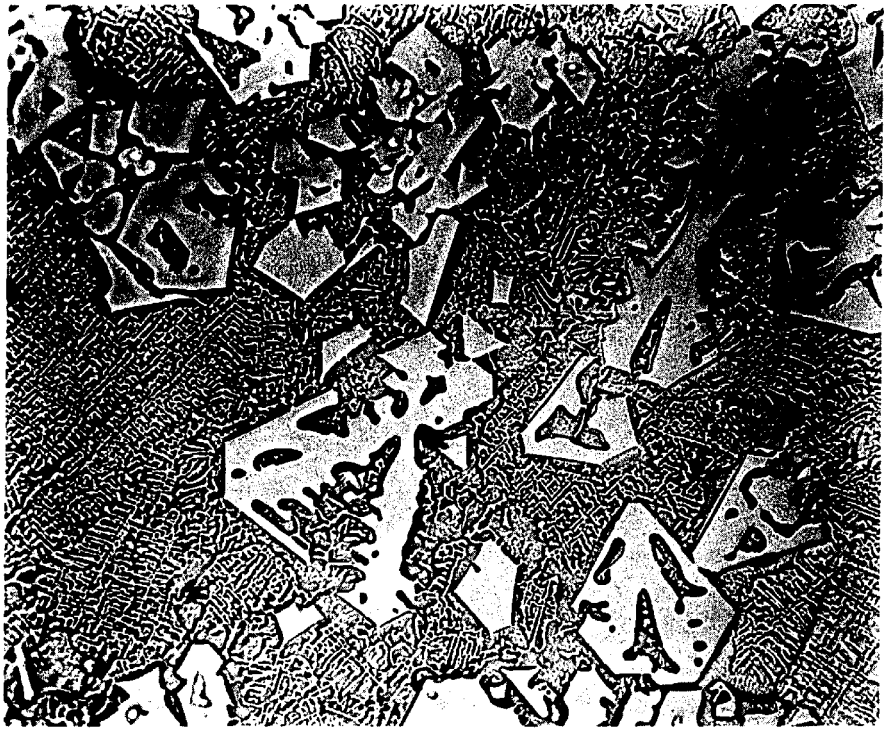


Figure 24 Schematic Illustration of Runs 55 and 83 in the Fe-Mo-O System

Arrows represent compositional change in charge as molybdenum was added by reaction with crucible.



Unetched X500

Figure 25 Microstructure of Oxide Phase in Sample 83-1

Oxide phase was liquid at the 1600 C equilibration temperature.

Equilibrium oxide composition was approached from the molybdenum-rich side.

Light angular phase is believed to be Fe_2MoO_4; dark matrix is believed to be FeO.

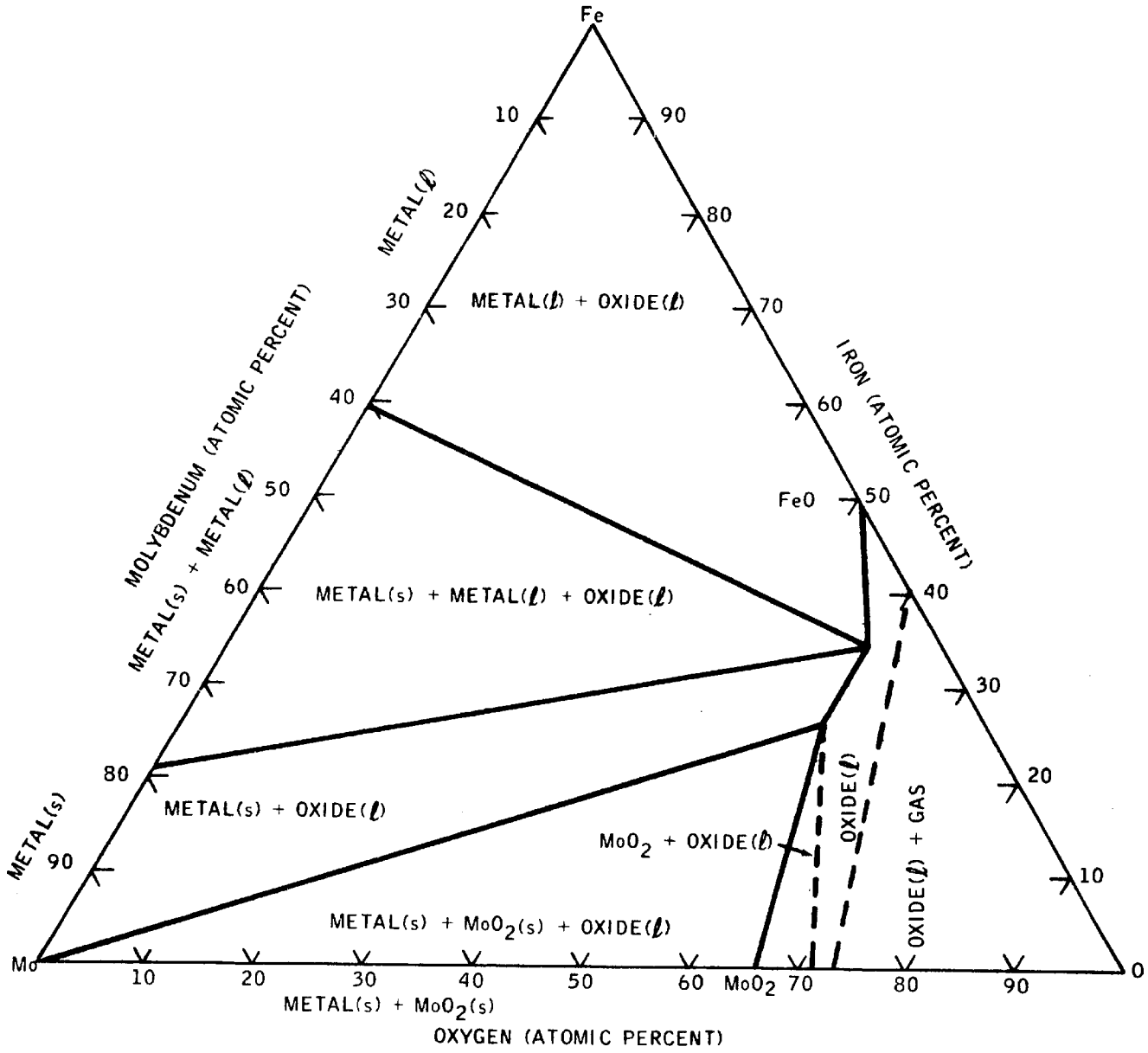


Figure 26 1600 C Isothermal Section through the Fe-Mo-O Phase Diagram Based on the Experimental Results of This Investigation

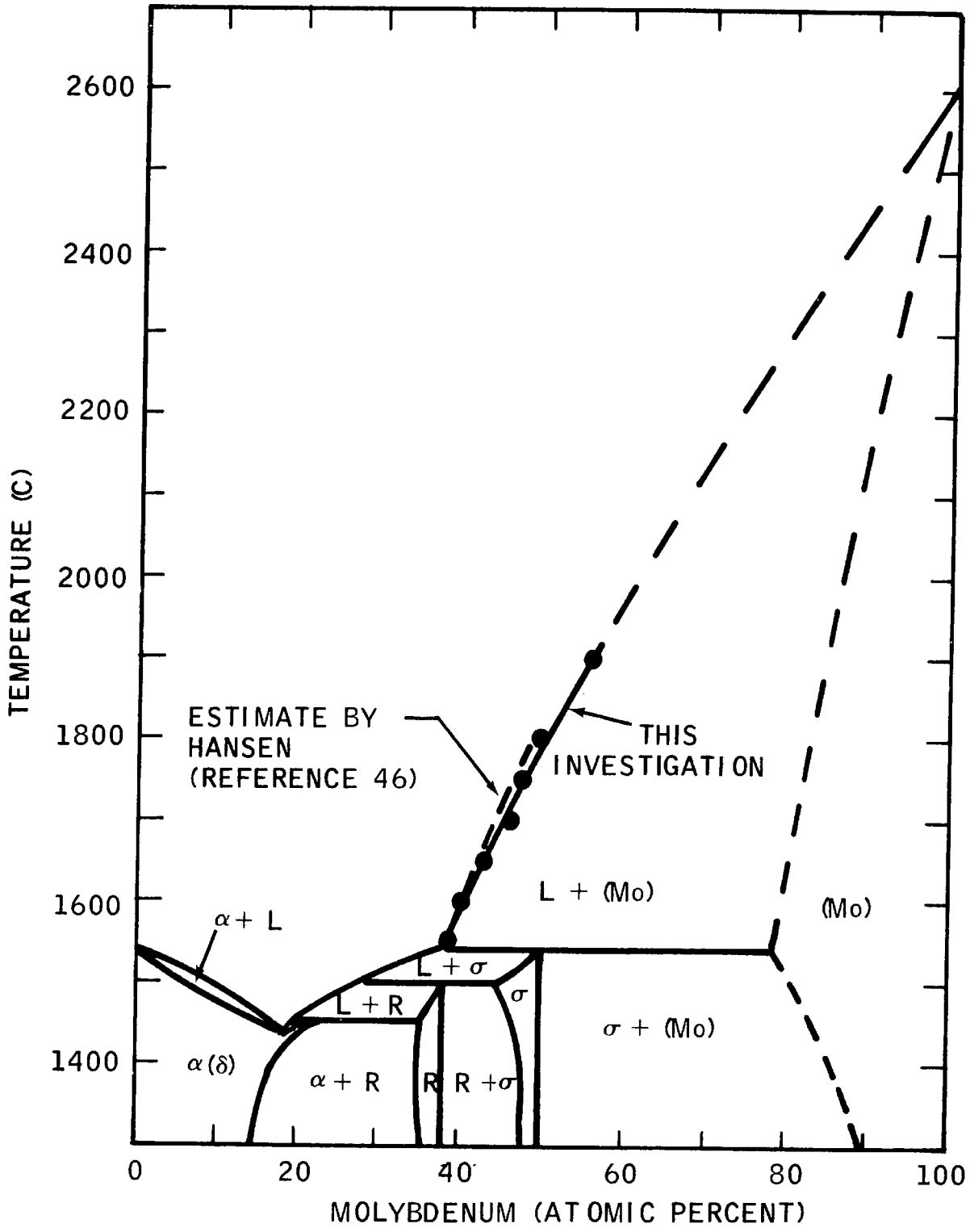


Figure 27 Iron-Molybdenum Equilibrium Phase Diagram Showing the Best Estimate of Liquidus Composition Using Data from Fe-Mo, Fe-Mo-O, and Fe-Mo-Si-O Equilibrations

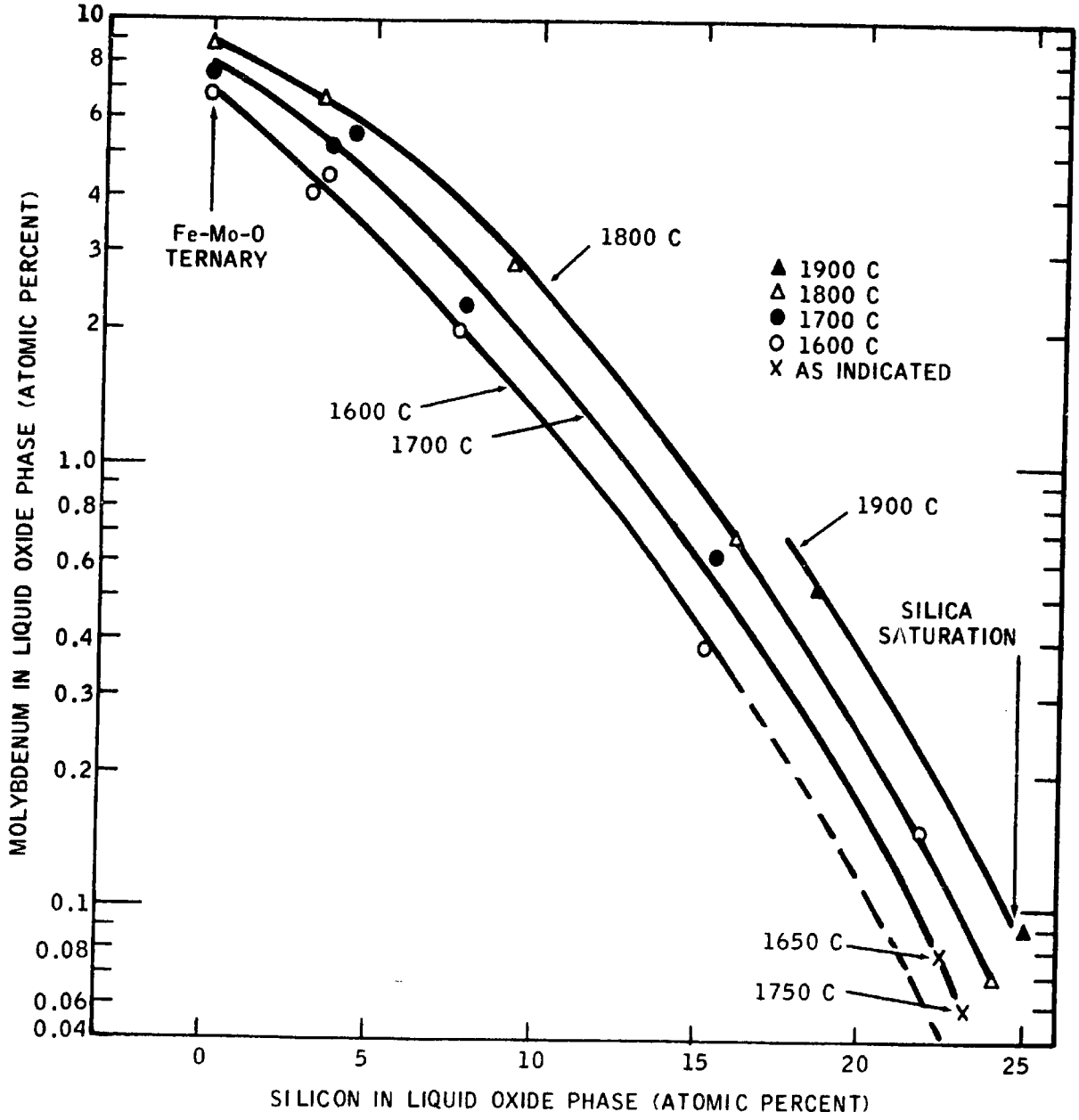


Figure 28 Effect of Temperature and Silicon Concentration of Molybdenum-Saturated Fe-Mo-Si-O Slags in Equilibrium with Liquid Fe-Mo Metal on Molybdenum Concentration of These Slags

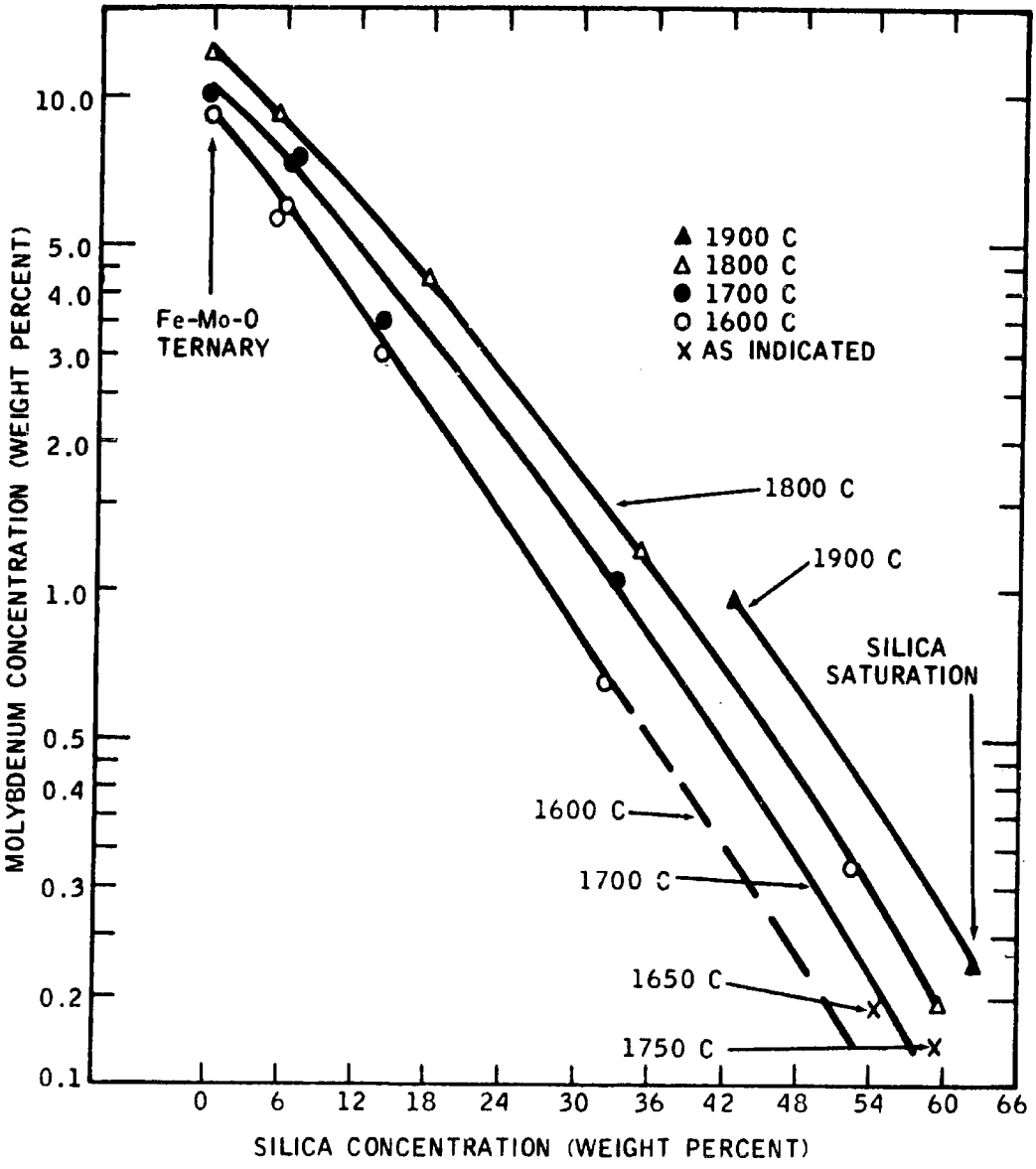


Figure 29 Effect of Temperature and Silica Concentration of Molybdenum-Saturated Fe-Mo-Si-O Slags in Equilibrium with Liquid Fe-Mo Metal on the Molybdenum Concentration of These Slags

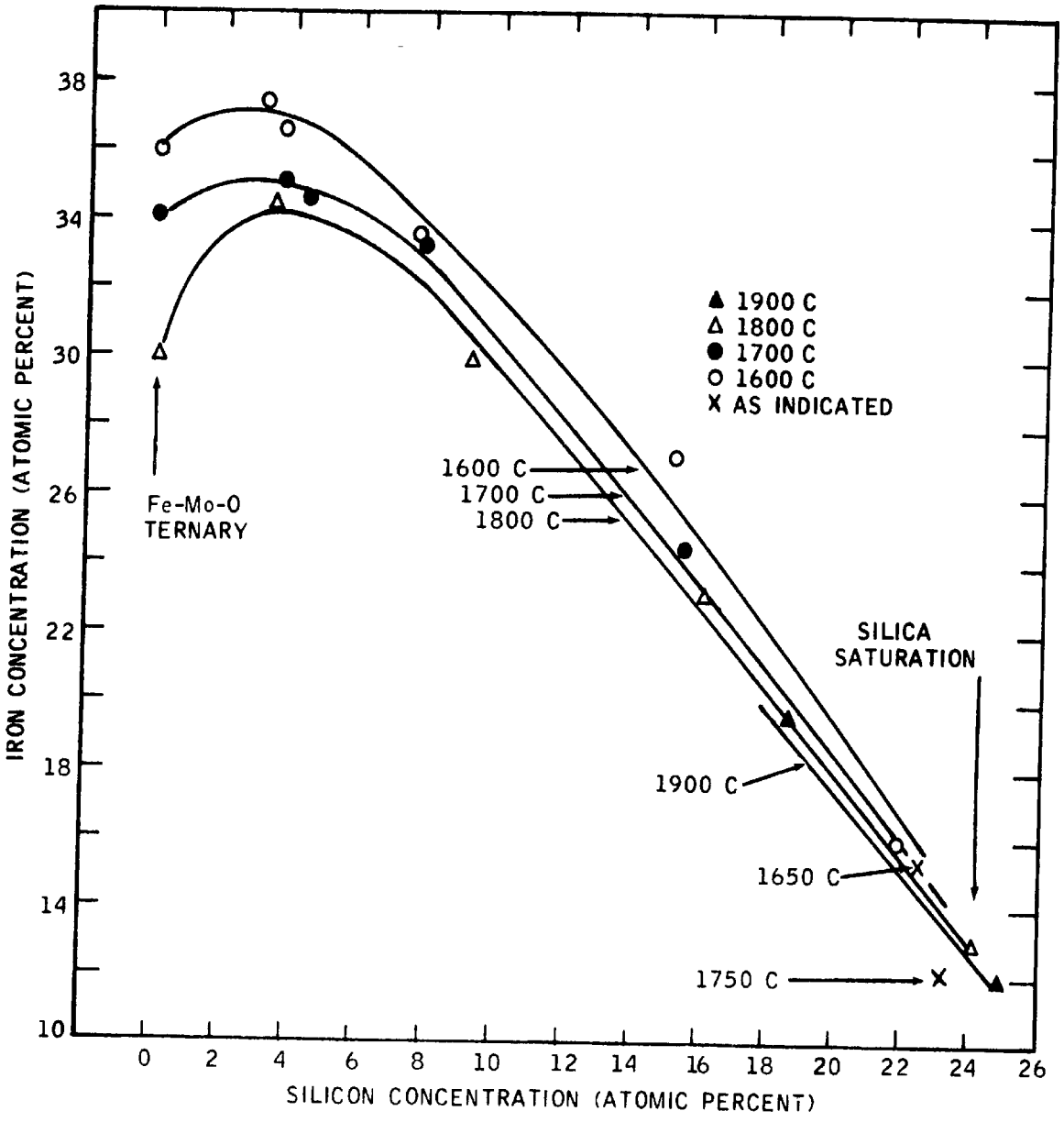


Figure 30 Effect of Temperature and Silicon Concentration of Molybdenum-Saturated Fe-Mo-Si-O Slags in Equilibrium with Liquid Fe-Mo Metal on Iron Concentration of These Slags



Unetched X500

Figure 31 Microstructure of Oxide Phase in Sample 84-1

Oxide phase was liquid at the 1600 C equilibration temperature.

Quenched sample contains dendrites of Fe_2MoO_4 (lighter phase), dendrites of wustite (darker phase), and a fayalite matrix.

Sample contains 6.5 weight percent SiO_2.



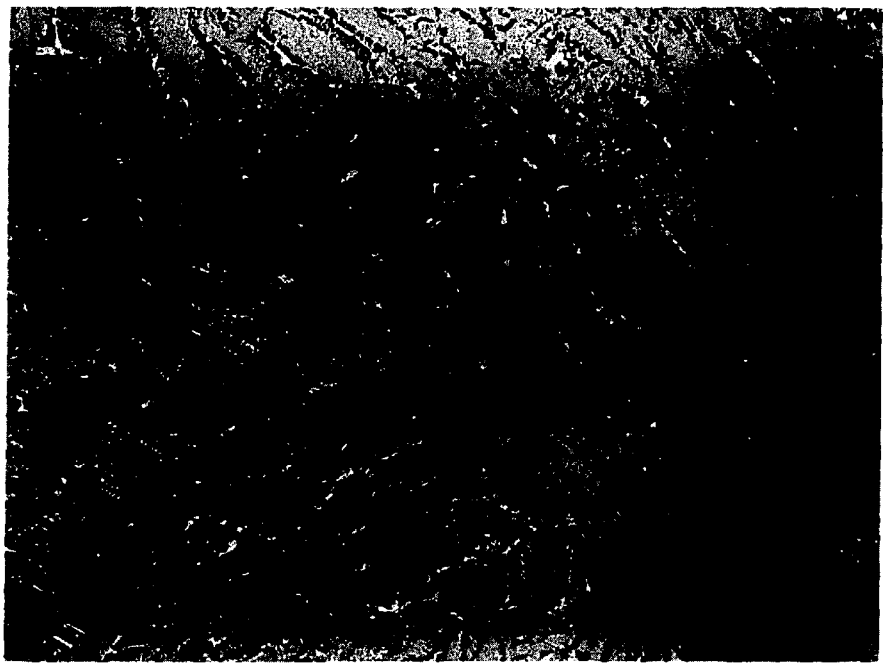
Unetched X500

Figure 32 Microstructure of Oxide Phase in Sample 57-1

Oxide phase was liquid at the 1600 C equilibration temperature.

Quenched sample contains dendrites of Fe_2MoO_4 (lighter phase), dendrites of wustite (darker phase), and a fayalite matrix.

Sample contains 14.2 weight percent SiO_2.



Unetched X500

Figure 33 Microstructure of Oxide Phase in Sample 58-1

Oxide phase was liquid at the 1600 C equilibration temperature.

Quenched sample contains fayalite.

Sample contains 32.3 weight percent SiO_2.

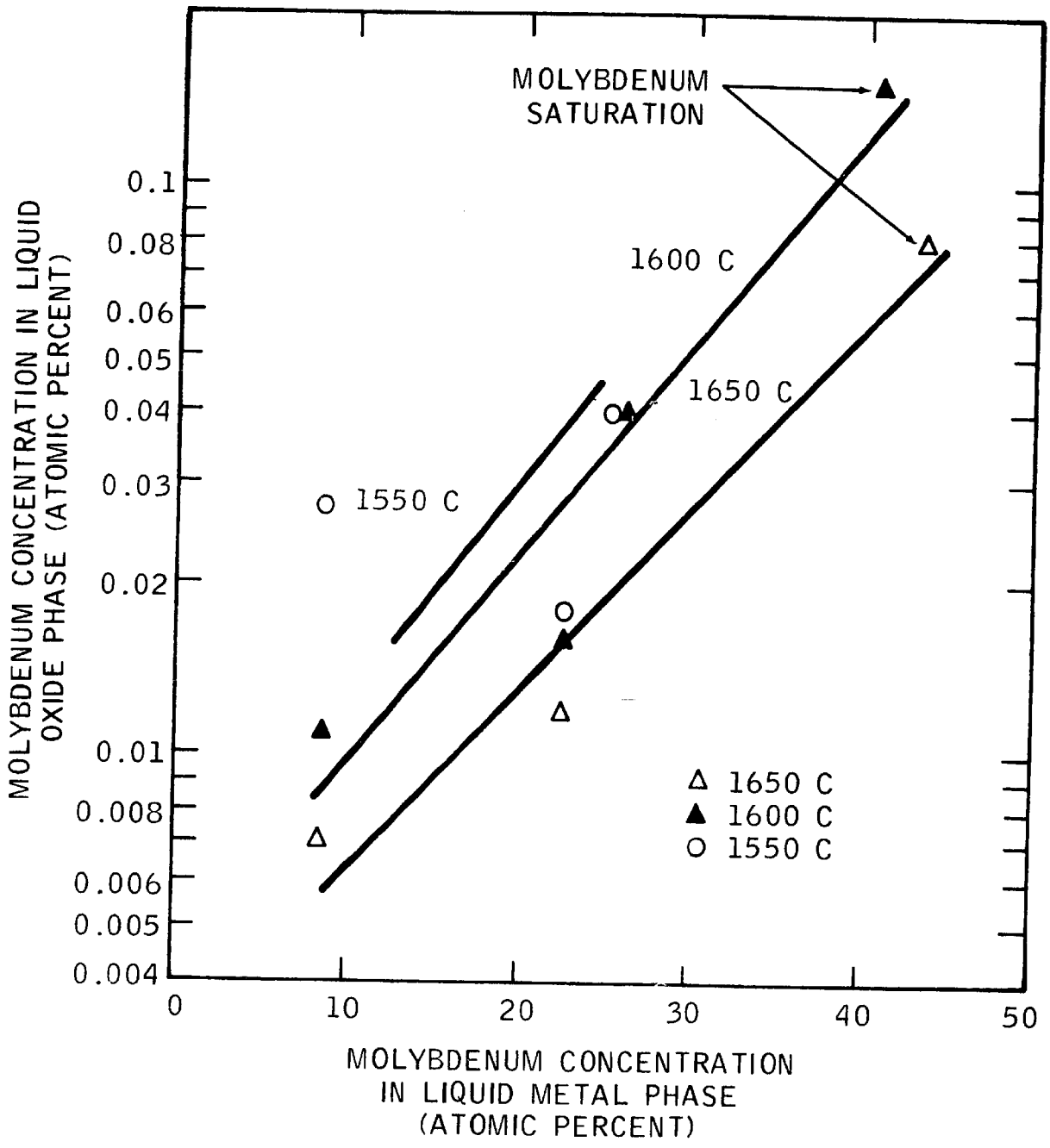


Figure 34 Effect of Temperature and Molybdenum Concentration of Liquid Fe-Mo Metal in Equilibrium with Silica-Saturated Fe-Mo-Si-O Slags on Molybdenum Concentration of These Slags

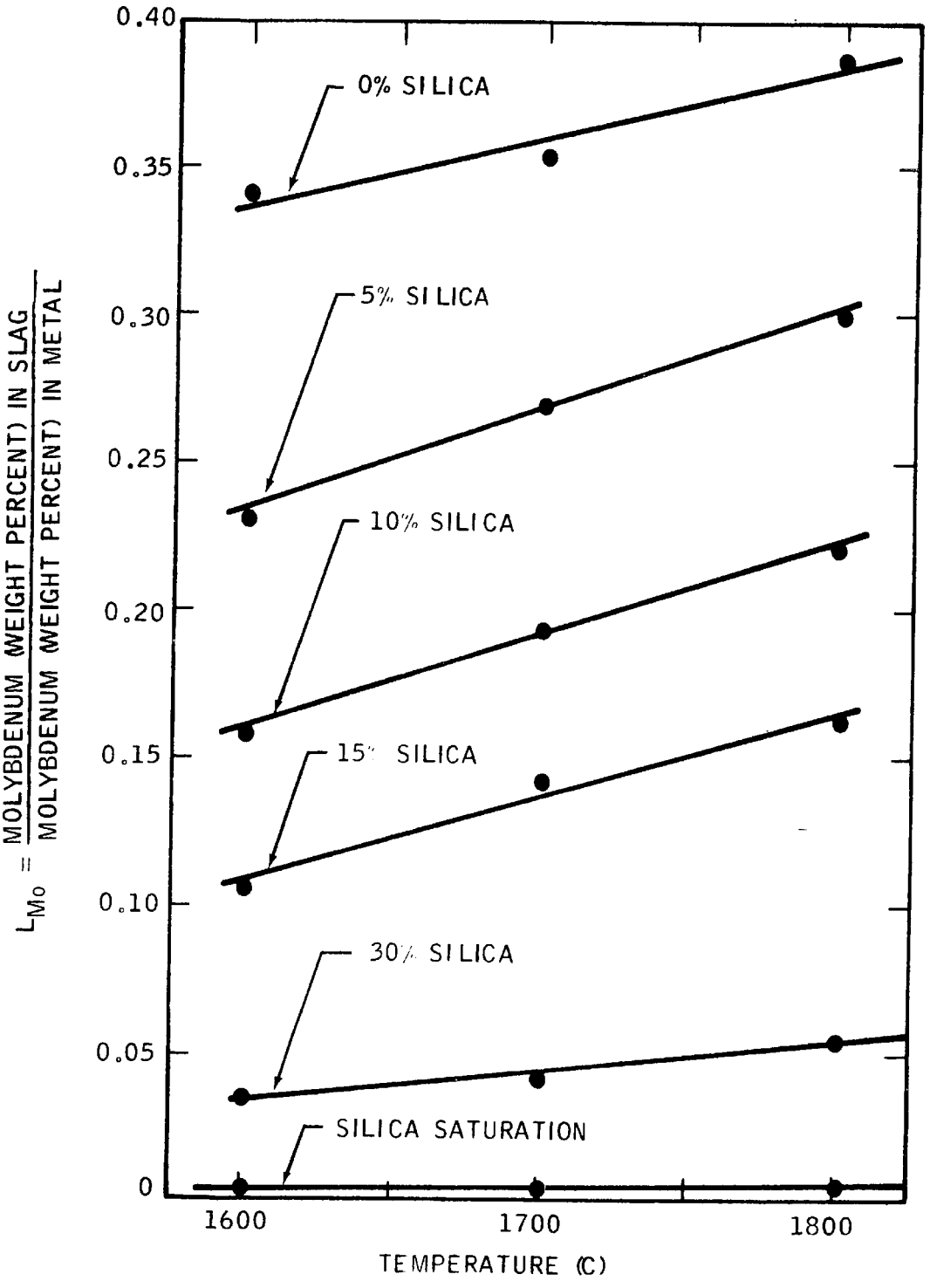


Figure 35 Partitioning of Molybdenum between an Fe-Mo-Si-O Slag and Fe-Mo Metal (Molybdenum Saturation) as a Function of Silica Content of the Slag

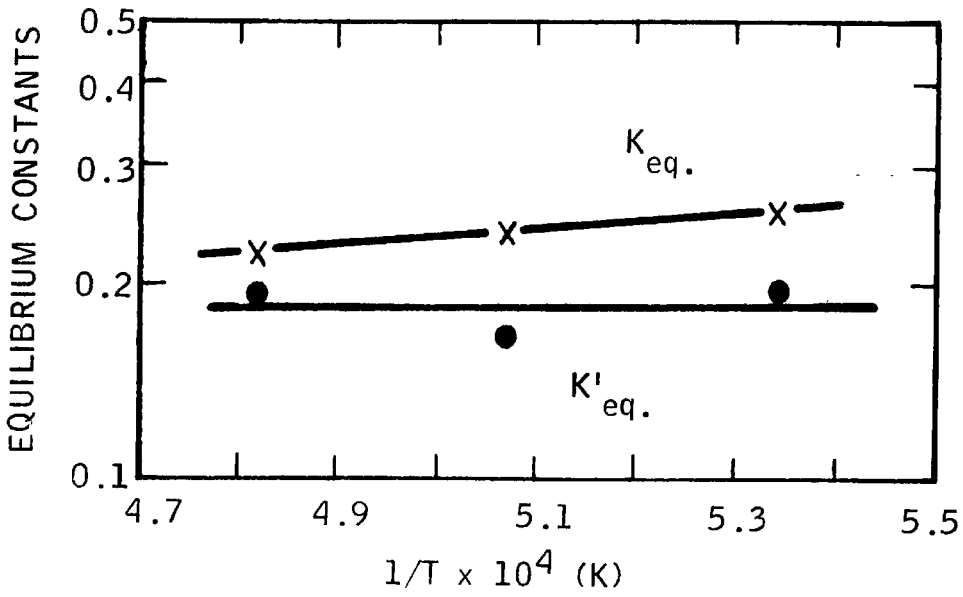


Figure 36 Equilibrium Constants versus Reciprocal of Absolute Temperature

$K_{eq.}$ was calculated from data in the literature.

$K'_{eq.}$ was calculated from experimental data of this study.

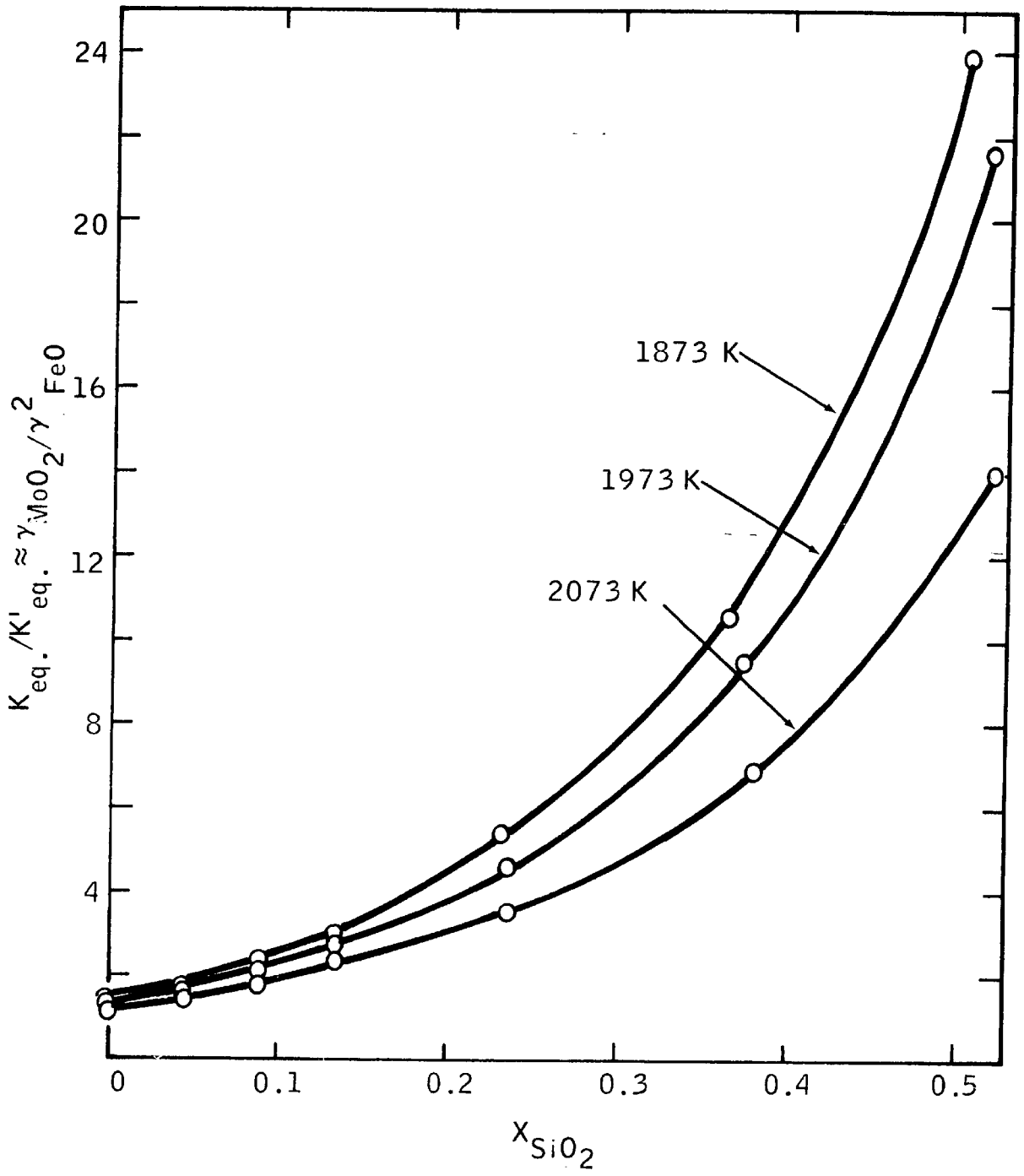


Figure 37 Effect of SiO_2 Additions to Molybdenum-Saturated Liquid Fe-Mo-Si-O Slag in Equilibrium with Liquid Fe-Mo Metal on the Activity Coefficient Ratio $\gamma_{MoO_2}/\gamma^2_{FeO} \approx K_{eq.}/K'_{eq.}$ at 1873, 1973, and 2073 K

APPENDIX A

USES OF FERROMOLYBDENUM

Ferromolybdenum, an alloy containing 60 to 70 weight percent molybdenum, is produced in the form of small chunks for consumption by the iron and steel industry as a molybdenum additive to ferrous melts. Ferromolybdenum powder is used in the production of welding rod coatings. Ferromolybdenum is considered preferable to pure molybdenum as a molybdenum additive because it melts at steelmaking temperatures, dissolves more readily, and is less expensive per pound of molybdenum contained. Molybdic oxide is readily reduced by liquid iron and is less expensive than ferromolybdenum per pound of molybdenum contained. It is also used in considerable quantities as a molybdenum additive to ferrous melts. Preference is given to ferromolybdenum where slag formation may be undesirable, such as in ladle additions and induction furnace melting.

APPENDIX B

DISCUSSION OF EXPERIMENTS UTILIZING A ROTATING CRUCIBLE APPARATUS

In the present study the use of a rotating crucible was investigated as a means of equilibrating liquid slag and liquid metal in a non-reactive container. The rotation of the crucible, as discussed by Taylor and Chipman,[B-1] causes the surface of the liquid slag and liquid metal to form paraboloids of revolution about the axis of rotation. If the slag completely wets the metal it can not be held in the liquid metal cup, since it creeps up the metal walls and permits reaction with the crucible. Under more favorable conditions of interfacial tension a finite contact angle exists which permits containment of the slag in the metal cup. In addition to eliminating slag-crucible reactions concentration of the slag in the base of the metal cup improves the possibilities for slag sampling. Slag-metal compositions below molybdenum or silica saturation could be studied by successfully applying this technique to the Fe-Mo-Si-O system. For example, the partitioning of molybdenum between slag and metal could be determined at a molybdenum activity below unity as a function of silica content of the slag phase. Although these experiments were not successful, a description of the apparatus and discussion of the results is included in this appendix.

The rotating crucible technique has been used by several investigators to study slag-metal equilibria under conditions where any reaction between slag and crucible is undesirable. Barrett et al.[B-2] have described several furnaces of this type. Taylor and Chipman[B-1] have studied equilibria between liquid iron and simple acid and basic slags in a rotating crucible furnace. More recent work by Hilty and Crafts,[B-3,B-4] and Hilty[B-5] incorporates similar equipment to determine oxygen solubilities in various liquid iron-slag systems.

The rotating crucible apparatus constructed in this investigation is shown schematically in Figure B-1. A molybdenum cup and shaft are used to hold a 3-3/8-inch-o.d. by 5-1/2-inch-tall magnesia crucible in an inert-atmosphere induction furnace. The molybdenum cup and shaft are carefully machined to be concentric and well balanced. The molybdenum shaft extends through the bottom of the furnace to an air-operated motor which turns the entire assembly on water-cooled bearings. A tungsten, tungsten-26% rhenium thermocouple is suspended into the hot zone of the furnace adjacent to the rotating assembly. Tank argon is fed through a molybdenum tube in the top of the furnace to flood the hot zone. A run is made by charging the crucible with metal of the desired composition. After heating the furnace to about 1600 C the crucible is spun at approximately 300 rpm to cause the surface of the metal to form a parabolic shape. The slag is then slowly charged through a hole in the top of the furnace and the melt is observed to note the position of the slag phase. The slag composition selected for preliminary experiments with this apparatus was 35 weight percent SiO_2 and 65 weight percent FeO. A slag of essentially this composition was successfully used by Taylor and Chipman[B-1] for equilibration with liquid iron at 1588 C.

Table B-I summarizes the results of four runs made with the rotating crucible apparatus. Each run required a new molybdenum cup and shaft assembly. Despite attempts to vary the speed of rotation of the crucible and the type of slag addition, the slag invariably penetrated the crucible at the metal surface shortly after being added to the melt. Leakage of molten iron onto the molybdenum cup and shaft then caused these components to be irreparably damaged.

It is concluded that the slag studied in these experiments wets the surface of the liquid metal and hence is not confined to the bottom of

Table B-I

Results of Rotating Crucible Experiments

Run	Metal Charge	Slag Charge	Results
54A	2000g Fe	--	Crucible cracked upon rotation of metal.
63	1000g Fe	35 weight percent SiO_2 and 65 weight percent FeO, added as pressed pellets of SiO_2, Fe, and Fe_2O_3	Rapid attack of crucible by slag at top of metal surface; complete penetration within 10 minutes after addition of about 50 grams of slag.
64	1500g Fe	SiO_2 pellets followed by small amount of FeO as pellets of Fe and Fe_2O_3	Crucible attacked at top of metal surface after iron oxide addition; some attack of molybdenum cup due to splashing of liquid metal over top of crucible during attempted sampling into Vycor tube.
70	1513g Fe, 267g Mo	Prefused pieces of 35 weight percent SiO_2 - 65 weight percent FeO slag; Composition confirmed by prior chemical analyses	Complete penetration of crucible at top of metal surface after about 1 hour at 1600 C.

the parabolic cavity formed by the metal. It is anticipated that iron-silicate slags higher in FeO than the 35 weight percent SiO_2 - 65 weight percent FeO trial slag would also wet the metal surface. More viscous slags higher in silica would be nearly silica saturated and more easily studied in silica crucibles. Based on these preliminary experiments the rotating crucible technique is considered inapplicable to the slag-metal system of interest in this investigation.

REFERENCES

B-1. C. R. Taylor and J. Chipman, "Equilibria of Liquid Iron and Simple Basic and Acid Slags in a Rotating Induction Furnace," AIME Trans. 154 (1943), 228-245.

B-2. E. P. Barrett, W. F. Holbrook, and C. E. Wood, "Induction Furnaces for Rotating Liquid Crucibles," AIME Trans. 135 (1939), 73-84.

B-3. D. C. Hilty and W. Crafts, "Solubility of Oxygen in Liquid Iron Containing Silicon and Manganese," AIME Trans. 188 (1950), 425-436.

B-4. D. C. Hilty and W. Crafts, "Solubility of Oxygen in Liquid Iron Containing Aluminum," AIME Trans. 188 (1950), 414-424.

B-5. D. C. Hilty, "Influence of Sulfur on Oxygen Solubility in Steel," J. Metals 18 (1966), 201-204.

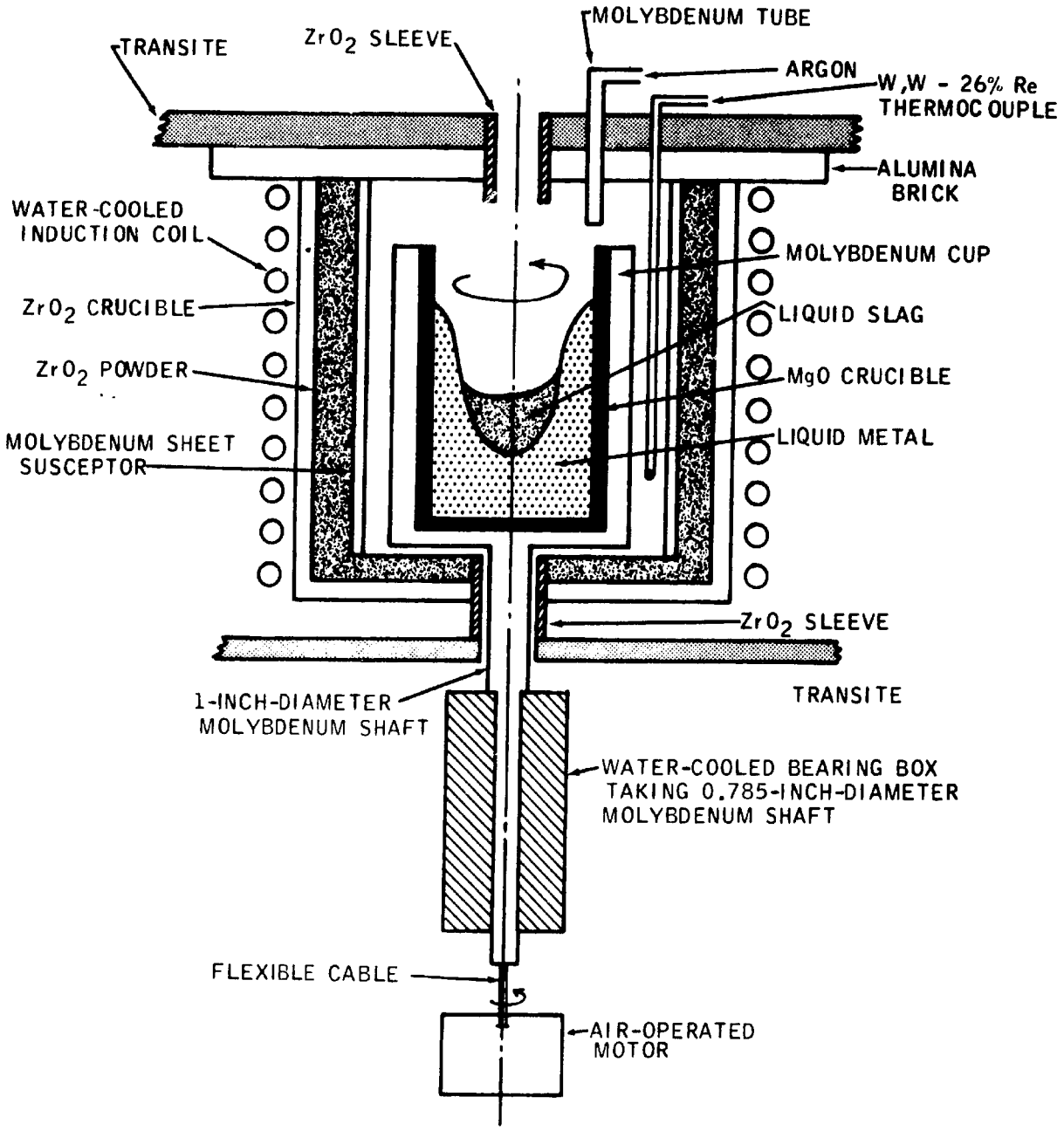


Figure B-1 Schematic Diagram of Inert Atmosphere Induction Heated Rotating Crucible Apparatus

The apparatus shown above was packed in alumina bubble to the top of the induction coil.